

UNIVERSITÄTSKLINIKUM HAMBURG-EPPENDORF

Institut für Biochemie und Molekulare Zellbiologie

Institutsdirektor: Prof. Dr. Dr. Andreas H. Guse

Role of the scavenger receptors CD36 and SR-B1 in adaptive thermogenesis and lipid handling

Dissertation

zur Erlangung des Doktorgrades PhD
an der Medizinischen Fakultät der Universität Hamburg.

vorgelegt von:

Kimberley M. Hurkmans

aus Harmelen, die Niederlande

Hamburg 2025

(wird von der Medizinischen Fakultät ausgefüllt)

**Angenommen von der
Medizinischen Fakultät der Universität Hamburg am: 06.06.2025**

**Veröffentlicht mit Genehmigung der
Medizinischen Fakultät der Universität Hamburg.**

Prüfungsausschuss, der/die Vorsitzende: Prof. Dr. Jörg Heeren

Prüfungsausschuss, zweite/r Gutachter/in: Prof. Dr. Hartmut Schlüter

The present work was performed at the Institute of Biochemistry and Molecular Cell Biology of the University Medical Center Hamburg-Eppendorf under the supervision of Prof. Dr. Jörg Heeren from December 2021 to February 2025. This work was co-supervised by Prof. Dr. Hartmut Schlüter from the Department of Clinical Chemistry and Laboratory Medicine of the University Medical Center Hamburg-Eppendorf.

“Blijf nieuwsgierig”

“Stay curious”

Toos Hurkmans

Publications, presentations and abstracts at national and international congresses

Manuscripts in preparation

1. Hurkmans KM, Heine M & Heeren J. CD36 expressed by brown adipocytes is indispensable for thermogenesis and lipid uptake in BAT, while CD36 expressed by endothelial cells is not. (In preparation)
2. Hurkmans KM, Heine M, Shaul PW, Rinniger F & Heeren J. SR-B1 expressed by endothelial cells is dispensable for thermogenesis and lipid handling in BAT. (In preparation)

Oral presentations at national and international congresses

- *Scavenger receptor B1 (SR-B1) expressed by endothelial cell is dispensable for handling of triglyceride-rich lipoproteins and for adaptive thermogenesis*
Hurkmans KM, Heine M, Shaul PW & Heeren J

2023, 46st European Lipoprotein Club (ELC), Tutzing, Germany

- *Role of CD36 expressed by brown adipocytes in adaptive thermogenesis and lipid disposal*
Hurkmans KM, Heine M & Heeren J

2024, EndoConnect Symposium on Endo-Lysosomes in Metabolic Regulation, Cambridge, United Kingdom

Posters at national and international congresses

- *The role of endothelial expressed SR-B1 in lipid handling under adaptive thermogenesis conditions*

Hurkmans KM, Heine M, Shaul PW & Heeren J

2023, BATenergy Conference, Hamburg, Germany

- *Role of CD36 expressed by brown adipocytes in adaptive thermogenesis and lipid disposal*

Hurkmans KM, Heine M & Heeren J

2024, 47st European Lipoprotein Club (ELC), Tutzing, Germany

Table of Contents

Publications, presentations and abstracts at national and international congresses	5
Manuscripts in preparation	5
Oral presentations at national and international congresses	5
Posters at national and international congresses	6
Abbreviations	11
Part A: Summary	17
Part B: Zusammenfassung	20
Part C: Introduction	23
Adipose tissues	23
White vs brown adipocytes	24
A third type of adipocyte: beige	25
Endothelial cells in adipose tissues	27
WAT is the main organ for energy storage	28
BAT and NST	29
Receptors	32
CD36	32
Discovery	32
Structure	33
Post-translational modifications	33
Regulation of CD36	34
Ligands of CD36	34
Transport of fatty acids	34
CD36 and its role in lipid uptake & thermogenesis	35
SR-B1	37
Discovery	37

Structure	38
Post-translational modifications	39
Regulation of SR-B1	39
Ligands of SR-B1	39
Reverse cholesterol metabolism, cholesterol efflux, atherosclerosis, cold exposure ...	40
Part D: Aims	42
Part E: Material and methods	43
Animals	43
Interventions	44
Indirect calorimetry	44
Cd36 ^{fl/fl} -Ucp1	44
Non fasting experiment	44
Fasting experiment	44
Cd36 ^{fl/fl} -Cdh5	44
Scarb1 ^{fl/fl} -Cdh5	45
Basal measurement	45
Cold challenge	45
Cold exposure	45
Postprandial uptake studies and organ distribution	46
Oral fat tolerance test (OFTT)	46
Cd36 ^{fl/fl} -Ucp1	46
Cd36 ^{fl/fl} -Cdh5	46
Oral glucose fat tolerance test (OGFT)	46
Workflow and analysis	46
HDL turnover	47
Genotyping	48
DNA isolation	48

PCR.....	48
CD36flox.....	48
SR-B1flox.....	51
CreCs.....	54
Plasma TG, cholesterol and NEFA levels determination	57
Magnetic-activated Cell sorting (MACS).....	57
Gene expression analysis	58
RNA isolation	58
qPCR	58
Western blot	60
Immunofluorescence	61
Statistical analysis	61
Part F: Results	62
Brown adipocyte-specific CD36ko mice.....	62
Validating brown adipocyte-specific knockout of CD36 in <i>Cd36^{fl/fl}-Ucp1^{Cre+}</i> mice	62
Are <i>Cd36^{fl/fl}-Ucp1^{Cre+}</i> mice able to maintain their body temperature when exposed to cold in a fed state?.....	66
Are <i>Cd36^{fl/fl}-Ucp1^{Cre+}</i> mice able to maintain their body temperature when exposed to cold in a fasted state?.....	69
Do <i>Cd36^{fl/fl}-Ucp1^{Cre+}</i> mice have altered lipid uptake compared control littermates at different housing temperatures?	72
Do <i>Cd36^{fl/fl}-Ucp1^{Cre+}</i> mice have altered gene expression in BAT and WAT compared to control littermates at different housing temperatures?	74
Endothelial-specific CD36ko mice.....	77
Validating endothelial-specific knockout of CD36 in <i>Cd36^{fl/fl}-Cdh5^{Cre+}</i> mice.....	77
Are <i>Cd36^{fl/fl}-Cdh5^{Cre+}</i> mice able to maintain their body temperature when exposed to cold in a fed and fasted state?	80
Do <i>Cd36^{fl/fl}-Cdh5^{Cre+}</i> mice have altered lipid uptake compared to control littermates at different housing temperatures?	82

Do <i>Cd36^{fl/fl}-Cdh5^{Cre+}</i> mice have altered gene expression in BAT and WAT compared to control littermates at different housing temperatures?	84
Endothelial-specific SR-B1ko mice	86
Validating endothelial-specific knockout of SR-B1 in <i>Scarb1^{fl/fl}-Cdh5^{Cre+}</i> mice	86
Can an endothelial knockout of SR-B1 be detected on gene expression on whole organ level in <i>Scarb1^{fl/fl}-Cdh5^{Cre+}</i> mice?	88
Are <i>Scarb1^{fl/fl}-Cdh5^{Cre+}</i> mice able to maintain their body temperature when the temperature is gradually decreased and is this influenced by diet?	91
Do <i>Scarb1^{fl/fl}-Cdh5^{Cre+}</i> mice have altered lipid uptake compared to control littermates at different housing temperatures and diet regiments?	96
Do <i>Scarb1^{fl/fl}-Cdh5^{Cre+}</i> mice have altered gene expression in BAT and WAT compared to control littermates at different housing temperatures and diet regiments?	100
Do <i>Scarb1^{fl/fl}-Cdh5^{Cre+}</i> mice have altered uptake of cholesteryl ethers and selective cholesterol uptake compared to <i>Scarb1^{fl/fl}-Cdh5^{Cre-}</i> mice?	104
Part G: Discussion	106
CD36	107
CD36 in brown adipocytes	108
CD36 in endothelial cells	109
SR-B1	112
SR-B1 in endothelial cells	113
Part H: References	115
Part I: Attachments	135
Part J: Register of figures	137
Part K: Register of tables	141
Acknowledgements	138
Curriculum vitae	145
Eidesstattliche Versicherung	145

Abbreviations

μL	microlitre
μm	micrometre
¹²⁵ I-TC	¹²⁵ I-tyramine cellobiose
¹⁸ F-FDG	¹⁸ F-fluoro-2-deoxy-D-glucose
ABCA1	ATP-binding cassette A1
ABCG1	ATP-binding cassette G1
Abhd5, CGI-58	ATGL-activating protein comparative gene identification-58
acLDL	acetylated low-density lipoprotein
ACTH	adrenocorticotrophic hormone
Ad-CD36ko	adipocyte-specific CD36 knockout
Adgre	adhesion G protein-coupled receptor E
Adipoq	adiponectin
AGE	advanced glycation endproducts
Angptl4	angiopoietin-like protein 4
ARL15	ADP ribosylation factor-like GTPase 15
ATGL	adipose triglyceride lipase
BAT	brown adipose tissue
BLT-1	blocker of lipid transport 1
Brite	brown-in-white
cAMP	cyclic adenosine monophosphate
CAV-1	caveolin-1
CD11b	CD11b ⁺ macrophages
CD31	CD31 ⁺ endothelial cells

CD36	cluster of differentiation 36
CD36ko	CD36 knockout
Cdh5	VE-Cadherin
CE	cholesteryl ester
CEt	³ H-cholesteryl oleoyl ether
CETP	cholesteryl ester transfer protein
CHREBP-b	carbohydrate response element binding protein beta
CL	CL316,243
CoQ	coenzyme Q
CR	chylomicron remnants
CREB	cAMP response element-binding
Dio2	type II iodothyronine deiodinase
dl	decilitre
DNL	<i>de novo</i> lipogenesis
DOG	deoxyglucose
EC-CD36ko	endothelial-specific CD36 knockout
Elovl3	elongation of very long chain fatty acid 3
eNOS	endothelial nitric oxide synthase
ER	endoplasmic reticulum
FA	fatty acid
Fabp4	fatty acid binding protein 4
FABPc	fatty acid binding protein cytoplasmic
FABPpm	fatty acid binding protein plasma membrane
Fasn	fatty acid synthase

FATP1	fatty acid transporter 1
FC	free cholesterol
FFA	free fatty acid
γ-TUB	γ-Tubulin
g	gram
GLUT1	glucose transporter 1
GLUT4	glucose transporter 4
GPIHBP1	glycosylphosphatidylinositol anchored high density lipoprotein binding protein 1
gWAT	gonadal WAT
HDL	high-density lipoprotein
HFD	high-fat diet
HSL	hormone sensitive lipase
iBAT	interscapular BAT
IDL	intermediate-density lipoprotein
iWAT	inguinal WAT
L	litre
LAL	lysosomal acid lipase
LCAT	Lecitin:cholesterol acyltransferase
LCFA	long-chain fatty acid
LDL	low-density lipoprotein
LDLR	low-density lipoprotein receptor
LIMP-2	lysosomal integral membrane protein-2
LPL	lipoprotein lipase
Lrp1	LDL receptor–related protein–1

M	molar
mA	mature adipocytes
MACS	magnetic-activated cell sorting
mg	milligram
MGL	monoglyceride lipase
mL	millilitre
mM	millimolar
Myf5	myogenic factor 5
NE	norepinephrine
NEFA	non-esterified fatty acid
NHERF	Na ⁺ /H ⁺ Exchanger Regulatory Factors
NMR	nuclear magnetic resonance
NO	nitric oxide
NST	non-shivering thermogenesis
OFTT	oral fat tolerance test
OGFT	oral glucose fat tolerance test
OGTT	oral glucose tolerance test
organ-FCR	organ fractional catabolic rate
oxLDL	oxidized low-density lipoprotein
Pdgfra	platelet-derived growth factor receptor alpha
PDZK1	PDZ Domain Containing 1
PDZK1ko	PDZK1 knockout
PET-CT	positron emission tomography–computed tomography

Pgc1a (Ppargc1a)	peroxisome proliferator-activated receptor- gamma co-activator
PKA	protein kinase A
plasma-FCR	plasma fractional catabolic rate
PPAR γ	peroxisome proliferator-activated receptor γ
PPAR α	peroxisome proliferator-activated receptor α
PRDM16	PR domain containing 16
qPCR	quantitative PCR
RCT	reverse cholesterol transport
RER	respiratory exchange ratio
RT	room temperature
SR-B1	scavenger receptor B1
SR-B1ko	SR-B1 knockout
SSO	sulfo-N-succinimidyl oleate
SVF	stroma vascular fraction
T ₃	3,5,3'-triiodothyronine
T ₄	thyroxine
Tbp	TATA-box binding protein
TG	triglyceride
Tie2	TEK Receptor Tyrosine Kinase
TRL	triglyceride-rich lipoprotein
UCP1	uncoupling protein 1
UCP1ko	UCP1 knockout
VLDL	very-low-density lipoprotein

VLDLR	very-low-density lipoprotein receptor
WAT	white adipose tissue
WTD	western-type diet

Part A: Summary

Brown adipose tissue (BAT) is responsible for maintaining core body temperature via a process called non-shivering thermogenesis (NST). Upon cold-exposure, the peripheral sympathetic nervous system is activated, leading to the release of norepinephrine (NE) at the terminal nerve ends in BAT. Subsequently, NE binds to β 3-adrenergic receptors of brown adipocytes triggering an internal signaling cascade, which ultimately leads to lipolysis of triglycerides stored in intracellular lipid droplets. The liberated fatty acids (FAs) are then imported into the mitochondria for β -oxidation to generate a proton gradient at the inner mitochondrial membrane. However, instead of producing ATP, brown adipocytes contain a protein called uncoupling protein 1 (UCP1), which uncouples the proton gradient to produce heat.

Besides using intracellular lipid stores, BAT when activated, takes up increased amounts of lipids and glucose from the circulation. Glucose is taken up by glucose transporter 1 (GLUT1) and 4 (GLUT4) and stored as lipids via a process called *de novo* lipogenesis (DNL). On the other hand, lipids from triglyceride-rich lipoproteins (TRLs) are taken up by BAT to replenish the depleted energy stores of activated BAT. These TRLs are very-low-density lipoproteins (VLDLs) and chylomicrons that are produced in a fasted state by the liver and by the gut in a fed state, respectively. These TRLs are then marginalized by lipoprotein lipase (LPL) which is anchored to glycosylphosphatidylinositol-anchored high density lipoprotein binding protein 1 (GPIHBP1) on the luminal side of endothelial cells. LPL hydrolyzes the triglycerides (TGs) and liberated free FAs (FFAs) are taken up by endothelial cells via the fatty acid transporter 1 (FATP1) and by the scavenger receptor cluster of differentiation 36 (CD36). In addition to FFAs, endothelial CD36 can also mediate endocytosis of entire TRL remnants that follow an intracellular endolysosomal route. After endothelial transcytosis, FFAs are taken up by brown adipocytes probably again via FATP1 and CD36. Cold exposure and subsequent sympathetic stimulation also activates lipolysis in white adipose tissue (WAT). In contrast to BAT, lipolysis resulted in the release of FFAs into the circulation that can be taken up by BAT. It was shown that inhibiting lipolysis in WAT impaired thermogenic capacity of BAT, while inhibiting lipolysis in BAT did not, underlining the importance of exogenous lipids for BAT function. Lastly, it was also shown that acyl carnitines derived from the liver can be used as a fuel for BAT thermogenesis.

Taken together, in order for BAT to function properly, lipid uptake via lipid receptors in BAT is essential for efficient thermogenesis. In line, the full-body knockout of CD36 (CD36ko) resulted in decreased uptake of lipids into different BAT depots and impaired thermogenic function.

Since CD36 is expressed in many cell-types but highly expressed in brown adipocytes and endothelial cells, we aimed to elucidate the cell-type specific roles of CD36 in adaptive thermogenesis and lipid uptake. Moreover, lipid uptake in BAT is not fully ablated in CD36ko mice. Another member of the class B scavenger receptor family is scavenger receptor B1 (SR-B1). SR-B1 is mainly known for its role in reverse cholesterol metabolism where hepatic SR-B1 mediates the selective uptake of cholesteryl esters (CE) from HDL particles. In the context of atherosclerosis, it was demonstrated that endothelial SR-B1 can mediate transcytosis of LDL particles. Notably, we detected that SR-B1 is highly expressed in endothelial cells of murine BAT as well as WAT depots in mice and in humans. Based on these data, we aimed to investigate the role of SR-B1 expressed by endothelial cells in adaptive thermogenesis and lipid uptake.

The importance for CD36 in brown adipocytes was evident when mice lacking CD36 specifically in brown adipocytes (BAd-CD36ko) were cold exposed, as under these conditions they were unable to maintain their core body temperature in the fasted state. In line with the impaired BAT function, BAd-CD36ko mice had decreased uptake of lipids into BAT compared to control littermates. Gene expression analysis did not show a compensational mechanism regarding thermogenic marker expression or receptor expression. WAT of BAd-CD36ko mice showed decreased expression of thermogenic marker expression. In line with the decreased lipid uptake, the increase in lipid handling gene expression was blunted in cold-exposed BAd-CD36ko mice.

Conversely, mice with an endothelial-specific CD36 knockout (EC-CD36ko) were able to maintain their core body temperature regardless of the nutritional status. Moreover, in BAT lipid uptake was not altered in EC-CD36ko mice and thermogenic marker, receptor and lipid handling gene expression was not affected. On the other hand, EC-CD36ko mice had decreased expression of thermogenic markers in WAT. Interestingly, EC-CD36ko mice had higher levels of non-esterified FA (NEFAs) and lower glucose levels in blood, which were not observed in BAd-CD36ko mice. Hearts of EC-CD36ko mice did show higher uptake of glucose that could explain the lower blood glucose levels.

Similar to EC-CD36ko mice, endothelial-specific SR-B1 knockout (EC-SR-B1ko) mice were able to maintain their core body temperature regardless of diet. Moreover, lipid and glucose uptake was unaltered in EC-SR-B1ko mice. Moreover, the expression of thermogenic markers and lipid receptors was not affected. Interestingly, endothelial SR-B1 expression contributed majorly to whole organ level SR-B1 expression of not only BAT, but also WAT, quadriceps and heart. Surprisingly, when performing a HDL turnover study, we found that EC-SR-B1ko mice had decreased uptake of CE in BAT, heart and lungs. Future studies will have to elucidate the importance of CE uptake in BAT endothelial cells mediated by SR-B1.

Overall, we show that the importance of CD36 for adaptive thermogenesis and lipid uptake is dependent on its expression by thermogenic adipocytes but not endothelial cells. Lastly, endothelial SR-B1 is dispensable for thermogenesis and lipid uptake in BAT but mediates CE uptake in BAT.

Part B: Zusammenfassung

Braunes Fettgewebe (BAT) ist für die Aufrechterhaltung der Körperkerntemperatur über einen Prozess verantwortlich, der als Non-Shivering Thermogenesis (NST) bezeichnet wird. Bei Kälteeinwirkung wird das periphere sympathische Nervensystem aktiviert, was zur Freisetzung von Noradrenalin (NA) an den terminalen Nervenenden im BAT führt. Anschließend bindet NA an β 3-adrenerge Rezeptoren der braunen Adipozyten, was eine interne Signalkaskade auslöst, die letztlich zur Lipolyse der in intrazellulären Lipidtröpfchen gespeicherten Triglyceride führt. Die freigesetzten Fettsäuren (FS) werden dann zur β -Oxidation in die Mitochondrien importiert, um einen Protonengradienten an der inneren Mitochondrienmembran zu erzeugen. Anstatt jedoch ATP zu produzieren, enthalten braune Adipozyten ein Protein namens Uncoupling Protein 1 (UCP1), das den Protonengradienten entkoppelt, um Wärme zu erzeugen.

Neben der Nutzung intrazellulärer Lipidspeicher nimmt die aktivierte BAT auch erhöhte Mengen an Lipiden und Glukose aus dem Blutkreislauf auf. Glukose wird von den Glukosetransportern 1 (GLUT1) und 4 (GLUT4) aufgenommen und über einen Prozess namens De-novo-Lipogenese (DNL) als Lipide gespeichert. Andererseits werden Lipide aus triglyceridreichen Lipoproteinen (TRLs) von der BAT aufgenommen, um die erschöpften Energiespeicher der aktivierten BAT wieder aufzufüllen. Diese TRLs sind very-low-density Lipoproteine (VLDLs) und Chylomikronen, die im nüchternen Zustand von der Leber und im gefütterten Zustand vom Darm produziert werden. Diese TRLs werden dann durch Lipoproteinlipase (LPL) marginalisiert, die an Glycosylphosphatidylinositol-verankertes High-Density-Lipoprotein-Bindungsprotein 1 (GPIHBP1) auf der luminalen Seite von Endothelzellen verankert ist. LPL hydrolysiert die Triglyceride (TG) und die freigesetzten freien FS (FFS) werden von Endothelzellen über den Fettsäuretransporter 1 (FATP1) und den Scavenger-Rezeptor-Cluster-Differenzierung 36 (CD36) aufgenommen. Zusätzlich zu den FFS kann der endotheliale CD36 auch die Endozytose ganzer TRL-Reste vermitteln, die einem intrazellulären endolysosomalen Weg folgen. Nach der endothelialen Transzytose werden FS von braunen Adipozyten aufgenommen, wahrscheinlich wieder über FATP1 und CD36. Kälteexposition und anschließende sympathische Stimulation aktivieren auch die Lipolyse im weißen Fettgewebe (WAT). Im Gegensatz zur BAT führte die Lipolyse zur Freisetzung von Fettsäuren in den Blutkreislauf, die von der BAT aufgenommen werden können. Es wurde nachgewiesen, dass die Hemmung der Lipolyse in WAT die thermogene Kapazität von BAT beeinträchtigt, während die Hemmung der Lipolyse in BAT dies nicht tat, was die Bedeutung exogener Lipide für die BAT-Funktion unterstreicht.

Schließlich wurde auch nachgewiesen, dass aus der Leber stammende Acylcarnitine als Brennstoff für die BAT-Thermogenese verwendet werden können.

Zusammenfassend lässt sich sagen, dass die Lipidaufnahme über Lipidrezeptoren in BAT für eine effiziente Thermogenese unerlässlich ist, damit die BAT richtig funktioniert. Dementsprechend führte die vollständige Ausschaltung von CD36 (CD36ko) im gesamten Körper zu einer verminderten Aufnahme von Lipiden in verschiedene BAT-Depots und zu einer beeinträchtigten thermogenen Funktion. Da CD36 in vielen Zelltypen exprimiert wird, jedoch in braunen Adipozyten und Endothelzellen stark exprimiert wird, wollten wir die zelltypspezifischen Rollen von CD36 bei der adaptiven Thermogenese und der Lipidaufnahme aufklären. Darüber hinaus ist die Lipidaufnahme in BAT bei CD36ko-Mäusen nicht vollständig unterbunden. Ein weiteres Mitglied der Klasse-B-Scavenger-Rezeptorfamilie ist der Scavenger-Rezeptor B1 (SR-B1). SR-B1 ist vor allem für seine Rolle im reversen Cholesterinstoffwechsel bekannt, bei dem hepatisches SR-B1 die selektive Aufnahme von Cholesterylesteren (CE) aus HDL-Partikeln vermittelt. Im Zusammenhang mit Atherosklerose wurde nachgewiesen, dass endotheliales SR-B1 die Transzytose von LDL-Partikeln vermitteln kann. Insbesondere haben wir festgestellt, dass SR-B1 in Endothelzellen von BAT- und WAT-Depots bei Mäusen und Menschen stark exprimiert wird. Auf der Grundlage dieser Daten wollten wir die Rolle von SR-B1, das von Endothelzellen exprimiert wird, bei der adaptiven Thermogenese und der Lipidaufnahme untersuchen.

Die Bedeutung von CD36 in braunen Adipozyten wurde offensichtlich, als Mäuse, denen CD36 spezifisch in braunen Adipozyten fehlte (BAd-CD36ko), Kälte ausgesetzt wurden, da sie unter diesen Bedingungen nicht in der Lage waren, ihre Körperkerntemperatur im nüchternen Zustand aufrechtzuerhalten. Im Einklang mit der beeinträchtigten BAT-Funktion hatten BAd-CD36ko-Mäuse im Vergleich zu Kontrollgeschwistern eine verringerte Aufnahme von Lipiden in die BAT. Die Genexpressionsanalyse zeigte keinen Kompensationsmechanismus hinsichtlich der Expression thermogener Marker oder Rezeptoren. Das WAT von BAd-CD36ko-Mäusen zeigte eine verminderte Expression thermogener Marker. Im Einklang mit der verminderten Lipidaufnahme war die Zunahme der Genexpression im Zusammenhang mit dem Lipidstoffwechsel bei BAd-CD36ko-Mäusen, die Kälte ausgesetzt waren, gedämpft.

Im Gegensatz dazu konnten Mäuse mit endothelspezifischem CD36-Knockout (EC-CD36ko) ihre Körperkerntemperatur unabhängig vom Ernährungszustand aufrechterhalten. Darüber hinaus war die BAT-Lipidaufnahme bei EC-CD36ko-Mäusen nicht verändert und die Expression von thermogenen Markern, Rezeptoren und Lipid-Handling-Genen war nicht beeinträchtigt. Andererseits wiesen EC-CD36ko-Mäuse eine verminderte Expression von thermogenen Markern in WAT auf. Interessanterweise wiesen EC-CD36ko-Mäuse höhere Werte an nicht veresterten Fettsäuren (NEFS) und niedrigere Glukosewerte im Blut auf, was bei BAd-CD36ko-Mäusen nicht beobachtet wurde. Die Herzen von EC-CD36ko-Mäusen zeigten eine höhere Glukoseaufnahme, was die niedrigeren Blutglukosewerte erklären könnte. Ähnlich wie bei EC-CD36ko-Mäusen konnten endothelspezifische SR-B1-Knockout-Mäuse (EC-SR-B1ko) ihre Körperkerntemperatur unabhängig von der Ernährung aufrechterhalten. Darüber hinaus war die Lipid- und Glukoseaufnahme bei EC-SR-B1ko-Mäusen unverändert. Außerdem wurde die Expression von thermogenen Markern und Lipidrezeptoren nicht beeinflusst. Interessanterweise trug die endotheliale SR-B1-Expression wesentlich zur SR-B1-Expression auf Ganzorganebene bei, und zwar nicht nur in der BAT, sondern auch in der WAT, im Quadrizeps und im Herzen. Überraschenderweise stellten wir bei der Durchführung einer HDL-Umsatzstudie fest, dass EC-SR-B1ko-Mäuse eine verringerte Aufnahme von CE in BAT, Herz und Lunge aufwiesen. In zukünftigen Studien muss die Bedeutung der durch SR-B1 vermittelten CE-Aufnahme in BAT-Endothelzellen untersucht werden.

Insgesamt zeigen wir, dass die Bedeutung von CD36 für die adaptive Thermogenese und die Lipidaufnahme von seiner Expression durch thermogene Adipozyten, nicht aber durch Endothelzellen abhängt. Schließlich ist endotheliales SR-B1 für die Thermogenese und die Lipidaufnahme in der BAT nicht erforderlich, vermittelt aber die CE-Aufnahme in der BAT.

Part C: Introduction

Adipose tissues

Adipose tissue is a heterogeneous organ, found in multiple depots in the body. In general, adipose tissue can be divided into white adipose tissue (WAT) and brown adipose tissue (BAT).

In **Figure 1**, the different adipose tissue depots in humans are shown with the mouse counterparts. Large WAT depots are visceral and subcutaneous for WAT and the BAT depots are found in the in neck, supraclavicular, para aortic, paravertebral and suprarenal regions (Torres Irizarry *et al.*, 2022).

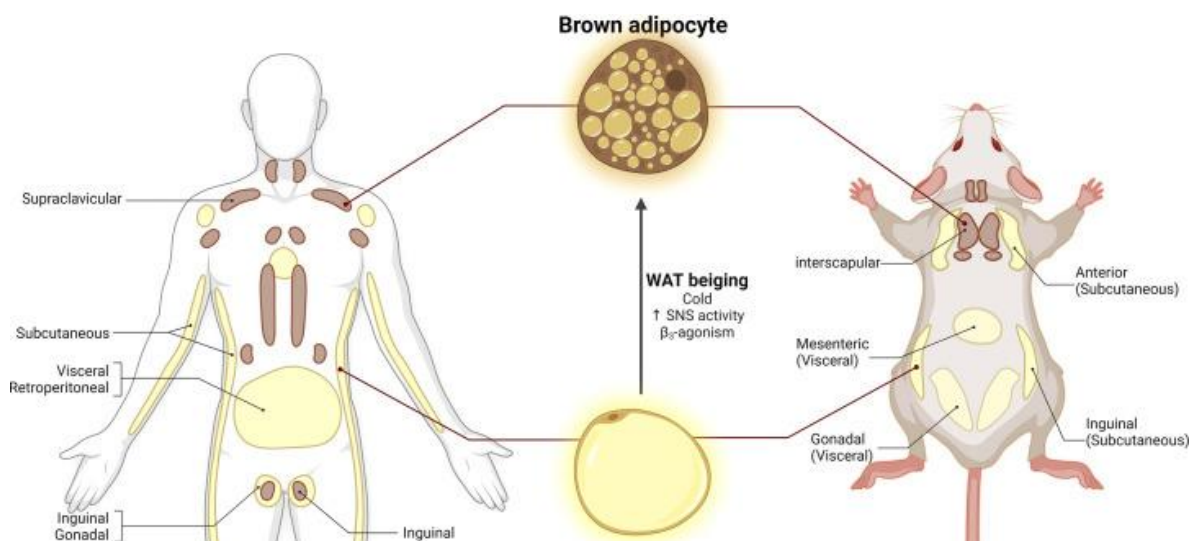


Figure 1. Location of different BAT and WAT depots in humans and mice. (Torres Irizarry *et al.*, 2022)

Adipose tissue is mainly comprised of adipocytes but also contains immune cells, endothelial cells, fibroblasts and pre-adipocytes (Luo and Liu, 2016). For the scope of this thesis, the focus will mainly be on adipocytes and endothelial cells.

White vs brown adipocytes

There are some differences between adipocytes derived from BAT or WAT. White adipocytes are derived from platelet-derived growth factor receptor alpha (*Pdgfra*) expressing (*Pdgfra*⁺) mesodermal stem cells and differentiate into white adipocytes through the activation of peroxisome proliferator-activated receptor γ (PPAR γ) (Rosen *et al.*, 1999) (**Figure 2**). On the other hand, brown adipocytes are derived from a myogenic factor 5 (*Myf5*) expressing (*Myf5*⁺) precursor, just like smooth muscle cells. The adipogenic transcription factor PR domain containing 16 (PRDM16) activates PPAR γ which induces the differentiation into brown adipocytes (Seale *et al.*, 2008) (**Figure 2**).

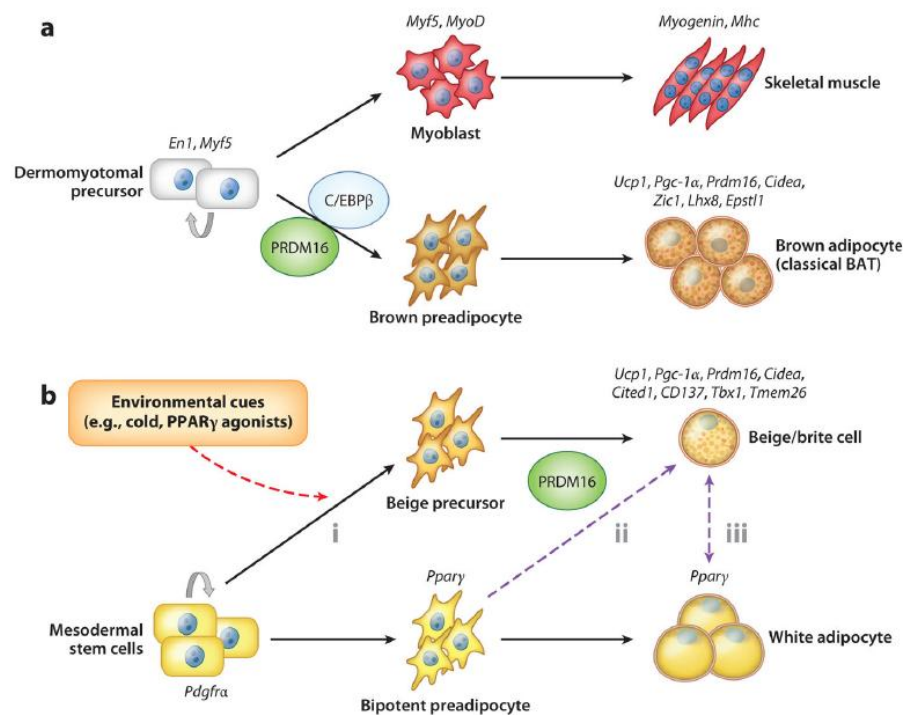


Figure 2. Cell origin and differentiation of skeletal muscle, brown, beige and white adipocytes. (Kajimura & Saito, 2014)

- Skeletal muscle and brown adipocytes stem from the same *Myf5*⁺ expressing precursor and brown adipocytes are differentiated into brown adipocytes with the help of PRDM16.
- White and beige adipocytes stem from *Pdgfra*⁺ expressing mesodermal stem cells. PPAR γ induces differentiation to white adipocytes, while PRDM16 can induce differentiation to beige adipocytes.

As shown in **Figure 3**, white adipocytes consist of one unilocular lipid droplet, while brown adipocytes have multilocular lipid droplets and numerous mitochondria which express uncoupling protein 1 (UCP1) (Luo and Liu, 2016; An, Cho and Yoon, 2023). Corresponding with their respective functions as white adipocytes main function is energy storage and brown adipocytes are metabolically active and are responsible for non-shivering thermogenesis (NST) (Cannon and Nedergaard, 2004; Luo and Liu, 2016).




	White adipocyte	Brown adipocyte	Beige adipocyte
			
Mitochondria abundance	Low	High	High
Lipid droplet	Large unilocular	Small multilocular	Small multilocular
UCP1	-	+	+ (Some -)
Function	Energy storage / Lipogenesis Lipolysis Glucose uptake Adipokine secretion	Thermogenesis Lipid clearance Glucose uptake / catabolism Biotokine secretion	Thermogenesis Glucose uptake / catabolism

Figure 3. Overview of characteristics of white, brown and beige adipocytes. (Adapted from: An et al. 2023)

A third type of adipocyte: beige

A third type of adipocyte is the beige or brown-in-white (brite) adipocytes. These beige adipocytes stem from the same precursor as white adipocytes and are found in WAT depots (Himms-Hagen *et al.*, 2000; Seale *et al.*, 2008; Petrovic *et al.*, 2010; Wu *et al.*, 2012). Upon cold exposure or treatment with PPAR γ -agonists, these adipocytes can differentiate to a more beige phenotype, which results in browning or beigeing of the WAT (**Figure 4**) (Barbatelli *et al.*, 2010; Petrovic *et al.*, 2010). Beige adipocytes also have multilocular lipid droplets, more mitochondria than a white adipocyte and express UCP1 which makes them metabolically active and contribute to NST (Wu *et al.*, 2012; Rosenwald *et al.*, 2013). Conversely, during a high-fat diet (HFD) or when no NST is needed during thermoneutrality, beige adipocytes can regain their white-adipocyte-like phenotype, called 'whitening' (**Figure 4**) (Rosenwald *et al.*, 2013).

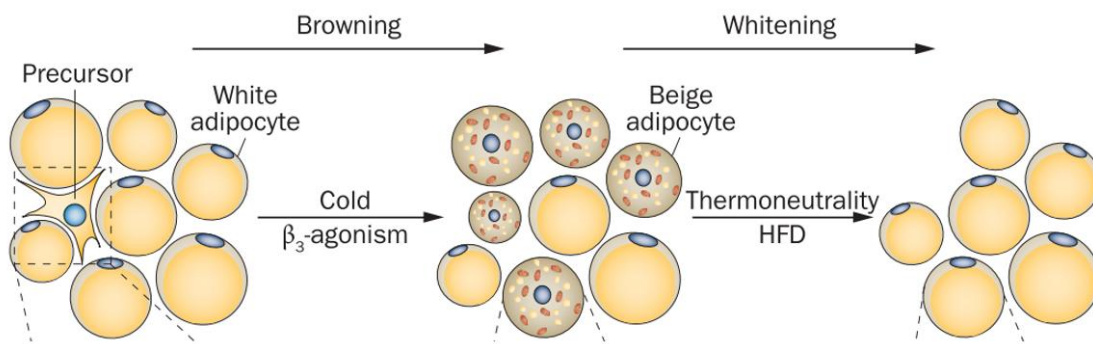


Figure 4. Browning and whitening of WAT. (Adapted from: Bartelt & Heeren, 2014)

Endothelial cells in adipose tissues

Endothelial cells form the lining of blood vessels and are therefore important for nutrient delivery, oxygen supply to organs and waste removal from organs. Endothelial cells show differences based on location (arteries, capillaries, veins, lymphatics) but even within the same vascular bed, endothelial cells show tissue-specific traits (Kalucka *et al.*, 2020). For example, in the liver the endothelium is discontinuous, meaning that there are gaps between the endothelial cells, therefore facilitating uptake of large particles from the blood without the need for transporters. While in adipose tissue, the endothelium is continuous, meaning that in order for proteins and nutrients to reach the adipocytes, they need receptors and transporters to get across the endothelium (Urbanczyk, Zbinden and Schenke-Layland, 2022).

BAT and to a lesser extent WAT are highly innervated. Different subpopulations within the endothelial cells of adipose tissue were reported in human WAT (Festa, AlZaim and Kalucka, 2023). Two interesting subpopulations are the pro-angiogenic and free fatty acid (FFA)-processing endothelial cells. Pro-angiogenic adipose tissue endothelial cell progenitors have high expression of *PRDM16* and ADP ribosylation factor-like GTPase 15 (*ARL15*) (Festa, AlZaim and Kalucka, 2023). Interestingly, these progenitors seem to be able to give rise to new brown and white adipocytes (Min *et al.*, 2016; Park *et al.*, 2022). On the other hand, the FFA-processing endothelial cells express high levels of lipid handling genes like cluster of differentiation 36 (*CD36*) and fatty acid binding protein 4 (*FABP4*) (Vijay *et al.*, 2020; Whytock *et al.*, 2022).

The importance of endothelial cells for adipose tissue health and function is evident in the case of obesity. Due to the expansion of the WAT and innervation not expanding at the same rate, hypoxic areas in the WAT emerge, which in turn attracts immune cells and causes inflammation (Elias *et al.*, 2012). Conversely, studies showed that promoting endothelial proliferation enhances thermogenesis in BAT, browning of WAT and protect against hypoxia in hypertrophic WAT under conditions of obesity (Elias *et al.*, 2012; Seki *et al.*, 2016, 2018).

WAT is the main organ for energy storage

As WAT is the main organ for energy storage, in a fed state, the WAT stores the dietary-derived lipids and converts glucose via *de novo* lipogenesis (DNL) into lipids. While upon fasting or high energy demand, white adipocytes initiate lipolysis and release FFAs back in the bloodstream (**Figure 5**) (Luo and Liu, 2016; Braun *et al.*, 2018). WAT is of particular interest as large amounts of WAT as seen with obesity, increase the risk of type 2 diabetes and cardiovascular diseases (Lee, Lee and Oh, 2019; Polkinghorne, West and Antoniadou, 2024).

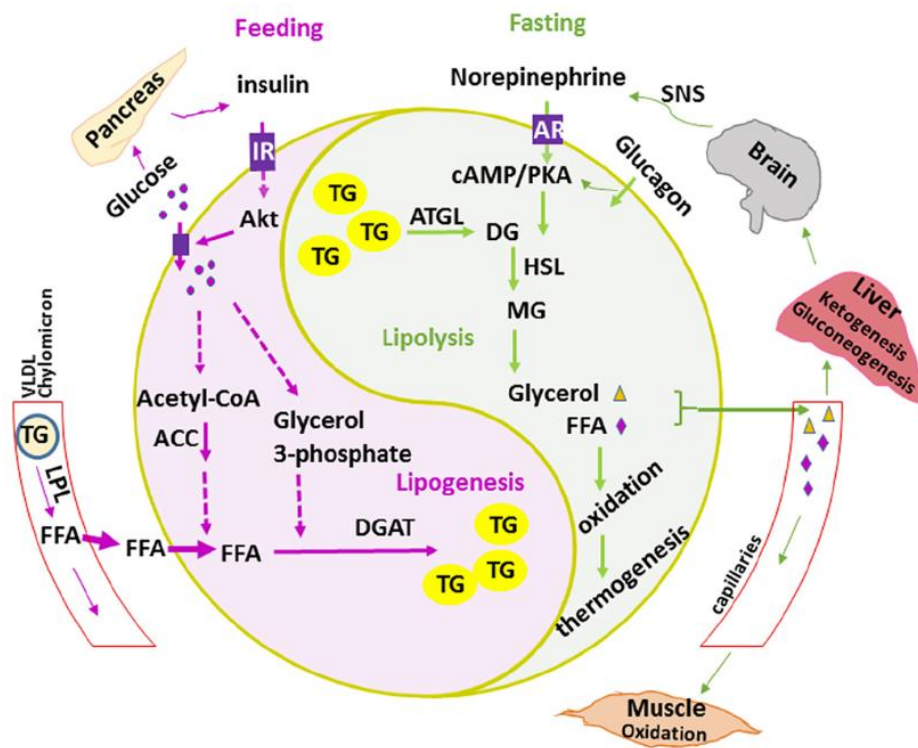


Figure 5. White adipocytes during feeding and fasting. (Luo and Liu, 2016)

During feeding white adipocytes take up liberated FFA by lipoprotein lipase (LPL) from very-low-density lipoprotein (VLDL) particles and chylomicrons and store them as triglycerides (TGs). Simultaneously, white adipocytes take up glucose and store them as TGs via DNL. Upon fasting or adrenergic stimuli, lipolysis of TGs is initiated and the FFAs and glycerol are released in the circulation for energy-demanding tissues and the liver.

BAT and NST

BAT is only found in mammals and the main function of BAT is maintaining core body temperature through the process of NST (Cannon and Nedergaard, 2004). As shown in **Figure 6**, upon cold-exposure the nervous system gets activated and releases norepinephrine (NE) that binds to β 3-adrenergic receptors (in rodents, β 2 in humans (Blondin *et al.*, 2020)). This triggers activation of protein kinase A (PKA) through cyclic adenosine monophosphate (cAMP)-dependent internal signaling cascades. Activated PKA phosphorylates cAMP response element-binding protein (CREB) which in turn results in enhanced transcription of thermogenic genes like *Ucp1* and *Pgc1a* (Cannon and Nedergaard, 2004).

Moreover, PKA enhances the activity of the lipolytic enzymes adipose triglyceride lipase (ATGL), hormone sensitive lipase (HSL) and monoglyceride lipase (MGL) (Cannon and Nedergaard, 2004; Pagnon *et al.*, 2012; Zechner, Madeo and Kratky, 2017). These enzymes are located at the lipid droplets and break down the stored TGs into FFAs (Cannon and Nedergaard, 2004). The FFAs can then be imported into the mitochondria to be used for β -oxidation and to allosterically activate UCP1 (Fedorenko, Lishko and Kirichok, 2012). UCP1 is located at the inner mitochondrial membrane of mitochondria and uncouples the proton gradient, which instead of generating ATP, allows for the generation of heat (Fedorenko, Lishko and Kirichok, 2012).

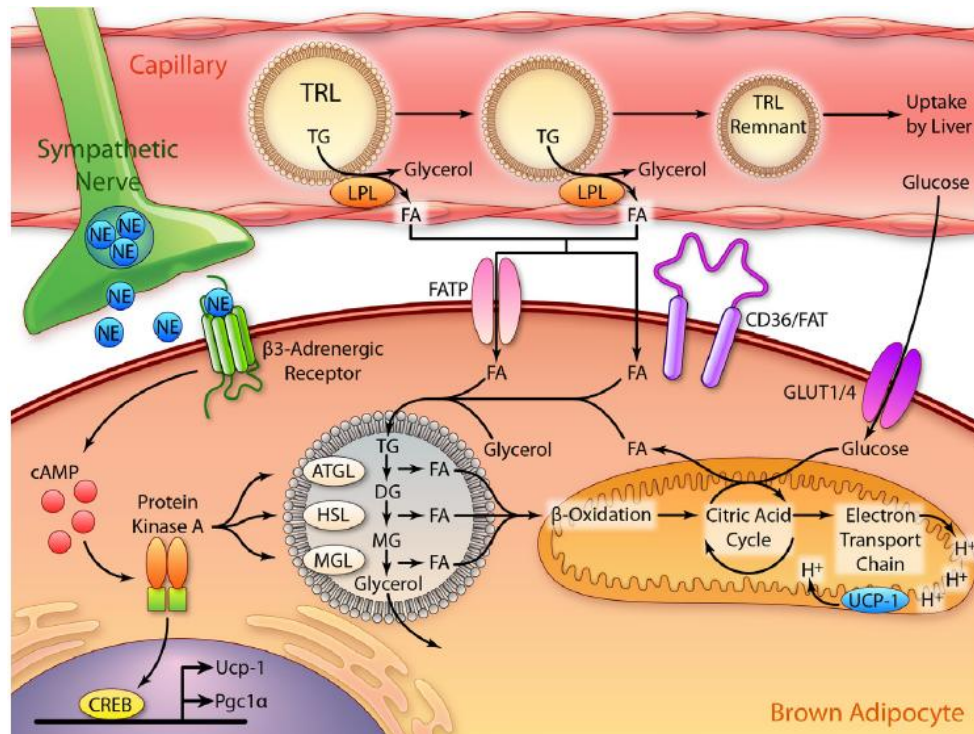


Figure 6. Signalling cascade upon adrenergic stimulation of BAT. (Hoeke et al., 2016)

Upon adrenergic stimulation of BAT, NE binds to the β 3-adrenergic receptor. This triggers activation of PKA through cAMP-dependent internal signaling cascades. Activated PKA phosphorylates CREB which in turn results in enhanced transcription of thermogenic genes. PKA enhances lipolysis by activating lipolytic enzymes. Subsequently the FFAs are imported in the mitochondria and heat is generated by UCP1 uncoupling the electron transport chain. Glucose and exogenous FFAs liberated by LPL from triglyceride-rich lipoproteins (TRLs) are imported via different transporters and stored as TGs.

Interestingly, when lipolysis in BAT was ablated by knocking out Atgl (Schreiber *et al.*, 2017) or the ATGL-activating protein comparative gene identification-58 (CGI-58, Abhd5) (Shin *et al.*, 2017) specifically in brown adipocytes, thermogenic capacity was not impaired. However mice that had a knockout of Atgl or Abhd5 in BAT and WAT were cold sensitive (Schreiber *et al.*, 2017; Shin *et al.*, 2017), thereby underlining the importance of exogenous lipids for BAT function.

Besides the liberated FFAs from WAT, a major source of extracellular lipids are TGs packaged in lipoproteins (Bartelt *et al.*, 2011; Dijk *et al.*, 2015; Heine *et al.*, 2018). Chylomicrons are produced by the gut in a fed state while VLDL particles are produced by the liver in a fasted state. Both contain a high concentration of TGs and are therefore also called triglyceride-rich lipoproteins (TRLs) (Feingold, 2022).

One thing that all the exogenous lipid have in common is that they have to cross the endothelial barrier before reaching the BAT. At the luminal site, lipoprotein lipase (LPL) that is bound to the endothelial protein glycosylphosphatidylinositol anchored high density lipoprotein binding protein 1 (GPIHBP1), hydrolyzes fatty acids (FAs) from the TRLs. These liberated FAs are then transported to the brown adipocytes via fatty acid transporter 1 (FATP1) or CD36 (Goldberg,

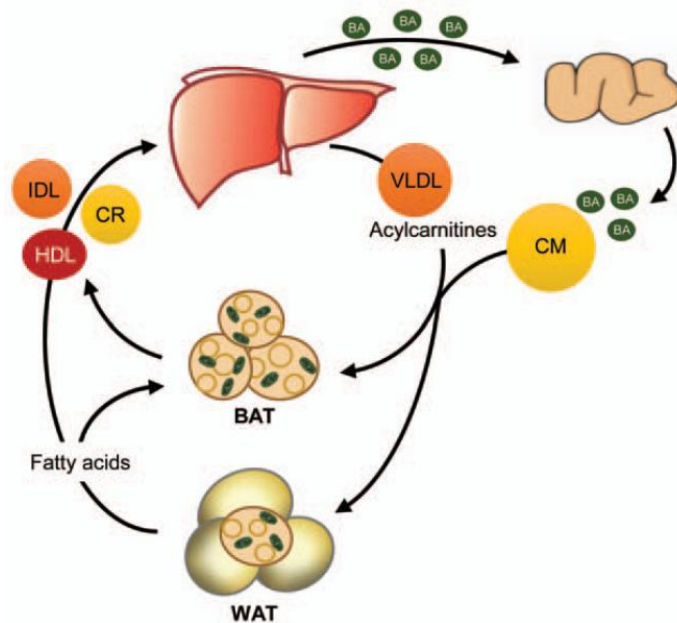


Figure 7. Lipoprotein metabolism during NST. (Heeren & Scheja, 2018)

TRLs are produced by the liver (VLDL) in a fasted state and chylomicrons by the gut in a fed state. VLDL and chylomicrons are able to deliver lipids to the BAT and WAT. Upon adrenergic stimulation or in a fasted state, WAT releases FFAs which can be taken up by the BAT. BAT can also take up liver-derived acyl carnitines as a fuel. Chylomicron remnants (CR), high-density lipoprotein (HDL) and intermediate-density lipoprotein (IDL) can then be transported back to the liver.

Eckel and Abumrad, 2009; Bartelt *et al.*, 2011; Lynes *et al.*, 2017). The FFAs can then be re-esterified and stored in the lipid droplets or imported in the mitochondria and used for heat generation.

The marginalized TRLs also called TRL-remnants can then be taken up by endothelial cells (Fischer *et al.*, 2021) or be taken up by the liver.

Another pathway to fuel BAT thermogenesis was described by Simcox and colleagues, where they found that acyl carnitines derived from the liver can also be used as fuel for thermogenesis (**Figure 7**) (Simcox *et al.*, 2017).

Besides lipids, BAT also takes up large amounts of glucose when activated (Labbé *et al.*, 2015). Glucose is taken up by glucose transporter 1 (GLUT1) or by glucose transporter 4 (GLUT4) in a fed state or when stimulated with NE (Dallner *et al.*, 2006). Glucose is then converted into TGs via DNL mediated by carbohydrate response element binding protein beta (CHREBP-b) and stored in the lipid droplets. Sanchez-Gurmanches and colleagues showed that when mice were exposed to mild cold (22°C) genes that are associated with DNL were highly upregulated in BAT (Sanchez-Gurmanches *et al.*, 2018).

Receptors

Efficient lipid uptake in BAT is essential to maintain the thermogenic function (Bartelt *et al.*, 2011). For efficient lipid uptake, receptors and transporters expressed on endothelial cells and brown adipocytes are indispensable (Abumrad *et al.*, 2021; Wade *et al.*, 2021). For example knockout of the VLDL receptor (VLDLR) which mediates uptake of VLDL particles, resulted in cold intolerance when mice were put into the cold (Shin *et al.*, 2022). Another example is the fatty acid transporter CD36, as full body knockout mice were not able to maintain their core body temperature when faced with a cold challenge (Bartelt *et al.*, 2011), underlining the importance of lipid receptors and transporters for BAT thermogenic function.

For the scope of this thesis I will focus on CD36 and scavenger receptor B1 (SR-B1) which belong to the same receptor family (Abumrad *et al.*, 2021) and focus on their roles in lipid uptake and thermogenesis.

CD36

CD36 is highly expressed in BAT, on brown adipocytes as well as endothelial cells and its expression is increased upon cold exposure (Fischer *et al.*, 2021). Besides endothelial cells and adipocytes, CD36 is also expressed in immune cells (Cifarelli *et al.*, 2017), heart (Koonen *et al.*, 2005), muscle (Bonen *et al.*, 2000), gut (Nassir *et al.*, 2007; Cifarelli *et al.*, 2017), liver (Zhao *et al.*, 2018), tongue (Laugerette *et al.*, 2005) and platelets (Asch *et al.*, 1987). Therefore CD36 is involved in different processes in the body related to immune and metabolic regulation (Silverstein and Febbraio, 2009).

Discovery

CD36 was identified as a long-chain fatty acid (LCFA) receptor in adipocytes by Abumrad and colleagues in 1993 (Abumrad *et al.*, 1993). Upon treating rat adipocytes with radioactively labeled Sulfo-N-succinimidyl oleate (SSO), long chain fatty acid uptake (oleate) was diminished by 75% and SSO bound to a 88 kDa plasma membrane protein (Harmon *et al.*, 1991; Harmon and Abumrad, 1993). This plasma membrane protein showed a high similarity with the already known protein CD36 expressed in human platelets, human and bovine endothelia as well as PAS IV from bovine and human endothelia (Harmon and Abumrad, 1993).

Structure

CD36 is predicted to have 2 membrane spanning domains creating a hairpin like structure with both the N- and C-terminal tails are palmitoylated and located on the cytoplasmic side (**Figure 8**) (Tao, Wagner and Lublin, 1996).

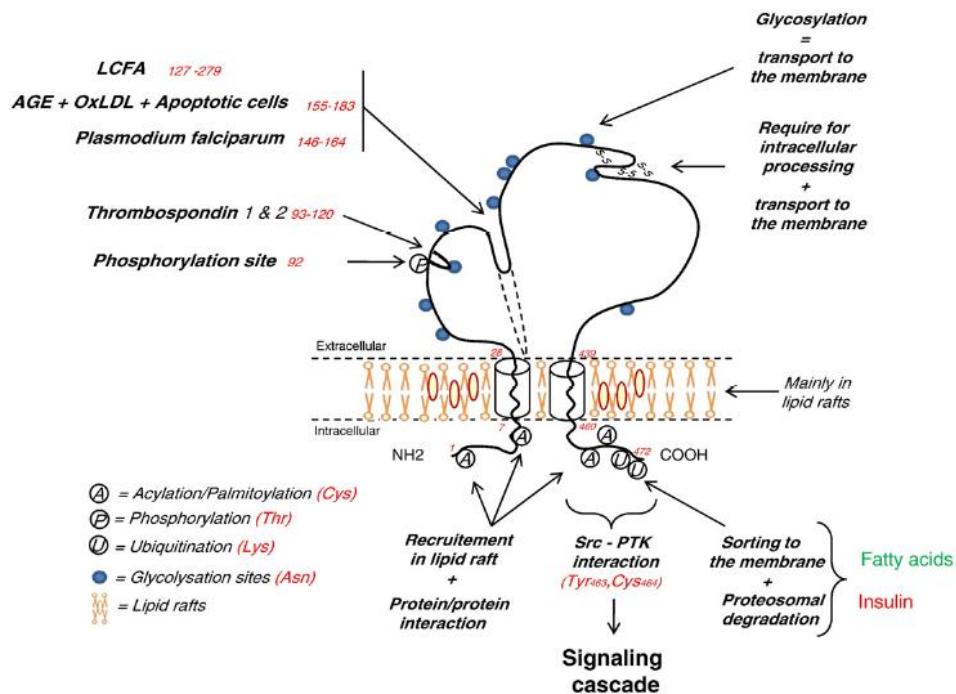


Figure 8. Schematic overview of structure of CD36. (Martin et al., 2011)

CD36 has two membrane spanning domains and N- and C-terminal tails are palmitoylated and located on the cytoplasmic side. CD36 has a cavity that spans the whole length of the protein and is proposed that FAs can be transported through the cavity. Other ligands that CD36 can bind such as advanced glycation endproducts (AGE), oxidized low-density lipoprotein (oxLDL), apoptotic cells, thrombospondin 1&2 and *plasmodium falciparum* are indicated in the figure.

protein and propose that lipids can attach to the receptor and travel to the membrane through the tunnel (Neculai *et al.*, 2013).

Post-translational modifications

CD36 is glycosylated and palmitoylated. Glycosylation is necessary for trafficking CD36 to the membrane (Hoosdally *et al.*, 2009). Inhibition of palmitoylation resulted in delayed processing at the endoplasmic reticulum (ER) and trafficking through the secretory pathway. Furthermore, the half-life of CD36 was reduced and more importantly, the palmitoylation-mutant of CD36 was not able to incorporate efficiently into the lipid rafts therefore impairing its function in FA uptake (Thorne *et al.*, 2010; Hao *et al.*, 2020).

Neculai and colleagues who determined the crystal structure of lysosomal integral membrane protein-2 (LIMP-2), another member of the scavenger receptor B family which CD36 belongs to, proposed how CD36 is able to transfer lipids to cells. They found that LIMP-2 had a large cavity that spans across the whole length of the

Regulation of CD36

CD36 is inhibited by SSO (Harmon *et al.*, 1991; Harmon and Abumrad, 1993; Coort *et al.*, 2002; Kuda *et al.*, 2013) and induced by peroxisome proliferator-activated receptor α (PPAR α) in liver and PPAR γ in adipose tissue (Motojima *et al.*, 1998; Teboul *et al.*, 2001). Furthermore, expression of CD36 is increased upon stimulation with LCFAs (Sfeir *et al.*, 1997).

Ligands of CD36

CD36 is known to act as a receptor for lipoproteins (VLDL, oxLDL, LDL, high-density lipoprotein (HDL)) (Endemann *et al.*, 1993; Calvo *et al.*, 1998; Kuniyasu, Hayashi and Nakayama, 2002; Zeng *et al.*, 2003; Hosomi *et al.*, 2023), coenzyme Q (CoQ) (Anderson *et al.*, 2015), thrombospondin (Asch *et al.*, 1987), anionic phospholipids (Rigotti, Acton and Krieger, 1995), *plasmodium falciparum* parasitized erythrocytes (Oquendo *et al.*, 1989; Baruch *et al.*, 1999), apoptotic cells (Ren *et al.*, 1995), micronutrients (Moussa *et al.*, 2011; Borel *et al.*, 2013), albumin (Raheel *et al.*, 2019) and LCFAs (Abumrad *et al.*, 1993; Baillie, Coburn and Abumrad, 1996).

Transport of fatty acids

Long there was a debate whether FAs needed transporters to be transported into the cells as the plasma membrane is a lipid bilayer. The theory that no transporters are needed is based on the observations that FA would be able to be transported through the membrane by a mechanism called 'flip-flop' where the polar carboxyl group of the fatty acid moves through the bilayer interior and re-positions at the opposite interface.

The theory that FA transport is protein-mediated is favored due to the fact that tissues can control the influx of FAs independently of the extracellular FA concentration. Meaning that the tissue is able to take up FAs when the extracellular concentrations are low or conversely limit FAs uptake when extracellular concentrations are high. Furthermore, when the fuel demands of the tissue change (suddenly), protein-mediated FAs uptake can be adjusted quickly. Lastly protein-mediated FA uptake may also select for specific fatty acid types (Reviewed in: Glatz, Luiken and Bonen, 2010).

The general consensus regarding FA uptake is that it follows the following steps (**Figure 9**):

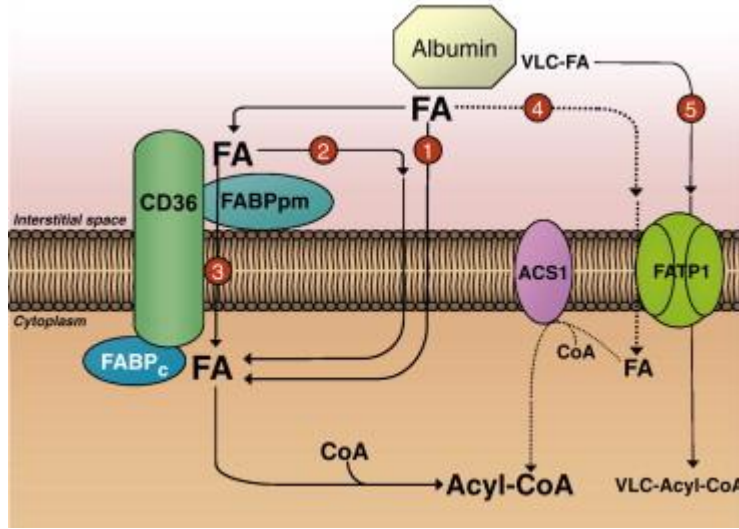


Figure 9. Schematic overview of FA uptake via CD36. (Schwenk et al., 2010)

FA are bound by FABPpm or CD36 and are helped to insert the FA into the outer leaflet of the lipid bilayer. Then via flip-flop mechanism the FA moves to the inner leaflet of the lipid bilayer and lastly, FA is bound by FABPc and processed intracellularly.

1. Adsorption step. After hydrolyzation, fatty acids are bound by CD36 or fatty acid binding protein plasma membrane (FABPpm) to stabilize the fatty acid and to help to insert the fatty acids into the outer leaflet of the lipid bilayer.

2. Translocation step. Subsequently, fatty acids move to the inner leaflet by the use of the flip-flop mechanism.

3. Desorption step. Lastly, the fatty acid moves to the aqueous phase and is bound by FABP cytoplasmic (FABPc) (Review in: Glatz and Luiken, 2017).

CD36 and its role in lipid uptake & thermogenesis

The role of CD36 in lipid uptake was confirmed by the mouse models where CD36 was ablated. Febbraio and colleagues were the first to generate a full-body CD36 knockout (CD36ko) mouse model. CD36ko mice have higher levels of plasma cholesterol, FFAs and TGs. Lower blood glucose levels after a prolonged (18h) fast and an increase in VLDL-associated TGs while low-density lipoprotein (LDL) particles were TG-poor. Oleate uptake was reduced in adipocytes of CD36null mice (Febbraio *et al.*, 1999). Moreover, CD36ko mice have reduced uptake of FAs in heart, muscle and adipose tissue (Coburn *et al.*, 2000). To compensate, heart and muscle took up more glucose in CD36ko mice and CD36ko mice cleared glucose faster than control littermates after an oral glucose tolerance test (OGTT) (Hajri *et al.*, 2002; Goudriaan *et al.*, 2003; McFarlan *et al.*, 2012).

Consistent with the mouse data, certain SNPs in the CD36 gene resulted in higher plasma TGs and FFA levels in humans (Ma *et al.*, 2004; Yamashita *et al.*, 2007; Masuda *et al.*, 2009; Shibao *et al.*, 2016).

When specifically focusing on BAT, CD36ko mice had a slower clearance of radioactively labelled ^3H -Triolein-TRLs (fatty acid label) and ^3H labeled oleate-bound-to-albumin (mimicking circulating FA in the bloodstream) in CD36ko mice compared to control littermates. This corresponded with decreased uptake of whole TRL particles and reduced uptake of radioactively labelled ^3H -Triolein-TRLs in different BAT depots (Bartelt *et al.*, 2011; Schlein *et al.*, 2016). When exposed to cold, the cold-induced uptake of whole particles and FAs was blunted in BAT of CD36ko mice (Fischer *et al.*, 2021). Similar effects were observed when CD36ko mice were treated with a β 3-adrenergic agonist CL316,243 (CL) (Heine *et al.*, 2018).

Impaired lipid uptake impairs the thermogenic capacity of BAT. For example, when CD36ko mice were cold-exposed for 24h, 60% of them died. When the cold-exposure time was reduced to 12h and the mice were fasted for the last 4h, CD36ko mice were shivering and had lower body temperatures compared to their control littermates (Bartelt *et al.*, 2011; Anderson *et al.*, 2015). The nutritional state is especially important, as CD36ko mice were able to keep their body temperature in the cold and at RT in a fed state, however upon fasting body temperature rapidly decreased after 1-2h (Putri *et al.*, 2015).

Since CD36 is expressed by many different cell-types, many different cell-specific knockout models are developed to unravel the cell-type specific CD36 contribution to lipid uptake. Interestingly, endothelial-specific CD36 knockout (EC-CD36ko) mice created using the Cre-lox system under the TEK Receptor Tyrosine Kinase (*Tie2*) promoter, recapitulated the CD36ko phenotype. EC-CD36ko mice had increased fasting plasma FFA levels and decreased plasma glucose levels. When given an olive oil gavage, plasma TG levels remained higher in EC-CD36ko mice while glucose was cleared faster than their control littermates after an OGTT. Furthermore, oleic acid clearance was delayed in EC-CD36ko mice and oleate uptake was 50% decreased in heart, quadriceps and BAT. Conversely, glucose uptake was increased in heart, muscle and WAT of EC-CD36ko mice. Similar results were found in another endothelial-specific CD36 knockout model (using the VE-Cadherin (*Cdh5*) promoter) (Son *et al.*, 2018). Moreover, male EC-CD36ko had lower levels of oxygen consumption and CO_2 production and lower energy expenditure (Rekhi *et al.*, 2021).

Daquinag and colleagues compared EC-CD36ko to an adipocyte-specific CD36ko (Ad-CD36ko) using the adiponectin (*Adipoq*) promoter, thereby knocking out CD36 in BAT and WAT. Both strains had increased levels of serum FFAs. After injection with fluorescently labeled BODIPY (lipid) both strains had decreased uptake of the BODIPY label in BAT and WAT (Daquinag *et al.*, 2021).

SR-B1

SR-B1 is together with LIMP-2 and CD36 part of the scavenger B class receptor family (Calvo and Vega, 1993; Acton *et al.*, 1994). It is highly expressed in many tissues and cell types, including intestine, adrenal gland, testis, ovaries, macrophages, endothelial cells, smooth muscle cells, keratinocytes, adipocytes and placenta (Shen, Azhar and Kraemer, 2018).

Discovery

Soon after it was discovered that the LDL receptor (LDLR) mediates the uptake of cholesterol in LDL particles via receptor-mediated endocytosis (Brown and Goldstein, 1986), a nonendocytic pathway of transferring cholesteryl esters (CEs) from HDL particles to cells was described (Pittman *et al.*, 1987). However, it was not till 1996 that Acton and colleagues showed that SR-B1 was responsible for the CE transfer and was coined the HDL receptor (Acton *et al.*, 1996). The role of SR-B1 in cholesterol metabolism was further underlined with the generation of the full-body knockout (SR-B1ko) mice. SR-B1ko mice had increased HDL size and total plasma cholesterol levels compared to control littermates. Furthermore, cholesterol stores in SR-B1ko mice were drastically reduced compared to control littermates (Rigotti, B. Trigatti, *et al.*, 1997). HDL particles were enlarged in SR-B1ko mice and plasma decay of radioactively labeled CE was decreased in SR-B1ko mice (Varban *et al.*, 1998). The importance of SR-B1 in the liver was underlined when a liver-specific SR-B1 mouse model was generated, which recapitulated the SR-B1ko elevated plasma total and free cholesterol (FC) levels and lipoprotein profile (Huby *et al.*, 2006). Conversely, when SR-B1 was overexpressed in mice livers it resulted in a reduction of plasma cholesterol levels (Kozarsky *et al.*, 1997; Wang *et al.*, 1998).

A lot of research has been done in regards to SR-B1 and the development of atherosclerosis. As liver-specific SR-B1ko mice or SR-B1ko mice fed a western-type diet (WTD) have increased risk of atherosclerosis (Trigatti *et al.*, 1999; Braun *et al.*, 2002; Van Eck *et al.*, 2003; Huby *et al.*, 2006). These effects can also be seen in humans, a SNP in the *SCARB1* gene results in increased HDL cholesterol and increased risk of coronary heart disease (Acton *et al.*, 1999; Roberts *et al.*, 2007; Manichaikul *et al.*, 2015; Zeng *et al.*, 2017). Interestingly, Vaisman and colleagues showed that overexpression of endothelial-expressed SR-B1 has atheroprotective effects when mice are fed a high-cholesterol diet (Vaisman *et al.*, 2015) while Huang and colleagues showed that an endothelial-specific knockout of SR-B1 had atheroprotective effects (Huang *et al.*, 2019).

Structure

SR-B1 is encoded by the gene *Scarb1* and has two splicing variants: SR-B1 and SR-B1.1 (Webb *et al.*, 1998). SR-B1 is highly abundant in tissues and is more efficient in taking up HDL-CE compared to SR-B1.1 (Webb *et al.*, 1998). SR-B1 has, just like the other members of the scavenger class B family, short cytoplasmic N- and C-terminals, two transmembrane domains and a large extracellular domain (Powers and Sahoo, 2022). Although the X-ray crystal structure of SR-B1 is not known yet, as discussed before, it is proposed that SR-B1 and CD36, just like LIMP-2 have a large cavity that spans across the whole length of the protein which is believed to facilitate the lipid transfer (Neculai *et al.*, 2013). Moreover, Chadwick and colleagues showed with nuclear magnetic resonance

(NMR) spectroscopy that a transmembrane domain of SR-B1 is located at the C-terminal. This leucine zipper dimerization motif is important for the ability to bind HDL and mediate CE transfer, upon disruption, this function is ablated (Chadwick *et al.*, 2017). Earlier it was already shown that the extracellular domain of SR-B1 is important for HDL binding, import of CE and cholesterol efflux and when hydrophobicity was decreased due to mutations in the extracellular domain, all these functions were impaired (Papale *et al.*, 2010). In order for SR-B1 to function it needs to form oligomers (Reaven *et al.*, 2004; Sahoo *et al.*, 2007). Disruption in the glycine dimerization motif Gly 15_Gly 18_Gly 25 in the N-terminal or C-terminal leucine zipper motif of SR-B1 also reduces the ability to transfer lipids from HDL to cells and receptor oligomerization (**Figure 10**) (Gaidukov *et al.*, 2011; Marques *et al.*, 2019).

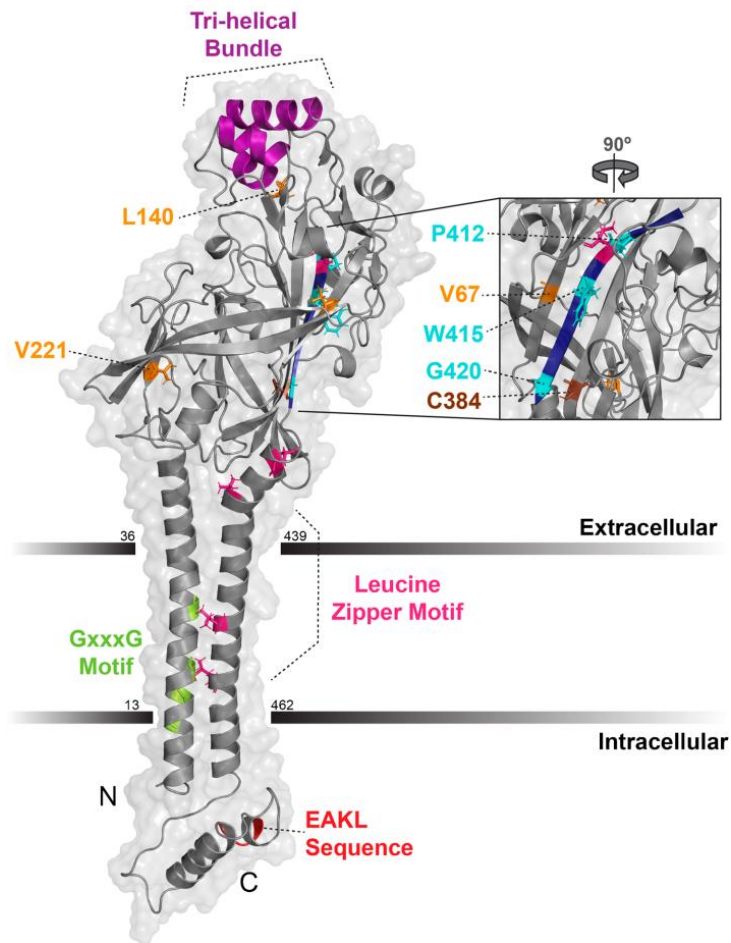


Figure 10. Schematic overview of structure of SR-B1. (Powers & Sahoo, 2022)

SR-B1 contains a leucine zipper dimerization motif at the C-terminal and a glycine dimerization motive at the N-terminal. It has two transmembrane domains and a large extracellular domain containing a tri-helical bundle.

Post-translational modifications

SR-B1 has a predicted molecular weight of 57 kDa, however SR-B1 is heavily N-glycosylated which results in an apparent molecular weight of 82 kDa (Acton *et al.*, 1994; Babitt *et al.*, 1997). Of the 11 N-linked glycosylation sites (in mice, 9 in humans), when disrupting Asn-108 and Asn-173 expression and function of SR-B1 was altered. Disruption of Asn-108 and Asn-173 resulted in decreased localization of SR-B1 at the plasma membrane and also reduced its ability to transfer lipids from HDL to the cells (Viñals *et al.*, 2003).

Regulation of SR-B1

The function and expression of SR-B1 is regulated by different factors. The adaptor protein PDZ Domain Containing 1 (PDZK1) regulates the expression and function of SR-B1 in liver and in moderate level in the proximal intestine, whereby PDZK1 knockout (PDZK1ko) had decreased SR-B1 expression in these organs. In endothelial cells, the interaction between SR-B1 and PDZK1 is needed for HDL activation of endothelial NO synthase and cell migration (Zhu *et al.*, 2008) but not needed for the transcytosis of HDL (Zhu *et al.*, 2008; Fung *et al.*, 2017). SR-B1 expression in the steroidogenic organs (adrenals, testis and ovaries) was not affected in PDZK1ko mice or by a knockdown of PDZK1 (Kocher *et al.*, 2003).

In steroidogenic organs expression of SR-B1 is regulated by Na⁺/H⁺ Exchanger Regulatory Factors (NHERFs), where NHERF1 and NHERF2 inhibit *de novo* synthesis of SR-B1. Thereby decreasing selective CE uptake and steroidogenesis (Hu *et al.*, 2013). Treating mice with adrenocorticotrophic hormone (ACTH) induced SR-B1 expression in adrenal gland while treatment with dexamethasone (which decreases ACTH levels) decreased SR-B1 expression (Rigotti *et al.*, 1996).

Besides PDZK1 and NHERFs, small-molecule inhibitor blocker of lipid transport 1 (BLT-1) is known as an irreversible inhibitor of SR-B1 (Yu *et al.*, 2011).

Ligands of SR-B1

SR-B1 binds acetylated LDL (AcLDL) and oxLDL (Acton *et al.*, 1994; Calvo *et al.*, 1997), anionic phospholipids (Rigotti, Acton and Krieger, 1995), ApoA-I, ApoA-II and ApoC-III (Xu *et al.*, 1997), VLDL, LDL and HDL (Calvo *et al.*, 1997).

Reverse cholesterol metabolism, cholesterol efflux, atherosclerosis, cold exposure

The main function of SR-B1 is its role in reverse cholesterol transport (RCT) in the liver and cholesterol efflux in the periphery. As cells in the periphery are unable to get rid of excess cholesterol internally, pre-nascent lipid-poor HDL particles are released into the circulation by the liver (Shen, Azhar and Kraemer, 2018). These lipid-poor HDL particles are then taking up FC from the cells or macrophages with the help of ATP-binding cassette A1 (ABCA1) while mature HDL particles take up FC via ATP-binding cassette G1 (ABCG1) (Phillips, 2014). Larger HDL particles bind more efficiently to SR-B1 and promote more cholesterol efflux compared to smaller HDL particles (Thuahnai *et al.*, 2004), however SR-B1 can also facilitate passive FC efflux independently of HDL (De La Llera-Moya *et al.*, 1999). The FC on the HDL particles are then esterified by the enzyme Lecitin:cholesterol acyltransferase (LCAT), thereby promoting maturation of HDL particles. The HDL particles are then transported back to the liver where SR-B1 extracts the CE, FC and TGs from the HDL particles without endocytosing HDL as opposed to the LDLR (Brown and Goldstein, 1986). The CEs are then broken down to FC and excreted or turned into bile acids (Shen, Azhar and Kraemer, 2018) (**Figure 11**).

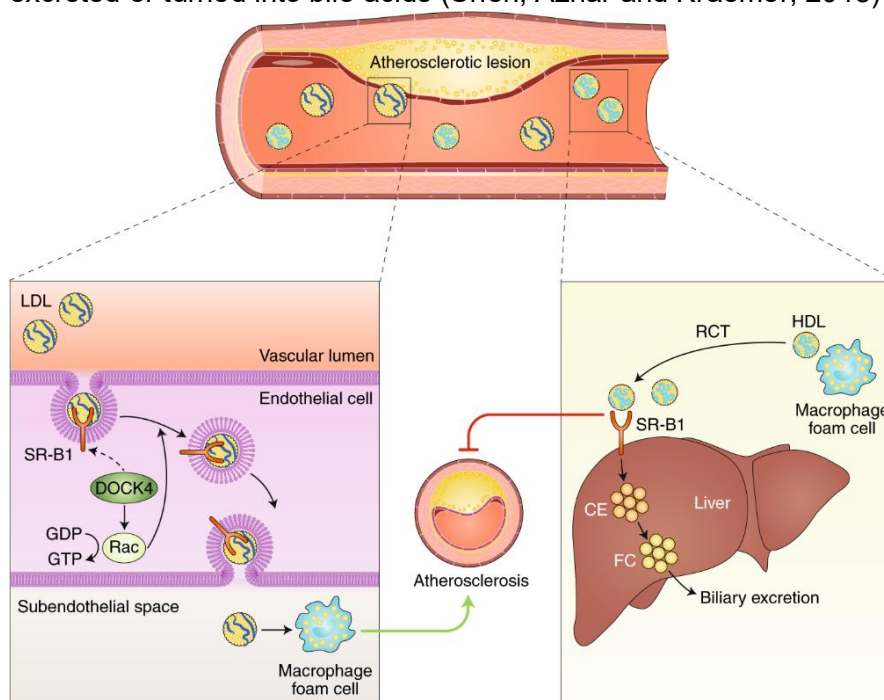


Figure 11. Role of SR-B1 in endothelial cells and RCT. (Zhang & Fernández-Hernando, 2019)

SR-B1 has a dual role in the development of atherosclerosis. During RCT, HDL particles take up excess cholesterol from the periphery and macrophage foam cells. Hepatic SR-B1 extracts the CEs from HDL which can then be excreted. This is thought to be anti-atherogenic. SR-B1 expressed by endothelial cells was shown to transcytosis LDL particles, which is thought to be pro-atherogenic.

The role of SR-B1 in RCT is thought to be atheroprotective. Endothelial SR-B1 is also responsible for transcytosis of HDL particles, therefore facilitating uptake of excess cholesterol by HDL particles (Rohrer *et al.*, 2009). However, besides the transcytosis of HDL, endothelial SR-B1 is also involved in LDL translocation, which is considered atherogenic (Armstrong *et al.*, 2015; Huang *et al.*, 2019).

There has been a lot of research in the context of atherosclerosis. Studying atherosclerosis development in mice was for a long time not directly translatable to humans as mice do not contain the cholesteryl ester transfer protein (CETP) which mediates exchange of CEs and lipids between chylomicrons, VLDL, LDL and HDL particles. Therefore, in mice HDL particles contain the majority of cholesterol. In order to properly study the development of atherosclerosis, APOE*3-Leiden.CETP mice were generated, which express the CETP protein (Westerterp *et al.*, 2006). This allowed to study the effect of cold exposure on HDL metabolism. BAT activation by CL decreased plasma cholesterol levels and promoted cholesterol-enriched remnants clearance by the liver in APOE*3-Leiden.CETP mice. Moreover, atherosclerosis development was also decreased upon BAT activation by CL (Berbeé *et al.*, 2015). Our group showed that pharmacological stimulation and cold exposure resulted in HDL remodeling in APOE*3-Leiden.CETP mice. Thereby, CL enhanced clearance of HDL particles via SR-B1 in the liver and enhanced RCT (Bartelt *et al.*, 2017). Besides, cold exposure also increases the conversion of cholesterol into bile acids, which results in changes in the microbiota, resulting in enhanced thermogenesis (Worthmann *et al.*, 2017).

Part D: Aims

Brown and beige adipocytes internalize large amounts of glucose and FAs from the circulation. Notably, up to 80% of the energy used for heat production is delivered by TRLs that are processed at the luminal site of the vascular endothelium. For efficient lipid uptake and thermogenesis, lipid and lipoprotein receptors and transporters expressed on endothelial cells and brown adipocytes are indispensable (Abumrad *et al.*, 2021; Wade *et al.*, 2021). This thesis will investigate the cell-type specific relevance of the two scavenger class B receptors CD36 and SR-B1.

CD36 facilitates LCFA uptake in cells (Coburn *et al.*, 2000) and the role for thermogenesis was evident when full-body CD36ko mice were unable to maintain their core body temperature when exposed to cold ambient temperatures (Bartelt *et al.*, 2011). Other groups have been making efforts to elucidate the cell-type specific role of CD36 in lipid uptake in endothelial cells (Son *et al.*, 2018; Daquinag *et al.*, 2021; Rekhi *et al.*, 2021; Dada *et al.*, 2024) and adipocytes (Daquinag *et al.*, 2021). However, the role of cell-type specific CD36 expression in endothelial cells and brown adipocytes in the context of adaptive thermogenesis is unclear. Therefore, the first aim of this thesis focuses on the role of CD36 expressed by brown adipocytes and by endothelial cells in adaptive thermogenesis and lipid handling.

SR-B1 is mainly known for its role in RCT in the liver and cholesterol efflux in the periphery (Shen, Azhar and Kraemer, 2018). Based on the observation that SR-B1 is highly expressed in the endothelial fraction of BAT and WAT in mice, in the second aim the hypothesis is tested whether SR-B1 expressed by endothelial cells plays a role in lipid handling and adaptive thermogenesis.

To address the hypotheses, metabolic tracer studies to quantify organ uptake of radiolabeled glucose and lipoprotein particles will be performed in endothelial- and adipose-specific mouse models fed a chow or an obesogenic HFD, which are housed at various ambient temperatures. The role of CD36 and SR-B1 in adaptive thermogenic responses will be investigated in cell-type specific knockouts by gene and protein expression analysis of thermogenic and metabolic markers in BAT and WAT. To measure energy expenditure and fuel selection at different ambient temperatures, indirect calorimetry will be performed. Overall, the results of these mechanistic studies will show whether CD36 expressed by brown adipocytes and endothelial CD36 and/or SR-B1 are important for the internalization of TRL particles, thermogenic adaptations, substrate utilization and energy expenditure mediated by BAT and/or WAT.

Part E: Material and methods

Animals

Mice with a specific endothelial deletion of SR-B1 and their control littermates were kindly gifted from the lab of Philip Shaul (Dallas, USA). Detailed description of the generation of the endothelial-specific knockout mice can be found in the paper of Huang (Huang *et al.*, 2019). In short, *Scarb1*^{fl/fl} mice have loxP sites inserted in intron 1 and intron 3 of the *Scarb1* gene. Heterozygous *Scarb1*^{fl/+} mice were crossed with *Cdh5*^{Cre+} mice to generate mice with an endothelial-specific knockout of SR-B1 (*Scarb1*^{fl/fl}-*Cdh5*^{Cre+}) and control littermates (*Scarb1*^{fl/fl}-*Cdh5*^{Cre-}).

Cd36^{fl/fl} mice with loxP sites flanking exon 3 and 4 of the *Cd36* gene were bought from Jackson laboratories. *Cd36*^{fl/fl} mice were crossed with mice with *Cre* under the *Cdh5* promoter (*Cdh5*^{Cre} mice) to create mice with an endothelial knockout of CD36 (*Cd36*^{fl/fl}-*Cdh5*^{Cre+}) and control littermates (*Cd36*^{fl/fl}-*Cdh5*^{Cre-}). To create a knockout of CD36 in brown adipocytes, *Cd36*^{fl/fl} mice were crossed with mice that express *Cre* under the *Ucp1* promoter (*Ucp1*^{Cre} mice) (*Cd36*^{fl/fl}-*Ucp1*^{Cre+}) and control littermates (*Cd36*^{fl/fl}-*Ucp1*^{Cre-}).

Mice were housed individually during the experiment with wood bedding in a light- and temperature-controlled facility with a 12h/12h dark regime. Mice were fed a standard laboratory chow diet *ad libitum* (19.10% protein, 4% fat, 6% fiber, from Altromin Spezialfutter GmbH&Co, Germany) or a HFD for 4 weeks (26.1% protein, 25.5% carbohydrates, 6.4% fiber, 34.8% fat, 6.4% mineral, 0.4% vitamins, 0.25% cholesterol from Research Diets, D14010701, USA) prior to the start of the experiment. At the end of the experiments, body weight was measured and blood glucose was determined using an Accu-Chek Aviva (Roche). Unless stated otherwise, mice were sacrificed by a lethal dosis of a mix of ketamine (180 mg/kg) and xylazin (24 mg/kg) in 0.9% NaCl. Blood samples were collected in syringes containing 0.5M EDTA by cardiac puncture and subsequently the animals were perfused with ice-cold PBS containing 10 U ml⁻¹ heparin. Harvested tissues were snap frozen in liquid nitrogen for quantitative PCR (qPCR) and western blot analysis and stored at -80°C for further analysis. Tissues used for immunofluorescence were kept in 3.7% formaldehyde solution. Animal studies were carried out in Hamburg and were approved by the Animal Welfare Officers at University Medical Center Hamburg-Eppendorf and the Behörde für Gesundheit und Verbraucherschutz Hamburg.

Interventions

Indirect calorimetry

A week before the start of the experiment, mice underwent surgery to transplant a transponder (STARR Life Sciences, USA) intraperitoneally. For metabolic studies, mice were put in metabolic cages (Sable Systems Europe GmbH, Germany) and the system was operated according to the manufactures guidelines. Mice were acclimated to the metabolic cages for 2 days at 22°C prior to recording. Change of temperature occurred at 7 am and the light phase was from 7 am – 7 pm. During the experiment consumption of O₂, production of CO₂, respiratory exchange ratio (RER), energy expenditure, food intake, water intake, body core temperature and activity were measured.

Cd36^{fl/fl}-Ucp1

Non fasting experiment

To test whether *Cd36^{fl/fl}-Ucp1^{Cre+}* mice were able to maintain their body temperature at different temperatures, 11-13 week old female *Cd36^{fl/fl}-Ucp1^{Cre+}* and *Cd36^{fl/fl}-Ucp1^{Cre-}* mice were put in metabolic cages. After acclimatization, temperature was kept for 2 days at 30 °C, then decreased to 22 °C for 2 days and the last 2 days were 6 °C. Mice were fasted for 2h before sacrifice.

Fasting experiment

To test whether *Cd36^{fl/fl}-Ucp1^{Cre+}* mice were able to maintain their body temperature at different temperatures while fasted, 15-17 week old female *Cd36^{fl/fl}-Ucp1^{Cre+}* and *Cd36^{fl/fl}-Ucp1^{Cre-}* mice were put in metabolic cages. After acclimatization, temperature was kept for 2 days at 30 °C, then decreased to 22 °C for 2 days and the last 2 days were 6 °C. On the day of the temperature change, mice were fasted from 6 am to 12 pm. Experiment was stopped when temperature of mice got critically low.

Cd36^{fl/fl}-Cdh5

To test whether *Cd36^{fl/fl}-Cdh5^{Cre+}* mice were able to maintain their body temperature at different temperatures while fasted, 13-19 week old female *Cd36^{fl/fl}-Cdh5^{Cre+}* and *Cd36^{fl/fl}-Cdh5^{Cre-}* mice were put in metabolic cages. After acclimatization, temperature was kept for 2 days at 30 °C, then decreased to 22 °C for 2 days and the last 2 days were 6 °C. Every day, mice were fasted from 6 am to 12 pm. After the 2 days of cold exposure, mice were fasted for 2h and received an oral fat gavage (see Oral fat tolerance test).

Scarb1^{fl/fl}-Cdh5

Basal measurement

To determine the metabolic parameters of *Scarb1^{fl/fl}-Cdh5^{Cre+}* and *Scarb1^{fl/fl}-Cdh5^{Cre-}* mice, at a basal level, fat mass, lean mass and water mass were measured using the EchoMRI machine (EchoMRI™, USA) of 17-18 week old male and female *Scarb1^{fl/fl}-Cdh5^{Cre+}* and *Scarb1^{fl/fl}-Cdh5^{Cre-}* mice. Afterwards they were kept in metabolic cages (Sable Systems Europe GmbH, Germany) for 5 days at 22°C.

Cold challenge

To test whether *Scarb1^{fl/fl}-Cdh5^{Cre+}* mice were able to maintain their body temperature at different temperatures, 13 week old male *Scarb1^{fl/fl}-Cdh5^{Cre+}* and *Scarb1^{fl/fl}-Cdh5^{Cre-}* mice were put in metabolic cages. After the acclimatization, the temperature was decreased from 30 °C to 6 °C by decreasing the temperature by 6 °C every day at 7 am. On the day of sacrifice, mice were fasted for 4 hours in the morning and received a CL (Tocris, 0.2 mg mL⁻¹ in 0.9 w/v % NaCl) subcutaneous injection (1 µg per g body weight) and were sacrificed by cervical dislocation for tissue collection 3 hours later.

Cold exposure

Half of the mice were kept at room temperature (RT, 22°C) and the other half was put into the cold (4°C) for 24 hours. Mice were fasted 4h in the morning before sacrifice. *Cd36^{fl/fl}-Cdh5* and *Cd36^{fl/fl}-Ucp1* mice were fasted only 2h due to risk of mice dying.

Postprandial uptake studies and organ distribution

Oral fat tolerance test (OFTT)

Cd36^{fl/fl}-Ucp1

To analyze lipid uptake and organ distribution at different temperatures, 13-16 week old female *Cd36^{fl/fl}-Ucp1^{Cre+}* and *Cd36^{fl/fl}-Ucp1^{Cre-}* mice were kept at RT and exposed to cold (4°C) for 24 hours. Mice were fasted 4h in the morning and 2h before sacrifice they received an oral gavage with radio-labelled ³H-Triolein and a tracer of ¹⁴C-Deoxyglucose (DOG).

Cd36^{fl/fl}-Cdh5

To analyze lipid uptake and organ distribution at different temperatures, 13-17 week old male *Cd36^{fl/fl}-Cdh5^{Cre+}* and *Cd36^{fl/fl}-Cdh5^{Cre-}* mice were kept at RT and exposed to cold (4°C) for 48h in metabolic cages. Mice were fasted 4h in the morning and 2h before sacrifice they received an oral gavage with radio-labelled ³H-Triolein and a tracer of ¹⁴C-DOG.

Oral glucose fat tolerance test (OGFT)

To analyze lipid and glucose uptake and organ distribution at different temperatures, 16-22 week old male *Scarb1^{fl/fl}-Cdh5^{Cre+}* and *Scarb1^{fl/fl}-Cdh5^{Cre-}* mice were kept at RT and exposed to cold (4°C) for 24 hours. Mice were fasted 4h in the morning and 2h before sacrifice they received an oral gavage with radio-labelled ³H-Triolein and ¹⁴C-DOG (2 g/kg).

Workflow and analysis

Organs were dissolved in Solvable™ (PerkinElmer, USA) (~0.1mL per 10 mg organ) in a 60°C shaker overnight. The next day, 400 µL of dissolved organ solution or 50 µL of plasma was mixed with 4 mL of scintillation fluid (Rotiszint® eco plus, Carl Roth) and radioactive particles were then counted using Liquid Scintillation Analyzer Tri-Carb® 2810 TR (PerkinElmer, USA).

For the analysis, counts per mg organ or µL plasma was calculated. For total organ uptake, counts per mg were multiplied with the total organ weight.

HDL turnover

As described in Bartelt *et al.* (2017), HDL was isolated from the blood of 4h fasted C57BL/6J WT mice by sequential ultracentrifugation ($d = 1.063\text{--}1.21\text{ g/ml}$) as described by Havel (Havel, Eder and Bragdon, 1955). HDL was then double-labelled with ^{125}I -tyramine cellobiose (^{125}I -TC) in the apolipoprotein moiety and with ^3H -cholesteryl oleoyl ether (CEt) in the lipoprotein core. Human plasma CETP was used to introduce ^3H -CEt into ^{125}I -TC-HDL by exchange from donor liposomal particles, containing ^3H -CEt. The final ^{125}I -TC-/ ^3H -CEt-HDL particles were dialyzed against PBS (pH 7.4, 4°C) with added 1 mM EDTA. In the following, ^{125}I -TC-/ ^3H -CEt-HDL (30 mg HDL protein per mouse; ca. 39 kBq ^{125}I -TC and 33 kBq ^3H -CEt, respectively) were injected into the tail vein of 4h fasted *Scarb1^{fl/fl}-Cdh5^{Cre+}* and *Scarb1^{fl/fl}-Cdh5^{Cre-}* mice for analysis of plasma decay and organ uptake of radiolabeled HDL. Blood samples were collected at: 10 min, 30 min; 2, 5, 9, 22 and 24h after injection. While plasma aliquots and tissues were directly assayed for ^{125}I radioactivity, ^3H -radioactivity was analyzed by scintillation counting after lipid extraction using the method of Dole (Dole, 1956).

Plasma fractional catabolic rates (plasma-FCRs) were determined for the two tracers per mouse. The uptake of the HDL-associated tracers were determined in the following organs: liver, kidney, heart, intestine, BAT and carcass. The fraction of total tracer uptake attributed to a specific organ was calculated as the radioactivity recovered in that organ divided by the total radioactivity recovered from all tissues and carcass.

Organ FCRs (organ-FCRs) were calculated to compare the rates of uptake of the apolipoprotein component and the CE moiety of HDL of the different organs. These rates are calculated as followed: (Organ-FCR in Tissue X) = (Plasma-FCR) \times (Fraction [%] of Total Body Tracer Recovery in Tissue X). This organ-FCR represents the fraction of the plasma pool of either HDL tracer cleared by an organ per hour. ^{125}I -TC represents the uptake of HDL holo-particles by tissues. Selective HDL CE uptake is calculated as the difference in organ-FCR between [^3H]CEt and ^{125}I -TC.

Genotyping

DNA isolation

Tail biopsies were lysed at 50°C for 1h or at 37°C overnight in a heat block at 700 rpm in a solution of 700 µL STE-Buffer and 10 µL Proteinase K. Afterwards 70 µL 10% SDS and 270 µL 5M NaCl were added and the samples centrifuged for 10 min at max g to let the protein fall out. 450 µL of the DNA-containing supernatant was transferred to a new Eppendorf tube with 900 µL 70% EtOH and thoroughly mixed. To pellet the DNA, samples were centrifuged at max g for at least 25 min. Then, the ethanol was removed and the DNA pellet dried for 1-2h at 45°C or 37°C overnight in a heat block at 700 rpm. Finally, the DNA pellet was dissolved in 50 µL aqua dest.

PCR

Genotyping was done for the following genes: CD36flox (*Cd36^{fl/fl}-Cdh5^{Cre}* and *Cd36^{fl/fl}-Ucp1^{Cre}* mice), SR-B1flox (*Scarb1^{fl/fl}-Cdh5^{Cre}* mice) and Cre in all mice.

CD36flox

Table 1. PCR reaction mix for CD36flox

Material	Amount (µL)
aqua dest.	19.4
10x PCR-Buffer GREEN	2.5
10 mM dNTP	1
10 µM PrimerMix	1
Taq-Polymerase (5U/µL)	0.1
DNA	1
Total	25

Table 2. PCR primer sequences of CD36flox from 5' to 3'

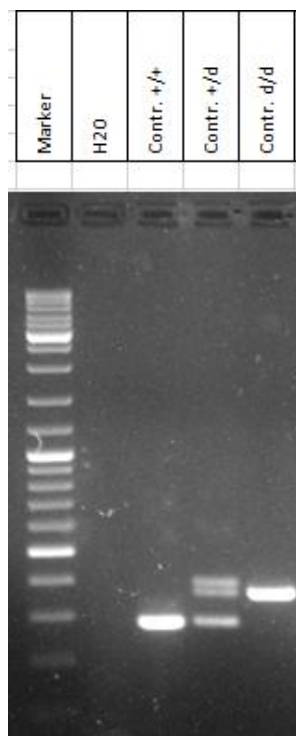
Primer	Sequence
CD36flox forward primer	CAT CTG TGT AGC GCT CTT GG
CD36flox reverse primer	TTG CTA CTA TGC ACT CCA TGC

A primer mix was made by diluting the stock solutions of the primers 1:10 and adding the primers in a proportion of 1:1. PCR tubes were briefly vortexed and spun down and then put in the thermocycler with the following program:

Table 3. PCR program CD36flox

Step	Temperature (°C)	Time
1	95	3 min
2	95	30s
3	57	30s
4	72	60s
	Repeat step 2-4 for 40 cycles	
5	72	5 min
6	4	oo

PCR products were then loaded on a 1.5% agarose gel (1.5g agarose/100mL TBE buffer, 5 µl Roti®-GelStain) and separated by electrophoresis for 1h at 120 mA. 8 µl of GeneRuler™ DNA Ladder Mix was used as marker. The bands were visualized under UV light with the GelStick Imager (INTAS, Germany) and images were analyzed in Excel.



The band corresponding with no CD36flox-alleles (+/+) was at 285 bp, the bands corresponding to one CD36flox-allele (+/d) were at 285 and 360 bp and two CD36flox-alleles (d/d) corresponded to a band at 360 bp (**Figure 12**). For experiments, only d/d mice were used.

Figure 12. Exemplary PCR results of the CD36flox PCR.

In addition to the marker, the gel picture shows the water control and the PCR products of no CD36flox-alleles (+/+), one CD36flox-allele (+/d) as well as two CD36flox-alleles (d/d).

SR-B1flox

Table 4. PCR reaction mix for SR-B1flox

Material	Amount (μL)
aqua dest.	17.25
10x PCR-Buffer GREEN	2.5
DMSO	1
10 mM dNTP	1
10 μM SR-B1flox forward primer	1
10 μM SR-B1flox reverse primer	1
Taq-Polymerase (5U/μL)	0.25
DNA	1
Total	25

Table 5. PCR primer sequences of SR-B1flox from 5' to 3'

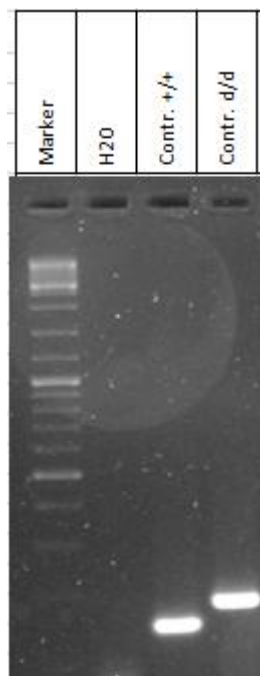
Primer	Sequence
SR-B1flox forward primer	GCACAGAGGACCCAACAGCGCACAAAATGG
SR-B1flox reverse primer	GCTGGGATTCAAGGTGTGTGCCACCACTAC

PCR tubes were briefly vortexed and spun down and then put in the thermocycler with the following program:

Table 6. PCR program SR-B1flox

Step	Temperature (°C)	Time
1	95	3 min
2	95	30s
3	69	30s
4	72	60s
	Repeat step 2-4 for 40 cycles	
5	72	5 min
6	4	oo

PCR products were then loaded on a 1.5% agarose gel (1.5g agarose/100mL TBE buffer, 5 µl Roti®-GelStain) and separated by electrophoresis for 1h at 120 mA. 8 µl of GeneRuler™ DNA Ladder Mix was used as marker. The bands were visualized under UV light with the GelStick Imager (INTAS, Germany) and images were analyzed in Excel.



The band corresponding with no SR-B1flox-alleles (+/+) was at 149 bp and two SR-B1flox-alleles (d/d) corresponded to a band at 188 bp (**Figure 13**). For experiments, only d/d mice were used.

Figure 13. Exemplary PCR results of the SR-B1flox PCR.

In addition to the marker, the gel picture shows the water control and the PCR products of no SR-B1flox-alleles (+/+) and two SR-B1flox-alleles (d/d).

CreCs

Table 7. PCR reaction mix for CreCs

Material	Amount (μL)
aqua dest.	19.9
10x PCR-Buffer GREEN	2.5
10 mM dNTP	1
10 μM 1+2+3+4 PrimerMix	1
Taq-Polymerase (5U/μL)	0.1
DNA	0.5
Total	25

Table 8. PCR primer sequences of CreCs from 5' to 3'

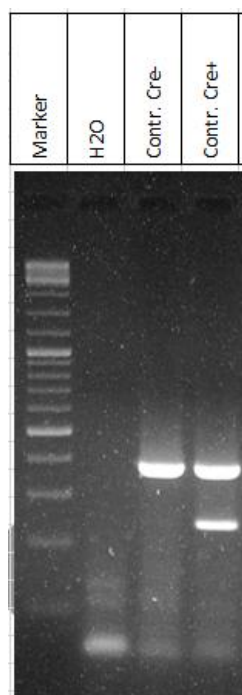
Primer	Sequence
Cre forward primer (1)	CCGTCTCTGGTGTAGCTGAT
Cre reverse primer (2)	CCGGTATTGAACTCCAGCG
Cre control forward primer (3)	ACTGGGATCTTCGAACTCTTTGGAC
Cre control reverse primer (4)	GATGTTGGGGCACTGCTCATTACCC

A primer mix was made by diluting the stock solutions of the primers 1:10 and adding the primers in a proportion of 1:1. PCR tubes were briefly vortexed and spun down and then put in the thermocycler with the following program:

Table 9. PCR program CreCs

Step	Temperature (°C)	Time
1	95	3 min
2	95	30s
3	57	30s
4	72	60s
	Repeat step 2-4 for 40 cycles	
5	72	5 min
6	4	oo

PCR products were then loaded on a 1.5% agarose gel (1.5g agarose/100mL TBE buffer, 5 µl Roti®-GelStain) and separated by electrophoresis for 1h at 120 mA. 8 µl of GeneRuler™ DNA Ladder Mix was used as marker. The bands were visualized under UV light with the GelStick Imager (INTAS, Germany) and images were analyzed in Excel.



The band corresponding with Cre gene (Cre+) was at 246 bp and the control band was at 397 bp, for Cre- only the control band was seen (**Figure 14**).

Figure 14. Exemplary PCR results of the CreCs PCR.

In addition to the marker, the gel picture shows the water control and the PCR products of the control (Cre-) and the Cre gene and control (Cre+).

Plasma TG, cholesterol and NEFA levels determination

Blood samples were centrifuged for 5 min, 10.000 rcf and subsequently plasma was collected. For plasma TG and cholesterol determination, 5 μ L of plasma was pipetted in duplicate in a 96-wells plate and determined with the commercial kits (DiaSys Diagnostic Systems GmbH). For plasma non-esterified FA (NEFA) concentrations 20 μ L of (diluted in PBS) plasma was pipetted in duplicate in a 96-wells plate and determined with the commercial kits (NEFA-HR(2) Assay (FUJIFILM)). Absorbance was read at 540 nm. NEFA concentrations were determined via linear regression with help of the standard curve.

Magnetic-activated Cell sorting (MACS)

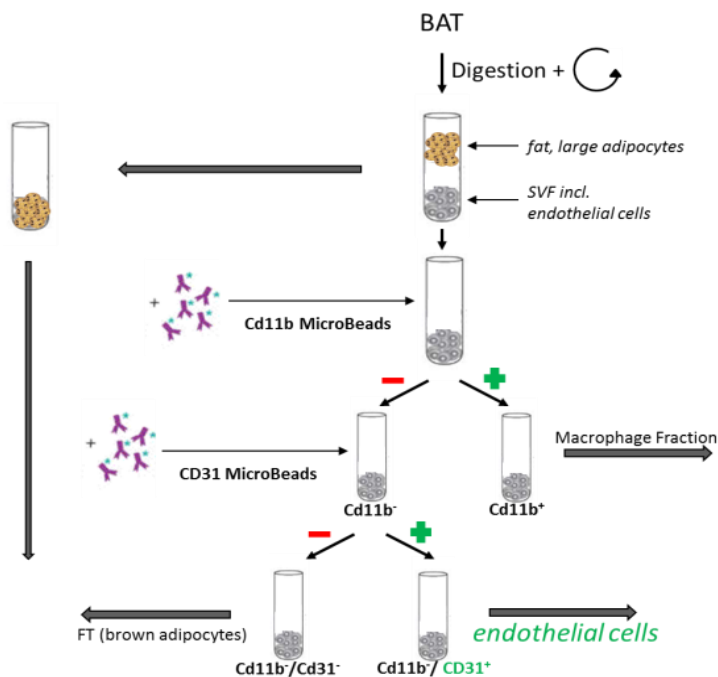


Figure 15. Workflow of MACS. (Figure provided by Kristina Gottschling)

Multiple BATs are pooled and then digested. Mature adipocytes are separated from the stroma vascular fraction (SVF) by low-speed centrifugation. Cd11b⁺ beads capture the macrophage fraction and Cd31⁺ beads the endothelial fraction. Final flow through contains premature adipocytes.

First the Cd11b⁺ or macrophage cell fraction was obtained, then the endothelial Cd31⁺ fraction and the final flow through was obtained as premature adipocytes (**Figure 15**). RNA was isolated as described in *RNA isolation, cDNA and qPCR*.

To test whether the SR-B1 knockout was endothelial-specific, interscapular BAT (iBAT) and inguinal WAT (iWAT) of 15-18 week old female *Scarb1^{fl/fl}-Cdh5^{Cre+}* and *Scarb1^{fl/fl}-Cdh5^{Cre-}* mice were pooled separately from 4 mice per pool, resulting in a n=3 per genotype and organ.

MACS analysis was performed as described previously (Tian *et al.*, 2020). Briefly, tissues were digested with collagenase (Sigma, USA). Mature adipocyte fraction was collected by collecting the floating fraction after low-speed centrifugation. Remaining fractions were collected with the use of magnetic beads (MiltenyiBiotec GmbH, Germany) and LS columns (MiltenyiBiotec GmbH, Germany).

Gene expression analysis

RNA isolation

To isolate the RNA, 1 mL of TRIzol™ Reagent was added to a piece of tissue which was subsequently homogenized in the tissue lyzer (Qiagen) using metal beads. After homogenization, chloroform was added in a 5:1 ratio and mixed well. To separate the phases, the lysate was centrifuged for 15 min at 13.000 rpm at 4°C. The aqueous phase was then mixed 1:1 with 70% ethanol. RNA was then further isolated using the Nucleo Spin RNA® (Macherey-Nagel™, Germany) according to the manufacturer's protocol and dissolved in nuclease-free aqua dest.

RNA content was measured using NanoPhotometer ® N60 (IMPLEN, Germany) and subsequently 400 ng of RNA was transcribed to cDNA using High-Capacity cDNA Reverse Transcription Kit (Applied Biosystems). For the MACS experiment, 100 ng of RNA was transcribed, as the RNA concentrations were too low to transcribe 400 ng.

qPCR

Gene expression was measured by mixing cDNA with Universal PCR MasterMix (Applied Biosystems) and TaqMan® Assay-on-demand primer sets (Table 10). PCR reaction was performed by Quantstudio™ 5 Real-Time PCR Systems (ThermoFischer Scientific).

Table 10. Gene names and TaqMan® Assays-on-Demand™

Gene name	Assay-on-Demand™
Tbp	Mm00446973_m1
Scarb1	Mm01198172_m1
Ucp1	Mm00494069_m1
Elovl3	Mm00468164_m1
Ppargc1a	Mm00447183_m1
Fasn	Mm00662319_m1
Dio2	Mm00515664_m1
Lpl	Mm00434764_m1
Cd36	Mm00432403_m1

Scarb2	Mm00446977_m1
Glut1	Mm00441480_m1
Glut4	Mm01245502_m1
Ldlr	Mm00440169_m1
Lrp1	Mm00464608_m1
Vldlr	Mm00443281_m1
Adgre1/Emr1	Mm00802530_m1
Gpihbp1	Mm01205849_g1
Pparg	Mm00440945_m1
Prdm16	Mm00712556_m1
Chrebp_beta	AIVI4CH
Fabp4	Mm00445880_m1
Fat1	Mm00449511_m1

Cycling parameters were as followed: 1 cycle of 95 °C for 10 min, 40 cycles of 95 °C for 15 s then 60 °C for 60 s, followed by melt curve analysis. Gene copy number was calculated with the formula $(10^{((Ct-35)/-3.3219)})$ and gene expression was normalized for copy number of TATA-box binding protein (*Tbp*). Normalized values could be used to calculate the relative values where the values for (RT) Cre- was set to 1.

Western blot

Total lysates were prepared by homogenizing the tissues with metal beads and tissue lyzer (Qiagen) in RIPA buffer ((10x (v/w), 20 mM Tris-HCl pH 7.4, 5 mM EDTA, 50 mM sodium chloride, 10 mM sodium pyrophosphate, 50 mM sodium fluoride, 1 mM sodium orthovanadate, 1 % NP-40, 0.1% SDS supplemented with cOmplete Mini Protease Inhibitor Cocktail Tablets (Roche) and phosphatase inhibitors (Sigma)). Lysates were centrifuged at 10.000 rcf, for 5 min at 4°C. The aqueous phase without the fatty layer was taken for protein determination using the Pierce™ BCA Protein Assay Kit (Thermoscientific). Samples were diluted to 20 µg protein per sample in RIPA and NuPAGE reducing sample buffer (Invitrogen) denatured for 10 min at 55°C.

Samples were separated by SDS-PAGE on a 10% SDS-polyacrylamide Tris-glycine gels. Samples were transferred to a nitrocellulose membrane overnight in a wet blotting system. Ponceau S (Sigma-Aldrich) staining was performed to ensure equal loading. The blots were blocked in 5% milk (Millipore) in TBST (0.2 M Tris, 1.37 M sodium chloride, 0.1 % (v/v) Tween 20) solution for 1h at RT. After washing with TBST, blots were incubated with primary antibody in 5% Bovine Serum Albumin (BSA, Sigma-Aldrich) in TBST overnight at 4°C. Blots for CD36 were blocked in Roti®Block (Carl Roth, 1:10 diluted with aqua dest) and primary and secondary antibodies were in Roti®Block as well. Primary antibodies used were SR-B1 ((ab217318, 1:1000); AKT (cs9272, 1:1000); CD36 (aliquot 201, 1:1000); γ -Tubulin (ab179503, 1:2000)). After washing with TBST, blots were incubated with secondary antibody in 5% milk in TBST for 1h at RT. Blots were then developed on Amersham Imager600 (GE Healthcare) using luminol (Sigma A4865) and para-hydroxycoumarinic acid-based (Sigma C9008) chemiluminescence substrate. Secondary antibody used was HRP-conjugated goat anti-rabbit (AB_2307391, Jackson ImmunoResearch laboratories, Inc, 1:5000).

Quantification of the bands was done in Image Studio Lite (version 5.2.5) and protein expression was normalized for AKT or γ -Tubulin. Then from the normalized values the relative values were calculated where the values for (RT) Cre- was set to 1.

Immunofluorescence

Tissues were fixed in 3.7% formaldehyde in PBS and embedded in paraffin. 4 μ m paraffin iBAT sections were deparaffinized and subsequently rehydrated in xylene and descending ethanol series. Next, slides were cooked in 10 mM citrate buffer (pH 6.0) for 30 minutes for antigen retrieval and left in the buffer for an additional 30 min to cool down. Next, to reduce auto fluorescence slides were incubated for 10 minutes at RT with 3% hydrogen peroxide in PBS. After washing, slides were blocked with 3% BSA in PBS for 1h at RT. Slices were then incubated with primary antibodies (CD36, AF2519, R&D Systems, 1:200; PLIN1, D1D8 #9349, Cell Signalling, 1:200; GPIHBP1, 11A12-SN, 1:500) in PBS overnight at 4°C. The following day, the slides were incubated (1:500) with Cy2 donkey-anti-rabbit secondary antibody (711-225-152, Jackson Laboratories), Cy3 donkey-anti-rat antibody (712-165-153, Jackson Laboratories) and Cy5 donkey-anti-goat secondary antibody (705-175-147, Jackson Laboratories) for 1 hour. Slides were then covered with ROTI®Mount FluorCare DAPI (Carl Roth). The negative control was incubated in PBS without primary antibody and treated using the same workflow.

Microscopy images were recorded using the Nikon A1R inverted Microscope with a 40x objective (Nikon, Shinagawa, Tokyo).

Statistical analysis

Results are expressed as mean \pm SEM. Outliers were identified by Graphpad prism (version 10) for Windows (GraphPad Software, USA) using the ROUT method with a Q cut-off value of 1%. When outliers were identified in basal body characteristics (body weight, plasma cholesterol and triglyceride levels, organ weights) the outlier was removed from all analyses.

All other statistical analysis were performed with RStudio version 2023.12.1+402 (RStudio, USA) with the following packages: readxl, tidyverse, car, ggpubr, rstatix. Data was tested for normal distribution and equal variances. In case parametric tests could be used the Student's t-test was performed for two groups, otherwise a two-way ANOVA was performed. When a non-parametric test was needed a Wilcox rank sum test was performed for two groups. A p-value <0.05 was considered significant.

Part F: Results

Brown adipocyte-specific CD36ko mice

Validating brown adipocyte-specific knockout of CD36 in *Cd36^{fl/fl}-Ucp1^{Cre+}* mice

To validate the knockout, female *Cd36^{fl/fl}-Ucp1^{Cre-}* and *Cd36^{fl/fl}-Ucp1^{Cre+}* mice were kept at RT or 24h at 4°C and after a 2h fast organs were collected. Aside from a slight increase in blood glucose levels in cold-exposed *Cd36^{fl/fl}-Ucp1^{Cre+}* mice compared to control littermates kept at RT (**Figure 16A**), no significant differences were observed in other body characteristics (**Figure 16B-F**).

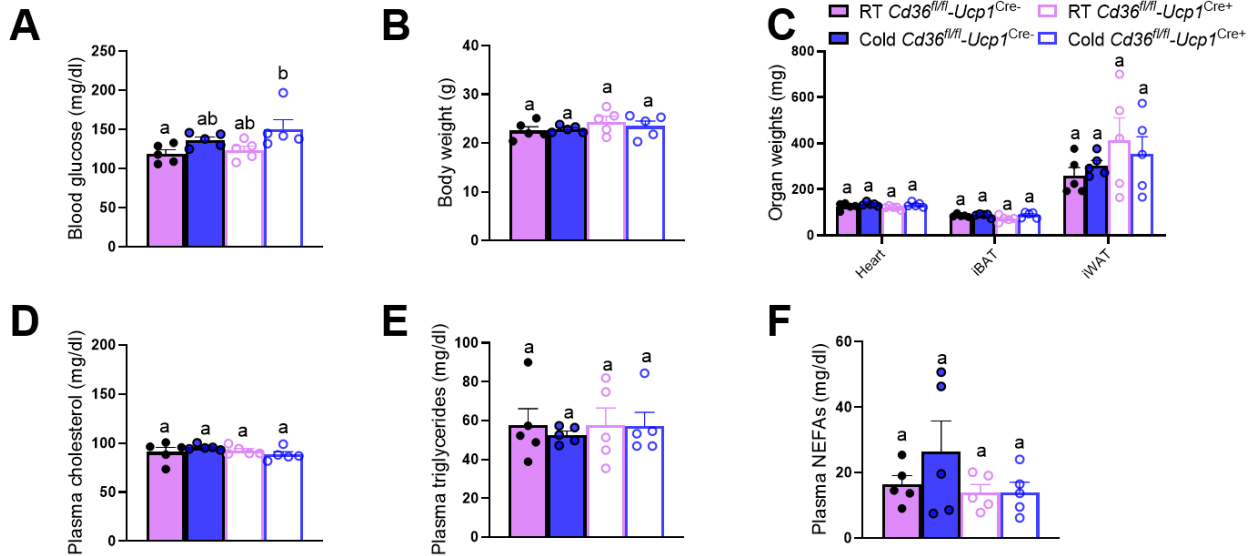


Figure 16. Body characteristics of *Cd36^{fl/fl}-Ucp1^{Cre+}* and *Cd36^{fl/fl}-Ucp1^{Cre-}* mice.

(A-F) 15-20 week old female *Cd36^{fl/fl}-Ucp1^{Cre+}* and *Cd36^{fl/fl}-Ucp1^{Cre-}* mice were housed at RT or 24h at 4°C. Mice were fasted 2h before sacrifice.

(A) Blood glucose (B) Body weight (C) Organ weights (D) Plasma cholesterol (E) Plasma TGs (F) Plasma NEFAs

Regarding *Cd36* expression as shown in **Figure 17A**, cold-exposed *Cd36^{fl/fl}-Ucp1^{Cre-}* mice had increased *Cd36* expression compared to mice housed at RT, as described before (Bartelt *et al.*, 2011). However, *Cd36^{fl/fl}-Ucp1^{Cre+}* mice kept at RT had decreased expression of *Cd36* compared to control littermates kept at RT. Moreover, *Cd36* expression in the BAT of *Cd36^{fl/fl}-Ucp1^{Cre+}* mice did increase upon cold exposure, however failed to reach the level of cold-exposed *Cd36^{fl/fl}-Ucp1^{Cre-}* mice. On protein level, the cold-induced increase of CD36 was not observed, but *Cd36^{fl/fl}-Ucp1^{Cre+}* mice had decreased levels of CD36 regardless of the housing temperature compared to their control littermates (**Figure 17B-C**).

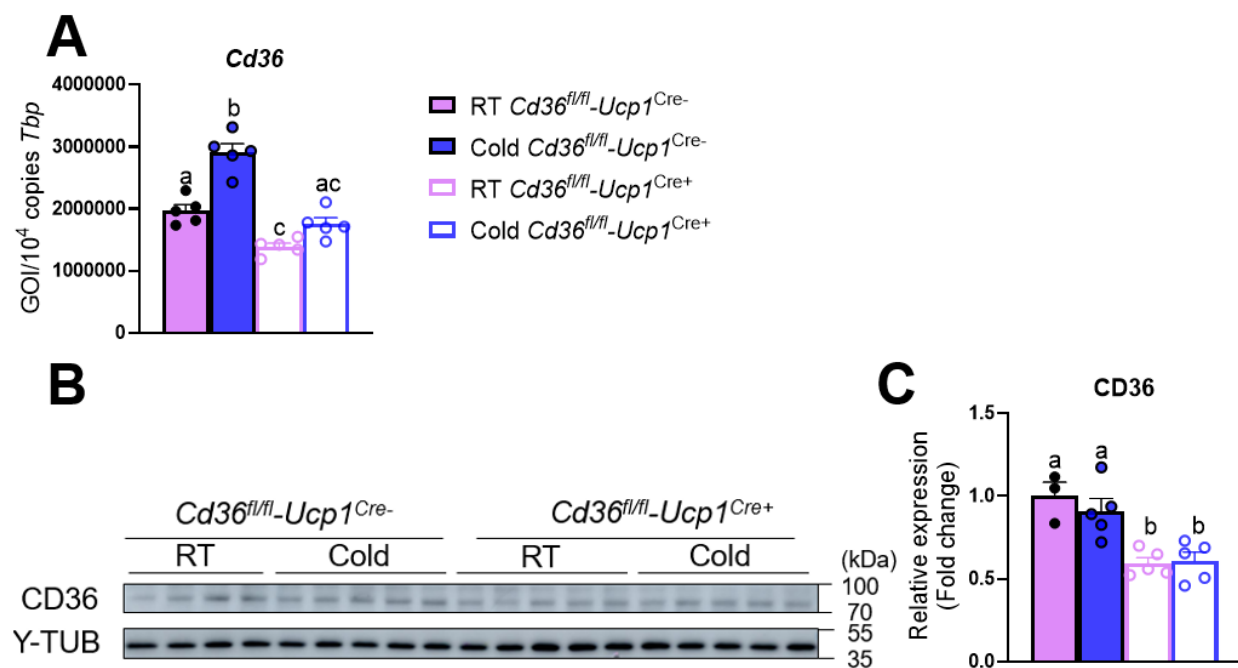


Figure 17. *Cd36^{fl/fl}-Ucp1^{Cre+}* mice have decreased *Cd36* gene and CD36 protein expression compared to control littermates.

(A-C) 15-20 week old female *Cd36^{fl/fl}-Ucp1^{Cre+}* and *Cd36^{fl/fl}-Ucp1^{Cre-}* mice were housed at RT or 24h at 4°C. Mice were fasted 2h before sacrifice.

(A) *Cd36* expression in iBAT. Gene expression was normalized for *Tbp*.

(B-C) CD36 expression in iBAT. Protein expression was normalized for y-Tubulin and RT *Cre-* group was set to 1.

In order to validate that the knockout is cell-type specific, pieces of iBAT were used for immunofluorescence to look at the localization of CD36. PLIN1 is a protein which surrounds the lipid droplets and can be used as a marker for adipose tissue (Yu *et al.*, 2015), while GPIHBP1 is expressed on endothelial cells (Fong *et al.*, 2016) and therefore used as an endothelial marker. In *Cd36^{fl/fl}-Ucp1^{Cre-}* mice regardless of housing temperature, CD36 staining displayed endothelial structures (tubular structures) and ring-like structures reflecting the plasma membrane of brown adipocytes (**Figure 18A-B**). Conversely, the staining in *Cd36^{fl/fl}-Ucp1^{Cre+}* mice regardless of temperature only shows the endothelial structures (**Figure 18C-D**).

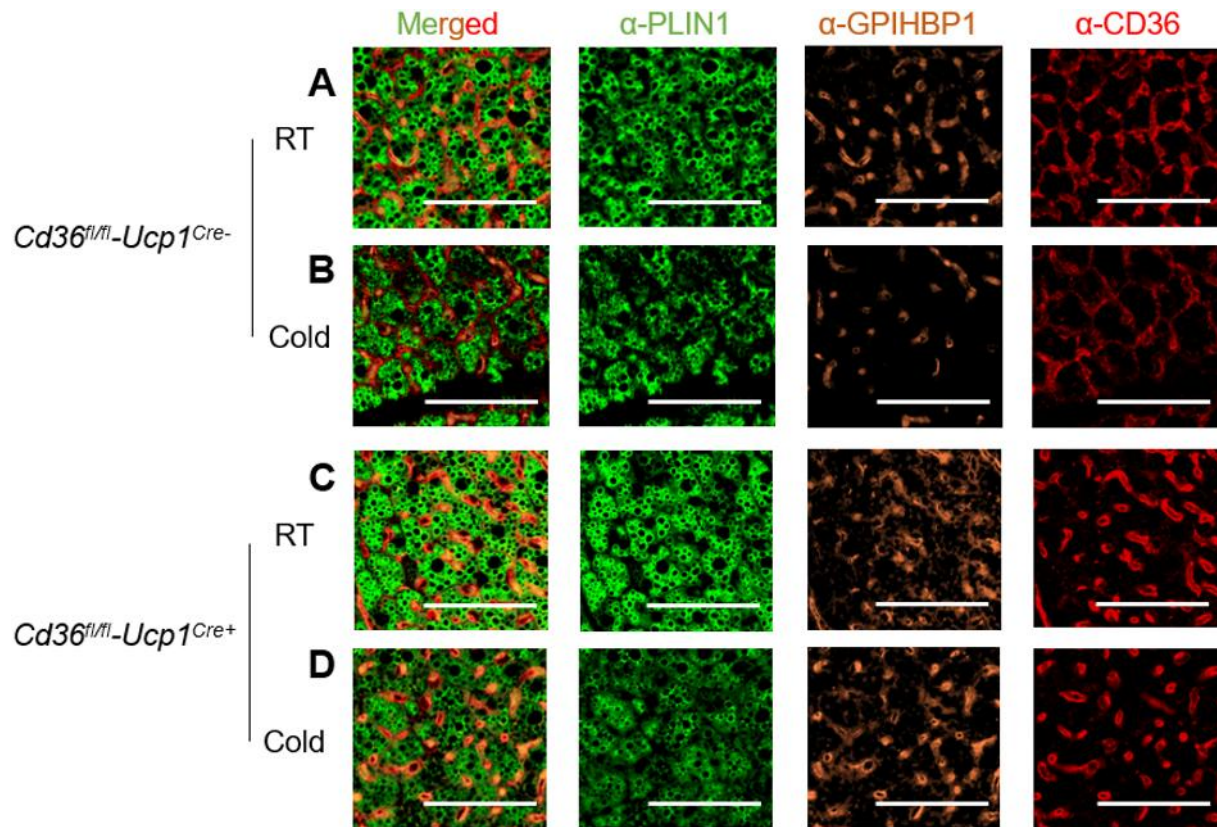


Figure 18. Localization of CD36 in iBAT of *Cd36^{fl/fl}-Ucp1^{Cre-}* and *Cd36^{fl/fl}-Ucp1^{Cre+}* mice.

(A-D) 15-20 week old female *Cd36^{fl/fl}-Ucp1^{Cre+}* and *Cd36^{fl/fl}-Ucp1^{Cre-}* mice were housed at RT or 24h at 4°C. Mice were fasted 2h before sacrifice. Paraffin sections were stained with PLIN1 (adipocyte marker), GPIHBP1 (endothelial marker) and CD36. Scale bar is 50 μ m.

(A-B) *Cd36^{fl/fl}-Ucp1^{Cre-}* mice (A) housed at RT (B) cold-exposed

(C-D) *Cd36^{fl/fl}-Ucp1^{Cre+}* mice (C) housed at RT (D) cold-exposed

In summary, brown adipocyte-specific knockout of CD36 can be observed on gene expression on whole organ level. Moreover, we conclude that based on the immunofluorescence data that CD36 is knocked out specifically in brown adipocytes in *Cd36^{fl/fl}*-Ucp1^{Cre+} mice.

Are $Cd36^{fl/fl}$ - $Ucp1^{Cre+}$ mice able to maintain their body temperature when exposed to cold in a fed state?

To test whether $Cd36^{fl/fl}$ - $Ucp1^{Cre+}$ mice were able to maintain their body temperature when faced a cold challenge, 11-13 week old female and male $Cd36^{fl/fl}$ - $Ucp1^{Cre-}$ and $Cd36^{fl/fl}$ - $Ucp1^{Cre+}$ mice were put in metabolic cages. Temperature was kept at 30°C for 2 days, then decreased to 22°C for 2 days and lastly decreased to 6°C for 2 days. Only data from female mice are shown, whereas male mice showed a similar pattern. No differences in body characteristics were observed (**Figure 19A-C**) except for a lower liver weight in $Cd36^{fl/fl}$ - $Ucp1^{Cre+}$ mice (**Figure 19C**). Interestingly, $Cd36^{fl/fl}$ - $Ucp1^{Cre+}$ mice also had lower plasma cholesterol levels compared to control littermates (**Figure 19D**), no differences in plasma TGs and plasma NEFAs were observed (**Figure 19E-F**).

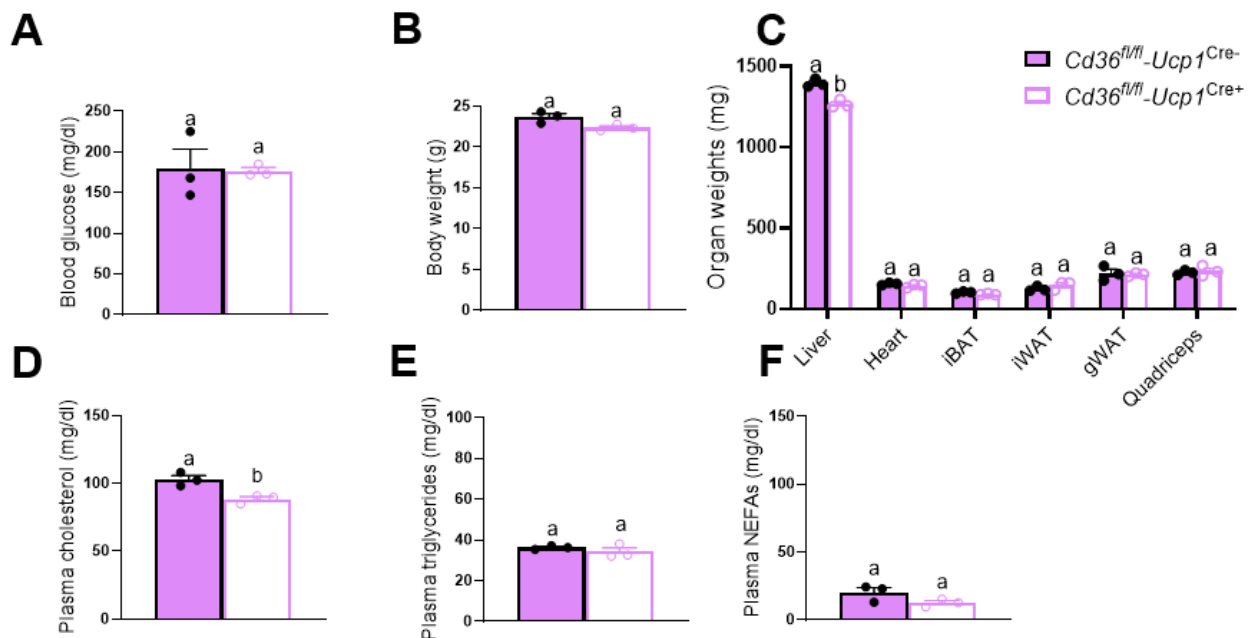


Figure 19. Body characteristics of $Cd36^{fl/fl}$ - $Ucp1^{Cre+}$ and $Cd36^{fl/fl}$ - $Ucp1^{Cre-}$ mice.

(A-F) 11-13 week old female $Cd36^{fl/fl}$ - $Ucp1^{Cre+}$ and $Cd36^{fl/fl}$ - $Ucp1^{Cre-}$ mice were put in metabolic cages. After acclimatization, temperature was kept for 2 days at 30 °C, then decreased to 22 °C for 2 days and the last 2 days were 6 °C. Mice were fasted for 2h before sacrifice.

(A) Blood glucose (B) Body weight (C) Organ weights (D) Plasma cholesterol (E) Plasma TGs (F) Plasma NEFAs

Both genotypes were able to maintain their body temperature at all temperatures (**Figure 20A**). Energy expenditure increased as the temperature decreased, as expected (Scholander *et al.*, 1950), but no differences were observed between the genotypes (**Figure 20B**). RER which indicates which fuel is used whether it's lipids (RER ~0.7) or glucose (RER ~1.0) (Simonson and DeFronzo, 1990) also showed no major differences (**Figure 20C**). Other mechanisms to maintain body temperature is increasing activity levels and food intake. Total distance in cage (**Figure 20D**) and food intake (**Figure 20E**) showed no differences.

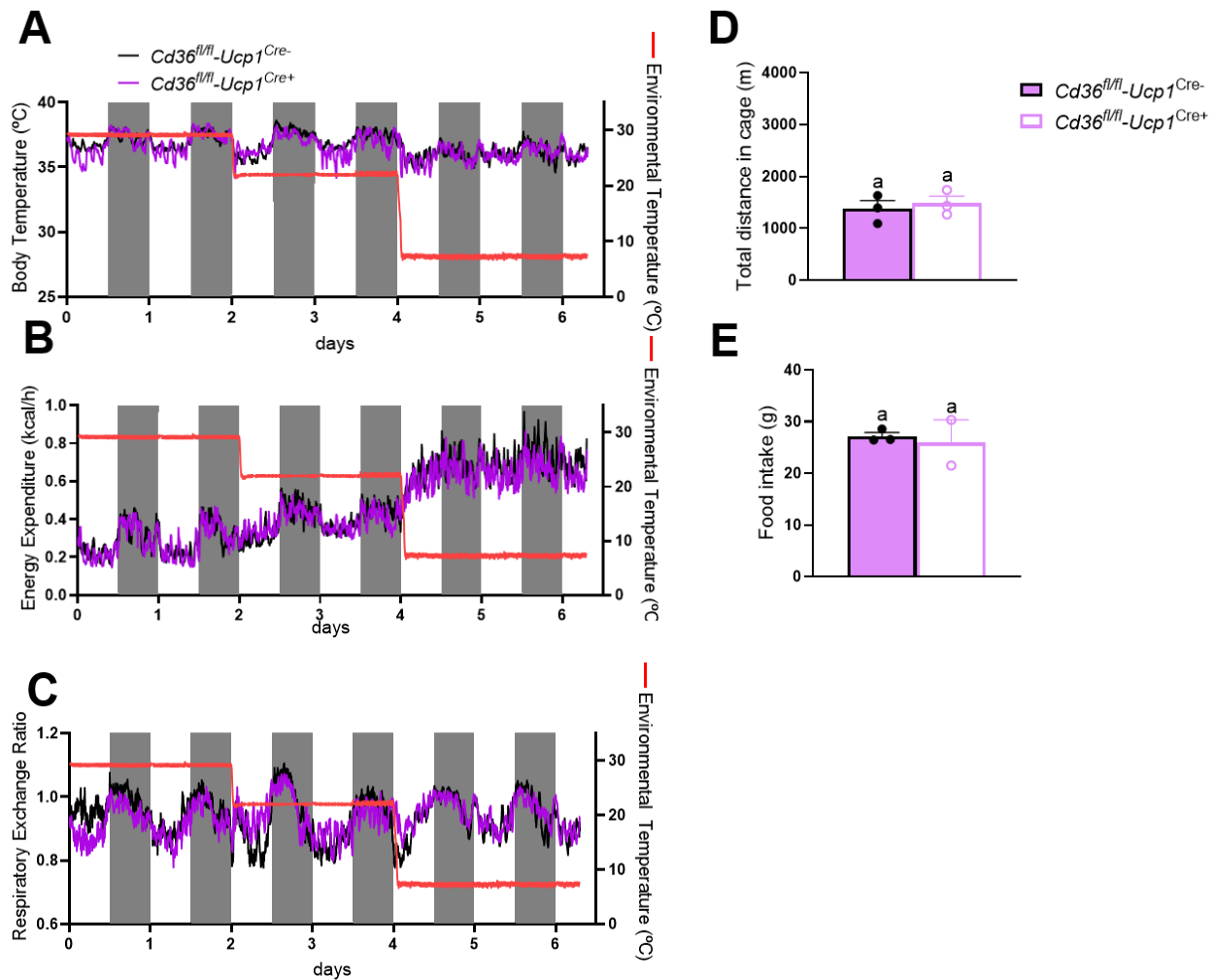


Figure 20. $Cd36^{fl/fl}-Ucp1^{Cre+/+}$ mice are able to maintain their body temperature when exposed to cold in a fed state.

(A-E) 11-13 week old female $Cd36^{fl/fl}-Ucp1^{Cre+/+}$ and $Cd36^{fl/fl}-Ucp1^{Cre-/-}$ mice were put in metabolic cages. After acclimatization, temperature was kept for 2 days at 30 °C, then decreased to 22 °C for 2 days and the last 2 days were 6 °C. Mice were fasted for 2h before sacrifice.

(A) Body temperature (B) Energy expenditure (C) RER (D) Total distance in cage (E) Food intake

We conclude that *Cd36^{fl/fl}-Ucp1^{Cre+}* mice are able to maintain their body temperature when exposed to cold in a fed state.

Are $Cd36^{fl/fl}$ - $Ucp1^{Cre+}$ mice able to maintain their body temperature when exposed to cold in a fasted state?

$CD36$ ko mice are able to maintain their body temperature in the cold in a fed state (Putri *et al.*, 2015). However, upon fasting, their body temperature rapidly decreases and become cold sensitive (Bartelt *et al.*, 2011; Putri *et al.*, 2015). Therefore, we wanted to test whether $Cd36^{fl/fl}$ - $Ucp1^{Cre+}$ mice were able to maintain their body temperature when faced a cold challenge when fasted. 15-17 week old female $Cd36^{fl/fl}$ - $Ucp1^{Cre-}$ and $Cd36^{fl/fl}$ - $Ucp1^{Cre+}$ mice were put in metabolic cages. The same temperature schedule was followed as before, except on the day of temperature change mice were fasted from 6 am – 12 pm.

No differences in body characteristics were observed (**Figure 21A-F**).

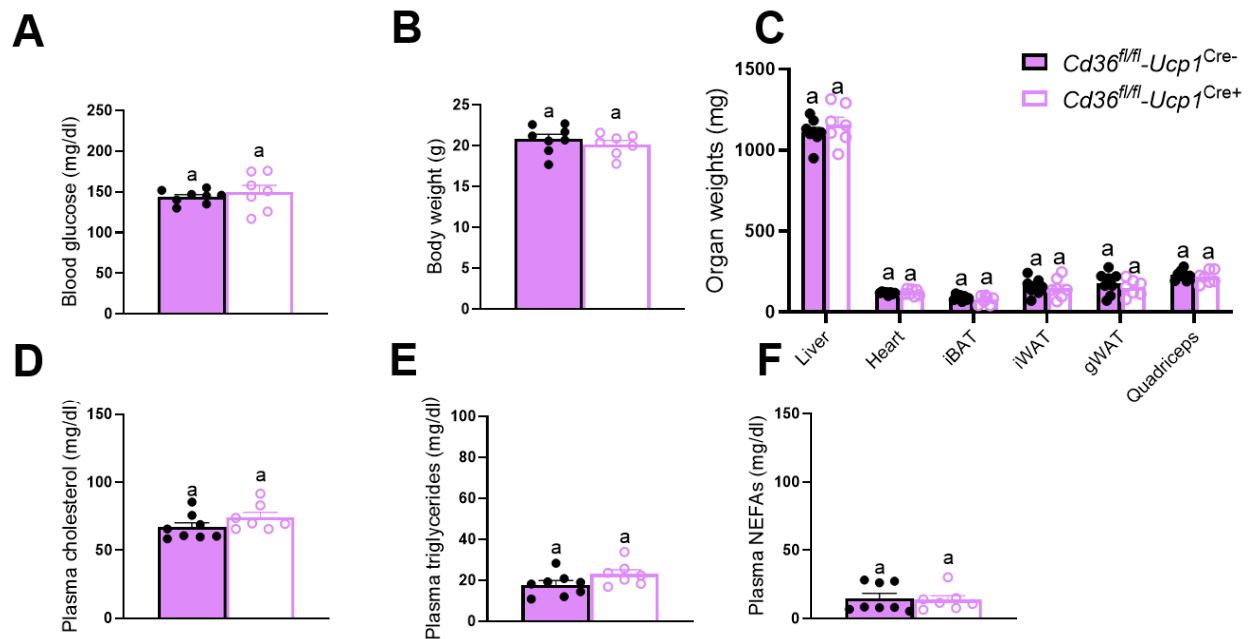


Figure 21. Body characteristics of $Cd36^{fl/fl}$ - $Ucp1^{Cre+}$ and $Cd36^{fl/fl}$ - $Ucp1^{Cre-}$ mice.

(A-F) 15-17 week old female $Cd36^{fl/fl}$ - $Ucp1^{Cre+}$ and $Cd36^{fl/fl}$ - $Ucp1^{Cre-}$ mice were put in metabolic cages. After acclimatization, temperature was kept for 2 days at 30 °C, then decreased to 22 °C for 2 days and the last 2 days were 6 °C. On the day of the temperature change, mice were fasted from 6 am to 12 pm.

(A) Blood glucose (B) Body weight (C) Organ weights (D) Plasma cholesterol (E) Plasma TGs (F) Plasma NEFAs

Cd36^{fl/fl}-Ucp1^{Cre+} mice were able to maintain their body temperature when fasted at 30°C and 22°C. However, during the fasting period at 6°C, half of the *Cd36^{fl/fl}-Ucp1^{Cre+}* mice were unable to maintain their body temperature (**Figure 22A-B**) and the experiment had to be stopped. Energy expenditure showed some tendencies to be lower in *Cd36^{fl/fl}-Ucp1^{Cre+}* mice compared to *Cd36^{fl/fl}-Ucp1^{Cre-}* mice already at 22°C (**Figure 22C**) and was also lower in *Cd36^{fl/fl}-Ucp1^{Cre+}* mice compared to *Cd36^{fl/fl}-Ucp1^{Cre-}* mice during the fasting period at 6°C (**Figure 22D**). RER, total distance in cage and food intake did not differ between the genotypes (**Figure 22E-H**).

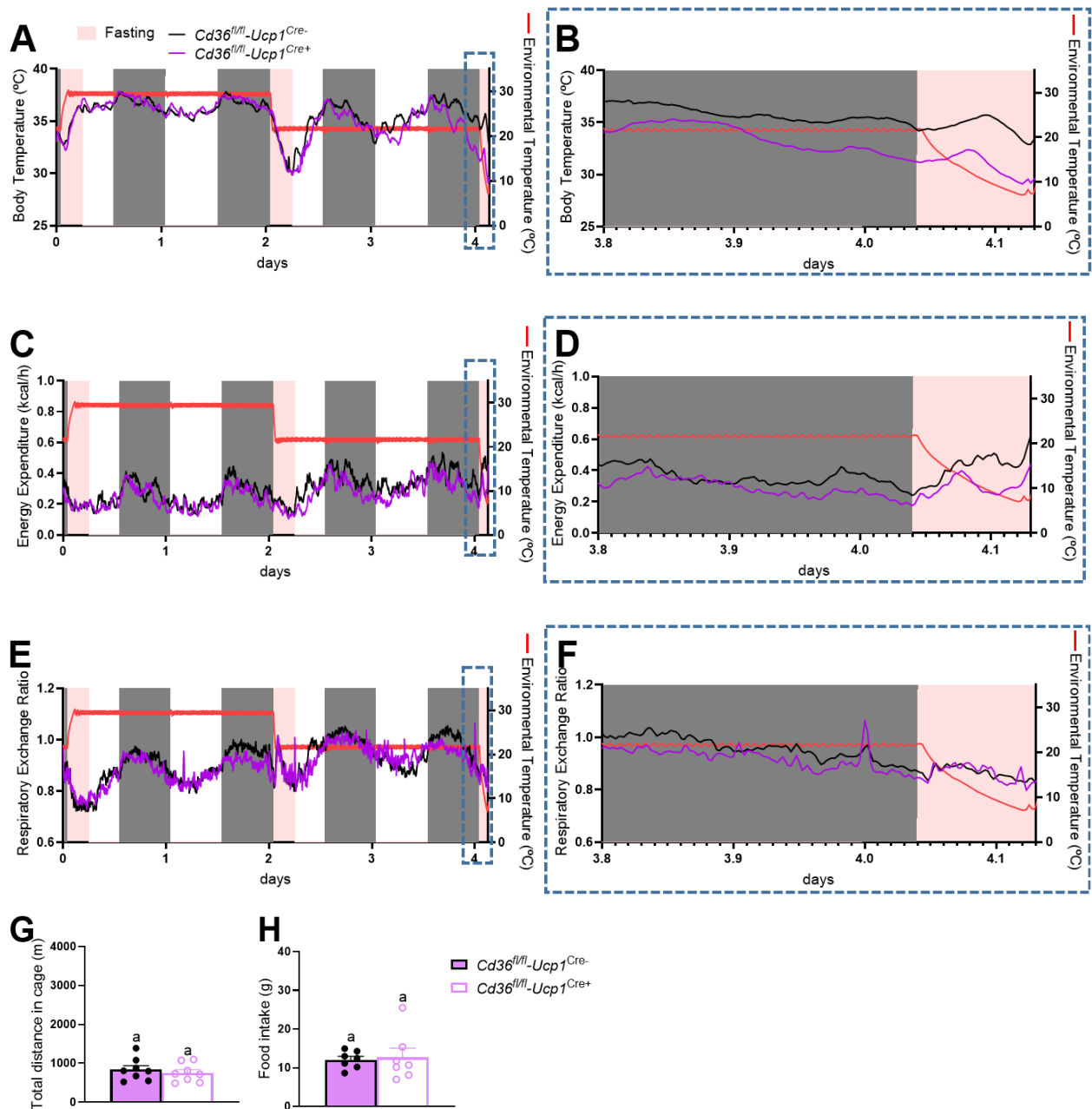


Figure 22. $Cd36^{fl/fl}-Ucp1^{Cre+}$ mice are unable to maintain their body temperature when exposed to cold in a fasted state.

(A-H) 15-17 week old female $Cd36^{fl/fl}-Ucp1^{Cre+}$ and $Cd36^{fl/fl}-Ucp1^{Cre-}$ mice were put in metabolic cages. After acclimatization, temperature was kept for 2 days at 30 °C, then decreased to 22 °C for 2 days and the last 2 days were 6 °C. On the day of the temperature change, mice were fasted from 6 am to 12 pm.

(A-B) Body temperature (C-D) Energy expenditure (E-F) RER

(B, D, F) last 5.5 h of the experiment, zoomed in (G) Total distance in cage (H) Food intake

We conclude that $Cd36^{fl/fl}-Ucp1^{Cre+}$ mice are unable to maintain their body temperature when exposed to cold in a fasted state.

Do $Cd36^{fl/fl}$ - $Ucp1^{Cre+}$ mice have altered lipid uptake compared control littermates at different housing temperatures?

To investigate whether $Cd36^{fl/fl}$ - $Ucp1^{Cre+}$ mice have altered lipid uptake, 13-16 week old female $Cd36^{fl/fl}$ - $Ucp1^{Cre-}$ and $Cd36^{fl/fl}$ - $Ucp1^{Cre+}$ mice were kept at RT or at 4°C for 24h and received an oral fat gavage with radioactively labelled ^3H -Triolein and a tracer of radioactively labelled ^{14}C -DOG.

No differences in body characteristics were observed (**Figure 23A-F**).

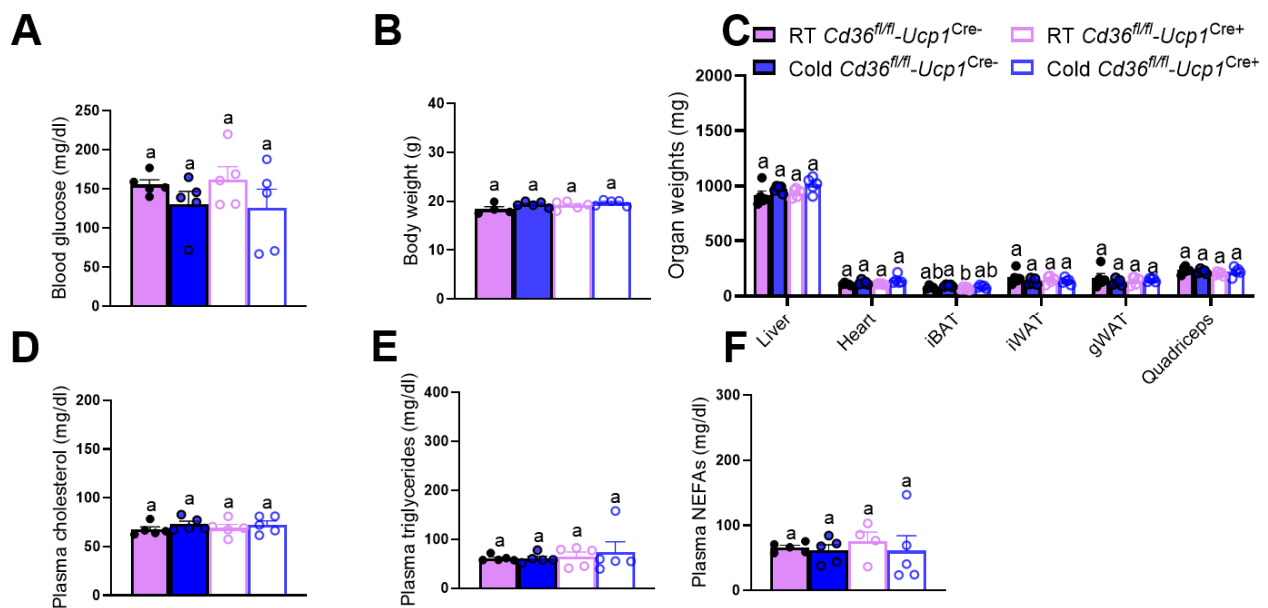


Figure 23. Body characteristics of $Cd36^{fl/fl}$ - $Ucp1^{Cre+}$ and $Cd36^{fl/fl}$ - $Ucp1^{Cre-}$ mice.

(A-F) 13-16 week old female $Cd36^{fl/fl}$ - $Ucp1^{Cre+}$ and $Cd36^{fl/fl}$ - $Ucp1^{Cre-}$ mice were kept at RT and exposed to cold (4°C) for 24h. Mice were fasted 4h in the morning and 2 hours before sacrifice they received an oral gavage with radio-labelled ^3H -Triolein and a tracer of ^{14}C -DOG.

(A) Blood glucose (B) Body weight (C) Organ weights (D) Plasma cholesterol (E) Plasma TGs (F) Plasma NEFAs

Cd36^{fl/fl}-Ucp1^{Cre+} mice show a tendency to have decreased ³H-Triolein uptake in iBAT when kept at RT compared to their control littermates. However, when cold-exposed, *Cd36^{fl/fl}-Ucp1^{Cre+}* mice have blunted uptake in iBAT compared to cold-exposed control littermates. In line with this, cold-exposed livers of *Cd36^{fl/fl}-Ucp1^{Cre+}* mice show an increase in ³H-Triolein uptake which is not observed in cold-exposed *Cd36^{fl/fl}-Ucp1^{Cre-}* mice (**Figure 24A**).

Regarding ¹⁴C-DOG uptake, heart and iBAT show increased uptake of ¹⁴C-DOG during cold-exposure but no major differences were observed between the genotypes (**Figure 24B**).

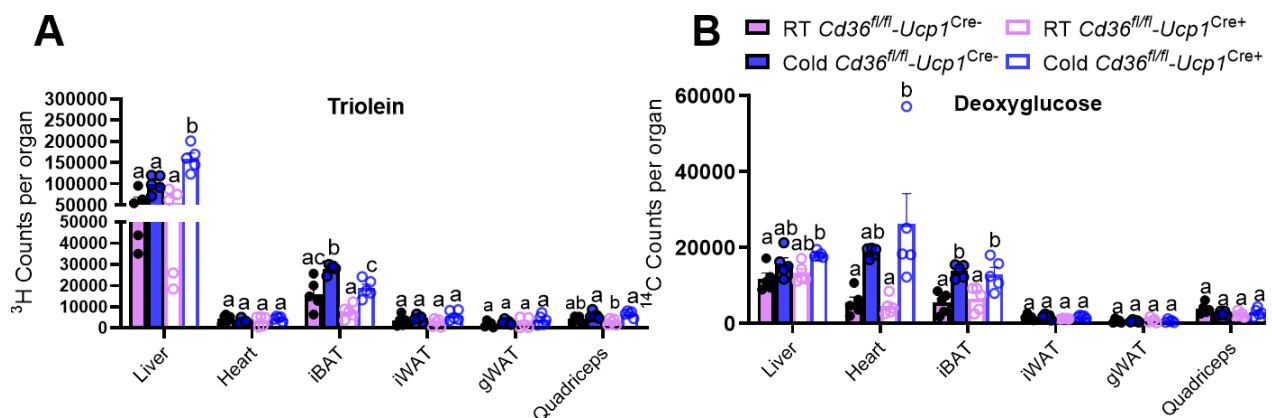


Figure 24. Cold-exposed *Cd36^{fl/fl}-Ucp1^{Cre+}* mice have blunted uptake in BAT compared to cold-exposed control littermates.

(A-B) 13-16 week old female *Cd36^{fl/fl}-Ucp1^{Cre+}* and *Cd36^{fl/fl}-Ucp1^{Cre-}* mice were kept at RT and exposed to cold (4°C) for 24h. Mice were fasted 4h in the morning and 2h before sacrifice they received an oral gavage with radio-labelled ³H-Triolein and a tracer of ¹⁴C-DOG.

(A) ³H-Triolein counts per organ (B) ¹⁴C-DOG counts per organ

We conclude that cold-exposed *Cd36^{fl/fl}-Ucp1^{Cre+}* mice have lower lipid uptake in iBAT compared to cold-exposed control littermates.

Do *Cd36^{fl/fl}-Ucp1^{Cre+}* mice have altered gene expression in BAT and WAT compared to control littermates at different housing temperatures?

To check whether a brown adipocyte-specific knockout of *Cd36* affects gene expression in BAT and WAT and order to identify potential compensational mechanism, we determined thermogenic markers, glucose and lipid handling genes as well as lipid receptor expression in iBAT and iWAT of *Cd36^{fl/fl}-Ucp1^{Cre-}* and *Cd36^{fl/fl}-Ucp1^{Cre+}* mice kept at RT or at 4°C for 24h .

Pparγ expression did not increase upon cold-exposure in BAT of *Cd36^{fl/fl}-Ucp1^{Cre+}* mice compared to control littermates while no differences were observed in *Prdm16* expression. Thermogenic markers *Dio2*, *Ucp1* and *Elovl3* were increased upon cold exposure and showed no differences between the genotypes except for *Elovl3*. elongation of very long chain fatty acid 3 (*Elovl3*) was shown to be highly upregulated during cold-exposure in BAT (Tvrdik *et al.*, 1997, 2000) and important for lipid recruitment and thermogenesis in BAT (Westerberg *et al.*, 2006). *Elovl3* expression did increase in BAT of cold-exposed *Cd36^{fl/fl}-Ucp1^{Cre+}* mice but was blunted compared to cold-exposed littermates (**Figure 25A**).

In WAT, cold-exposure did increase *Ucp1* and *Dio2* expression in *Cd36^{fl/fl}-Ucp1^{Cre-}* mice but in cold-exposed *Cd36^{fl/fl}-Ucp1^{Cre+}* mice this increase was blunted (**Figure 25B**). Type II iodothyronine deiodinase (*Dio2*) is an enzyme which catalyzes the conversion of thyroid hormones thyroxine (T₄) to its active metabolite 3,5,3'-triiodothyronine (T₃). T₃ is able to stimulate thermogenesis in BAT via UCP1 (Silva, 2003; Yau *et al.*, 2019). No major differences in *Pparγ*, *Prdm16* and *Elovl3* expression were seen between the genotypes and housing temperatures.

In BAT, *Cd36* expression was decreased in *Cd36^{fl/fl}-Ucp1^{Cre+}* mice compared to *Cd36^{fl/fl}-Ucp1^{Cre-}* mice housed at RT while the cold-induced increase of *Cd36* was blunted in *Cd36^{fl/fl}-Ucp1^{Cre+}* mice (**Figure 25C**). In line with the brown adipocyte-specific *Cd36* knockout, no differences in *Cd36* expression were observed in WAT (**Figure 25D**). Regarding expression of other receptors, aside from cold-induced effects no major differences were observed in BAT and WAT between the genotypes and housing temperatures (**Figure 25C-D**).

Aside from cold-induced increase in *Glut4* expression in BAT (**Figure 25E**), no major differences in gene expression of glucose handling were observed in BAT and WAT (**Figure 25E-F**). Interestingly, cold-exposure did increase *Fabp4* and *Lpl* expression in BAT, however in cold-exposed *Cd36^{fl/fl}-Ucp1^{Cre+}* mice this increase was lower compared to cold-exposed littermates (**Figure 25E**) and this effect was not observed in WAT (**Figure 25F**). Moreover, expression of angiopoietin-like protein 4 (*Angplt4*) an inhibitor of LPL (Lafferty *et al.*, 2013), was decreased in *Cd36^{fl/fl}-Ucp1^{Cre+}* mice regardless of housing temperature compared to control littermates housed at RT (**Figure 25E**) but not in WAT (**Figure 25F**). No differences in *Fatp1* expression in BAT and WAT were observed between the genotypes and housing temperatures (**Figure 25E-F**).

These data indicated that cold-exposed *Cd36^{fl/fl}-Ucp1^{Cre+}* mice have decreased expression of lipid handling genes in BAT and decreased expression of thermogenic markers in WAT.

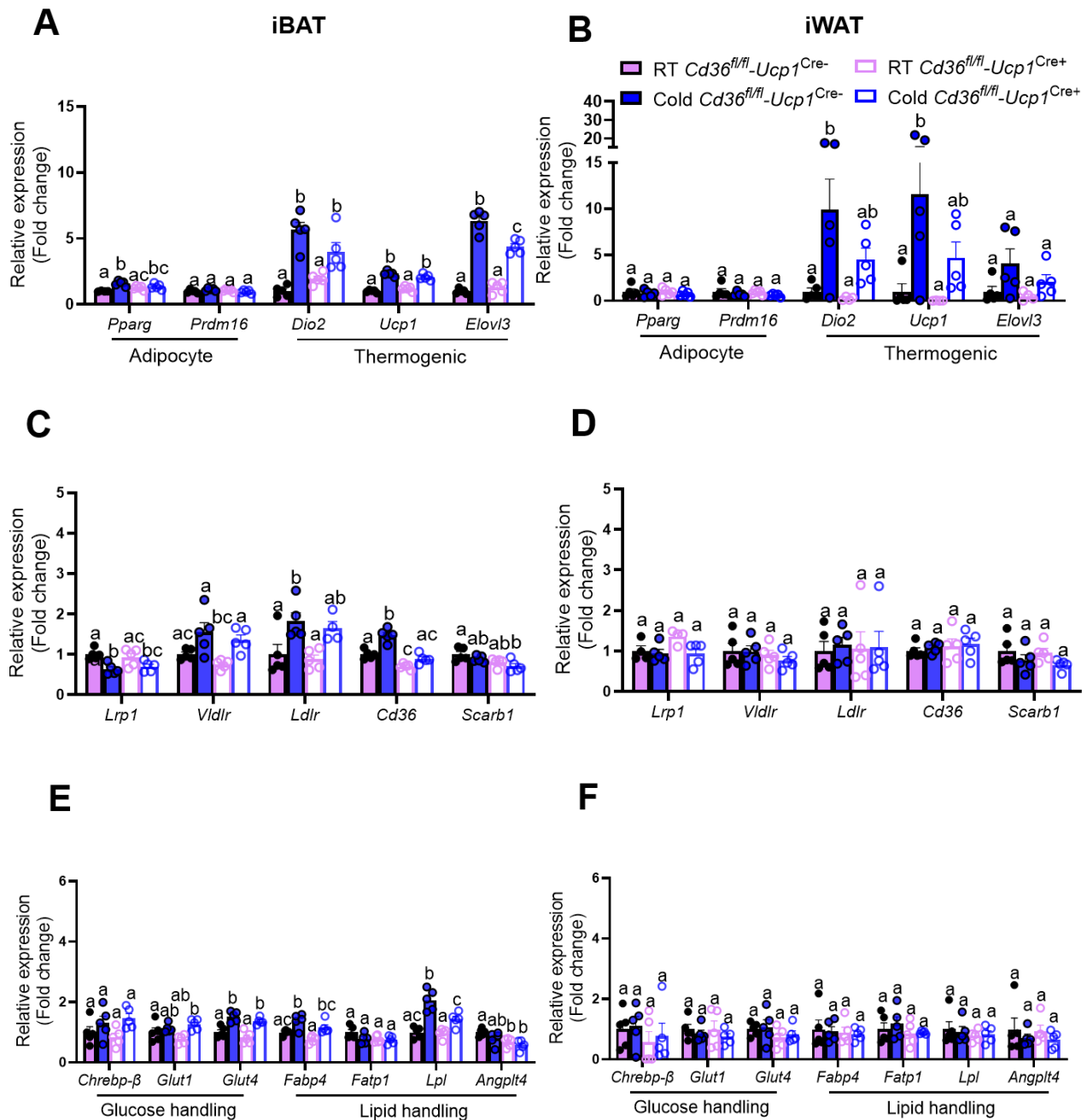


Figure 25. Cold-exposed $Cd36^{fl/fl}-Ucp1^{Cre+}$ mice have decreased expression of lipid handling genes in BAT and decreased expression of thermogenic markers in WAT.

(A-F) 15-20 week old female $Cd36^{fl/fl}-Ucp1^{Cre-}$ and $Cd36^{fl/fl}-Ucp1^{Cre+}$ mice were housed at RT or 24h at 4°C. Mice were fasted 2h before sacrifice.

(A, C, E) Gene expression in iBAT, (B, D, F) Gene expression in iWAT

Gene expression was normalized for *Tbp* and RT $Cre-$ group was set to 1.
(A-B) Adipocyte and thermogenic marker gene expression

(C-D) Receptor gene expression

(E-F) Glucose and lipid handling gene expression

Endothelial-specific CD36ko mice

Validating endothelial-specific knockout of CD36 in $Cd36^{fl/fl}-Cd36^{Cre+}$ mice

To validate the knockout, 12-14 week old male $Cd36^{fl/fl}-Cd36^{Cre-}$ and $Cd36^{fl/fl}-Cd36^{Cre+}$ mice were kept at RT or 24h at 4°C and after a 2h fast organs were collected. $Cd36^{fl/fl}-Cd36^{Cre+}$ mice had lower blood glucose levels compared to control littermates (**Figure 26A**) and higher plasma NEFA levels when cold-exposed compared to their cold-exposed control littermates (**Figure 26F**). Aside from cold-induced increase in heart weight (**Figure 26C**), no significant differences were observed in other body characteristics (**Figure 26B-E**).

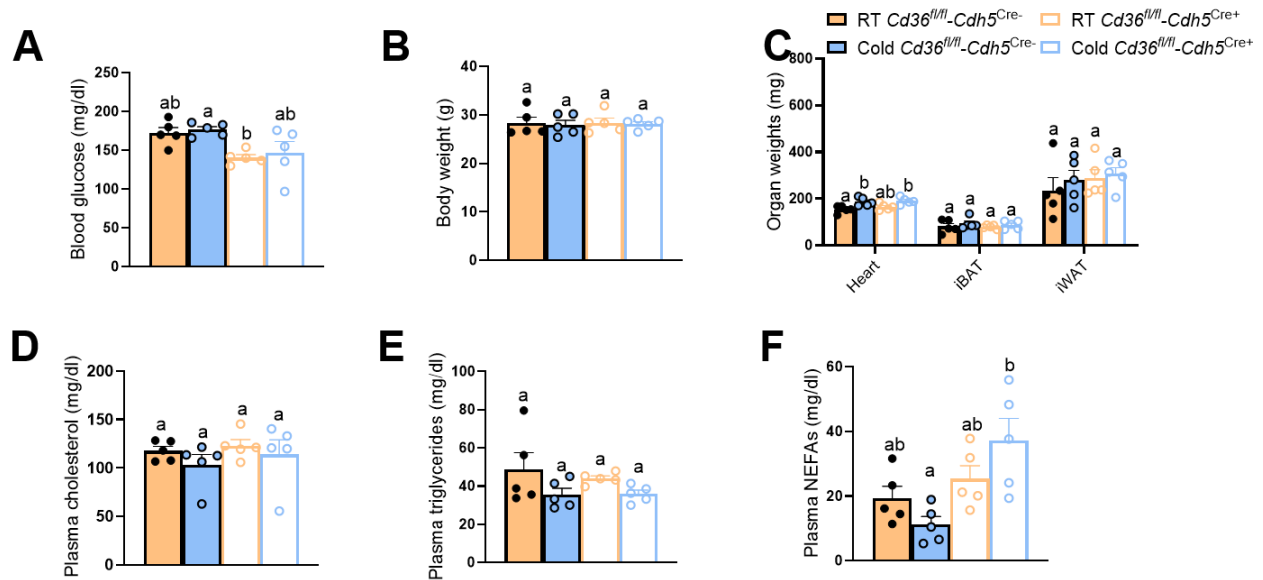


Figure 26. Body characteristics of $Cd36^{fl/fl}-Cd36^{Cre+}$ and $Cd36^{fl/fl}-Cd36^{Cre-}$ mice.

(A-F) 12-14 week old male $Cd36^{fl/fl}-Cd36^{Cre+}$ and $Cd36^{fl/fl}-Cd36^{Cre-}$ mice were housed at RT or 24h at 4°C. Mice were fasted 2h before sacrifice.

(A) Blood glucose (B) Body weight (C) Organ weights (D) Plasma cholesterol (E) Plasma TGs (F) Plasma NEFAs

Regarding *Cd36* expression as shown in **Figure 27A**, *Cd36* expression in the BAT of *Cd36^{fl/fl}-Cdh5^{Cre+}* mice did increase upon cold exposure but no knockout could be detected in *Cd36^{fl/fl}-Cdh5^{Cre+}* mice. On protein level, cold-exposed *Cd36^{fl/fl}-Cdh5^{Cre+}* mice did have decreased protein expression compared to control littermates housed at RT (**Figure 27B-C**).

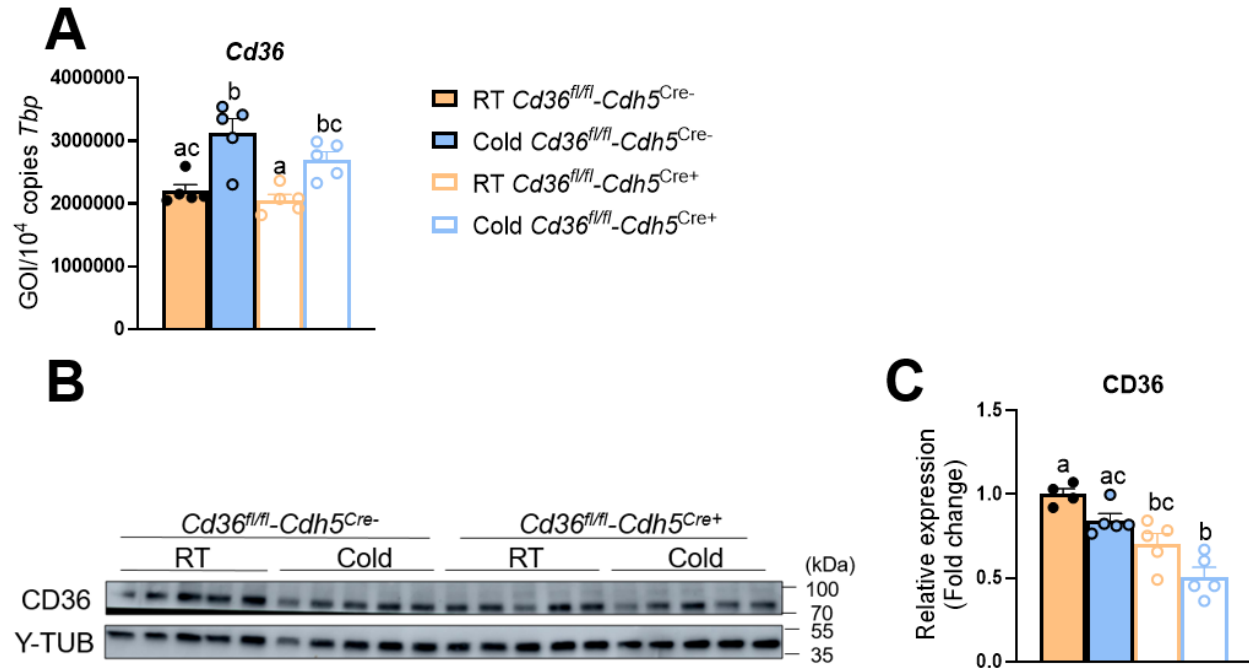


Figure 27. *Cd36^{fl/fl}-Cdh5^{Cre+}* mice have decreased CD36 protein expression compared to control littermates housed at RT.

(A-C) 12-14 week old male *Cd36^{fl/fl}-Cdh5^{Cre+}* and *Cd36^{fl/fl}-Cdh5^{Cre-}* mice were housed at RT or 24h at 4°C. Mice were fasted 2h before sacrifice.

(A) *Cd36* expression in iBAT. Gene expression was normalized for *Tbp*. (B-C) CD36 expression in iBAT. Protein expression was normalized for y-Tubulin and RT Cre- group was set to 1.

In order to validate that the knockout is cell-type specific, pieces of iBAT were used for immunofluorescence to look at the localization of CD36. In $Cd36^{fl/fl}-Cdh5^{Cre-}$ mice regardless of housing temperature, CD36 staining displays endothelial structures (tubular structures) and ring-like structures (plasma membrane of brown adipocytes) (**Figure 28A-B**). Conversely, the staining in $Cd36^{fl/fl}-Cdh5^{Cre+}$ mice regardless of temperature only shows the ring-like structures indicating adipocyte staining (**Figure 28C-D**).

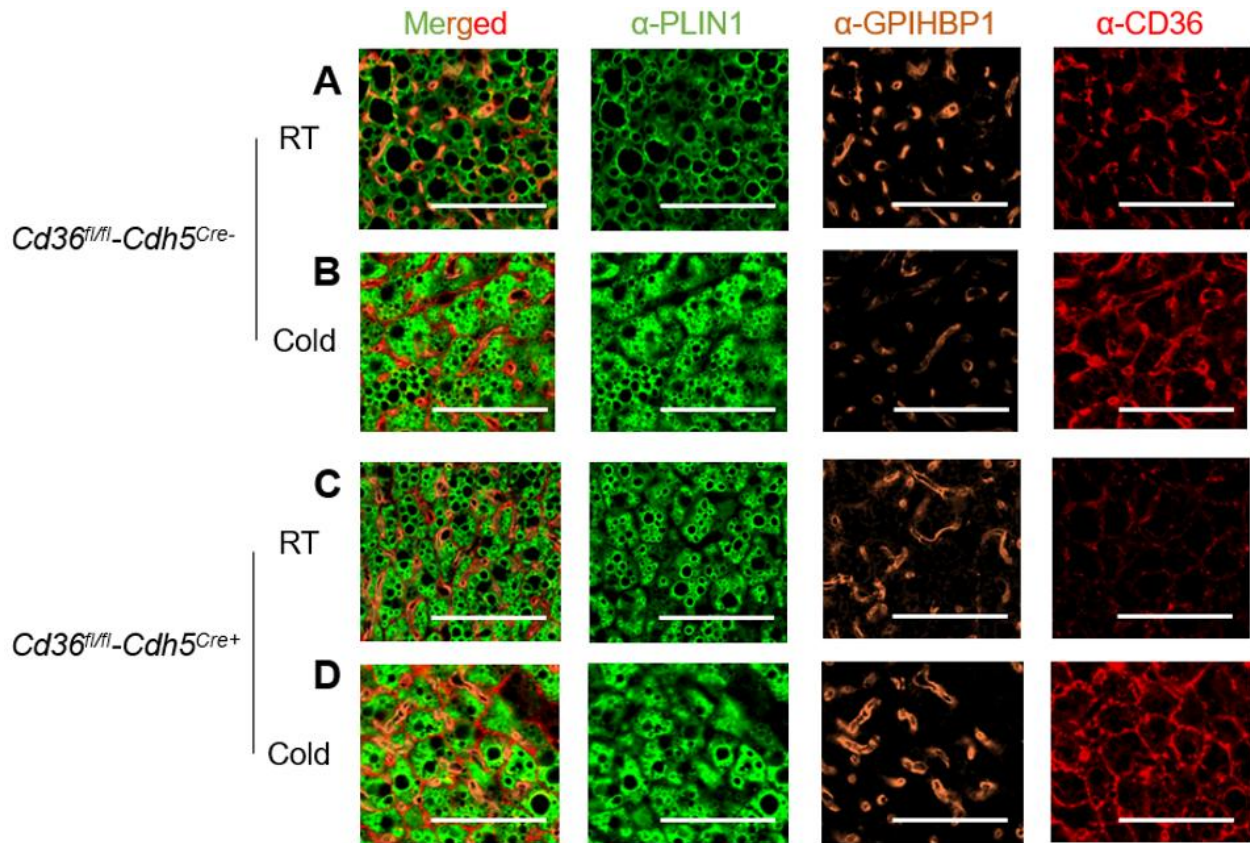


Figure 28. Localization of CD36 in iBAT of $Cd36^{fl/fl}-Cdh5^{Cre-}$ and $Cd36^{fl/fl}-Cdh5^{Cre+}$ mice.

(A-D) 12-14 week old male $Cd36^{fl/fl}-Cdh5^{Cre+}$ and $Cd36^{fl/fl}-Cdh5^{Cre-}$ mice were housed at RT or 24h at 4°C. Mice were fasted 2h before sacrifice. Paraffin sections were stained with PLIN1 (adipocyte marker), GPIHBP1 (endothelial marker) and CD36. Scale bar is 50 μ m.

(A-B) $Cd36^{fl/fl}-Ucp1^{Cre-}$ mice (A) housed at RT (B) cold-exposed

(C-D) $Cd36^{fl/fl}-Ucp1^{Cre+}$ mice (C) housed at RT (D) cold-exposed

Altogether, endothelial-specific knockout of CD36 was not detected on gene expression on whole organ level, but could be seen on protein level. Based on the immunofluorescence data, we conclude that CD36 is knocked out specifically in endothelial cells in $Cd36^{fl/fl}-Cdh5^{Cre+}$ mice.

Are $Cd36^{fl/fl}$ - $Cdh5^{Cre+}$ mice able to maintain their body temperature when exposed to cold in a fed and fasted state?

To test whether $Cd36^{fl/fl}$ - $Cdh5^{Cre+}$ mice were able to maintain their body temperature when exposed to cold, 13-19 week old female $Cd36^{fl/fl}$ - $Cdh5^{Cre-}$ and $Cd36^{fl/fl}$ - $Cdh5^{Cre+}$ mice were put in metabolic cages. Temperature was kept at 30°C for 2 days, then decreased to 22°C for 2 days and lastly decreased to 6°C for 2 days. To test whether $Cd36^{fl/fl}$ - $Cdh5^{Cre+}$ mice were able to maintain their body temperature during different nutritional states, mice were fasted each day from 6 am – 12 pm.

$Cd36^{fl/fl}$ - $Cdh5^{Cre+}$ mice had lower blood glucose levels compared to their control littermates (**Figure 29A**). No differences in body weight were observed (**Figure 29B**). $Cd36^{fl/fl}$ - $Cdh5^{Cre+}$ mice had increased heart weight and decreased iBAT weight compared to control littermates. Regarding plasma parameters in plasma cholesterol and TGs no differences were observed (**Figure 29D-E**) but $Cd36^{fl/fl}$ - $Cdh5^{Cre+}$ mice had increased plasma NEFA levels compared to $Cd36^{fl/fl}$ - $Cdh5^{Cre-}$ mice (**Figure 29F**).

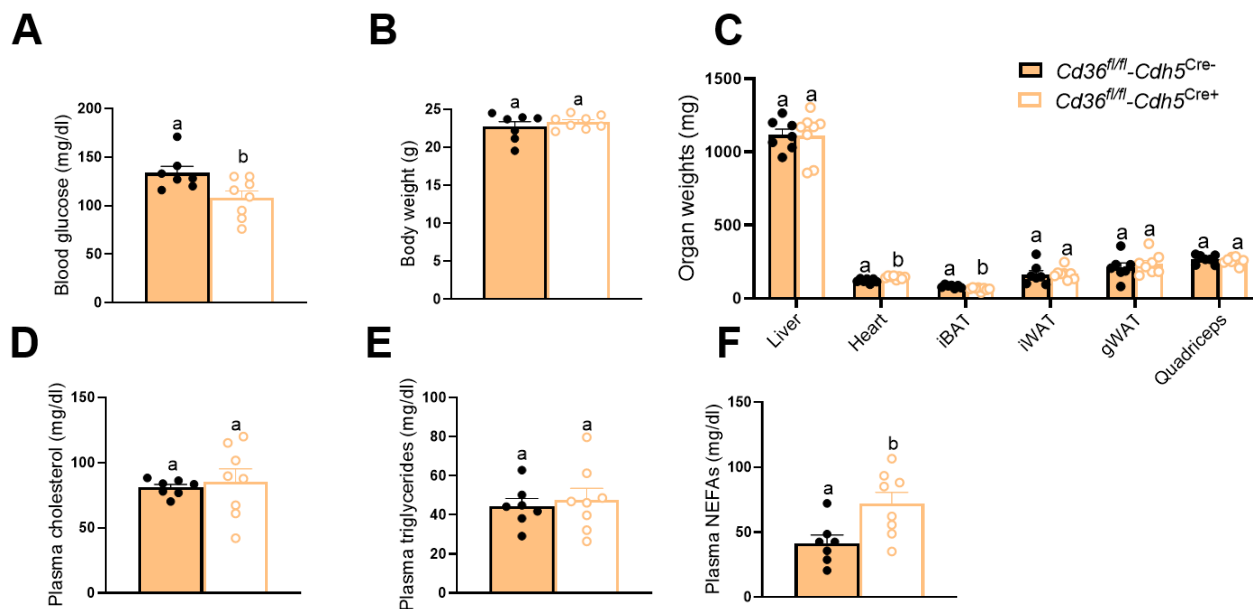


Figure 29. Body characteristics of $Cd36^{fl/fl}$ - $Cdh5^{Cre+}$ and $Cd36^{fl/fl}$ - $Cdh5^{Cre-}$ mice.

(A-F) 13-19 week old female $Cd36^{fl/fl}$ - $Cdh5^{Cre+}$ and $Cd36^{fl/fl}$ - $Cdh5^{Cre-}$ mice were put in metabolic cages. After acclimatization, temperature was kept for 2 days at 30 °C, then decreased to 22 °C for 2 days and the last 2 days were 6 °C. Mice were fasted every day from 6 am to 12 pm.

(A) Blood glucose (B) Body weight (C) Organ weights (D) Plasma cholesterol (E) Plasma TGs (F) Plasma NEFAs

Both genotypes were able to maintain their body temperature at all temperatures and in all nutritional conditions (**Figure 30A**). Energy expenditure and RER showed no major differences between the genotypes (**Figure 30B-C**). Total distance in cage (**Figure 30D**) and water intake (as a proxy for food intake) (**Figure 30E**) showed no differences.

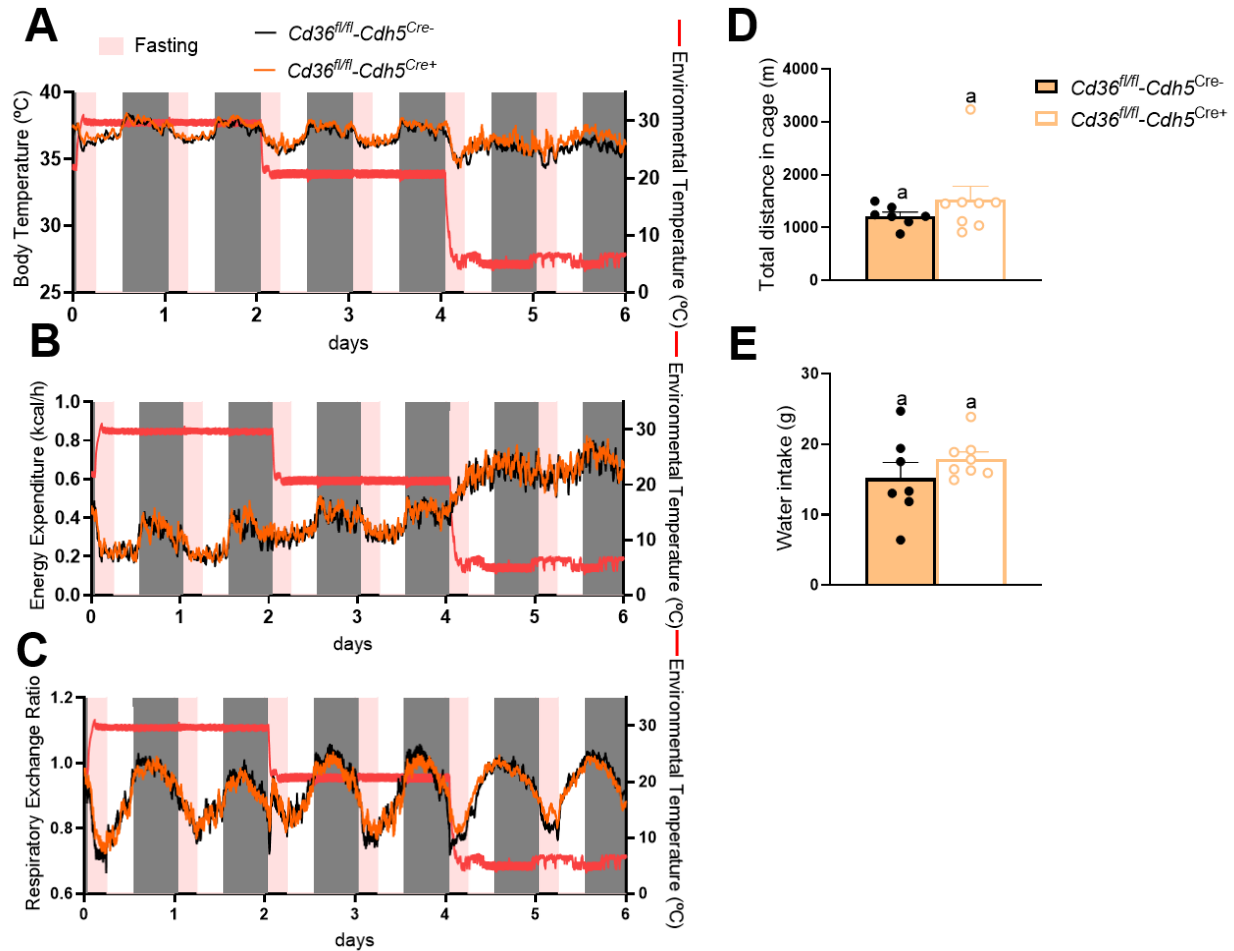


Figure 30. $Cd36^{fl/fl}-Cdh5^{Cre+/+}$ mice are able to maintain their body temperature when exposed to cold in a fed and fasted state.

(A-E) 13-19 week old female $Cd36^{fl/fl}-Cdh5^{Cre-/-}$ and $Cd36^{fl/fl}-Cdh5^{Cre+/+}$ mice were put in metabolic cages. After acclimatization, temperature was kept for 2 days at 30 °C, then decreased to 22 °C for 2 days and the last 2 days were 6 °C. Mice were fasted every day from 6 am to 12 pm.

(A) Body temperature (B) Energy expenditure (C) RER (D) Total distance in cage (E) Water intake

Thus, $Cd36^{fl/fl}-Cdh5^{Cre+/+}$ mice are able to maintain their body temperature when exposed to cold regardless of the nutritional state.

Do $Cd36^{fl/fl}$ - $Cdh5^{Cre+}$ mice have altered lipid uptake compared to control littermates at different housing temperatures?

To investigate whether $Cd36^{fl/fl}$ - $Cdh5^{Cre+}$ mice have altered lipid uptake, 13-17 week old male $Cd36^{fl/fl}$ - $Cdh5^{Cre-}$ and $Cd36^{fl/fl}$ - $Cdh5^{Cre+}$ mice were kept at RT or at 4°C for 24h and received an oral fat gavage with radioactively labelled ^3H -Triolein and a tracer of radioactively labelled ^{14}C -DOG. No differences in body characteristics were observed (**Figure 31A-C**). Regarding plasma parameters, cold-exposed $Cd36^{fl/fl}$ - $Cdh5^{Cre+}$ mice had lower plasma cholesterol levels compared to $Cd36^{fl/fl}$ - $Cdh5^{Cre+}$ mice housed at RT (**Figure 31D**). Plasma TG levels were decreased upon cold-exposure in both genotypes (**Figure 31E**) while plasma NEFA levels were increased in $Cd36^{fl/fl}$ - $Cdh5^{Cre+}$ mice housed at RT and normalized upon cold-exposure (**Figure 31F**).

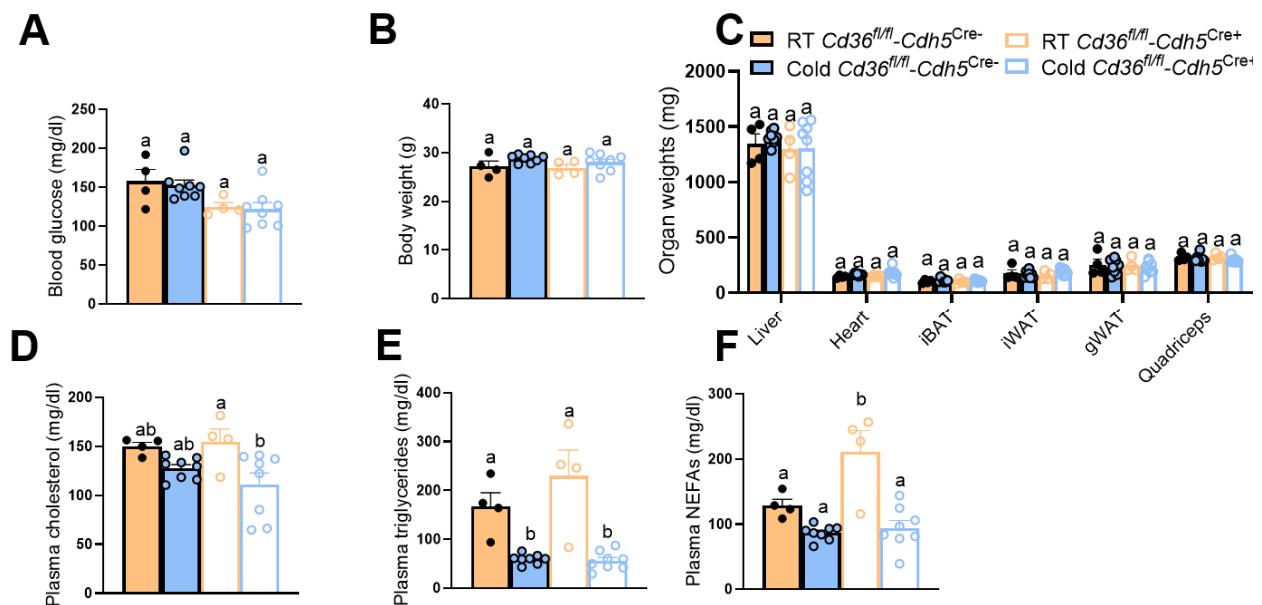


Figure 31. Body characteristics of $Cd36^{fl/fl}$ - $Cdh5^{Cre+}$ and $Cd36^{fl/fl}$ - $Cdh5^{Cre-}$ mice.

(A-F) 13-17 week old male $Cd36^{fl/fl}$ - $Cdh5^{Cre+}$ and $Cd36^{fl/fl}$ - $Cdh5^{Cre-}$ mice were kept at RT and exposed to cold (4°C) for 24h. Mice were fasted 4h in the morning and 2h before sacrifice they received an oral gavage with radio-labelled ^3H -Triolein and a tracer of ^{14}C -DOG.

(A) Blood glucose (B) Body weight (C) Organ weights (D) Plasma cholesterol (E) Plasma TGs (F) Plasma NEFAs

^3H -Triolein uptake was increased in cold-exposed mice regardless of the genotypes, whereas cold-exposed $\text{Cd}36^{\text{fl/fl}}\text{-Cd}h5^{\text{Cre}+}$ mice show a tendency to have decreased ^3H -Triolein uptake in RT compared to their cold-exposed control littermates. In line with this, cold-exposed livers of $\text{Cd}36^{\text{fl/fl}}\text{-Cd}h5^{\text{Cre}+}$ mice show an increase in ^3H -Triolein uptake which is not observed in cold-exposed $\text{Cd}36^{\text{fl/fl}}\text{-Cd}h5^{\text{Cre}-}$ mice (**Figure 32A**).

Regarding ^{14}C -DOG uptake, $\text{Cd}36^{\text{fl/fl}}\text{-Cd}h5^{\text{Cre}+}$ mice have increased uptake in the heart when housed at RT and increases even further when $\text{Cd}36^{\text{fl/fl}}\text{-Cd}h5^{\text{Cre}+}$ mice are cold-exposed. Aside from the cold-induced increase of ^{14}C -DOG in iBAT no further differences were observed (**Figure 32B**).

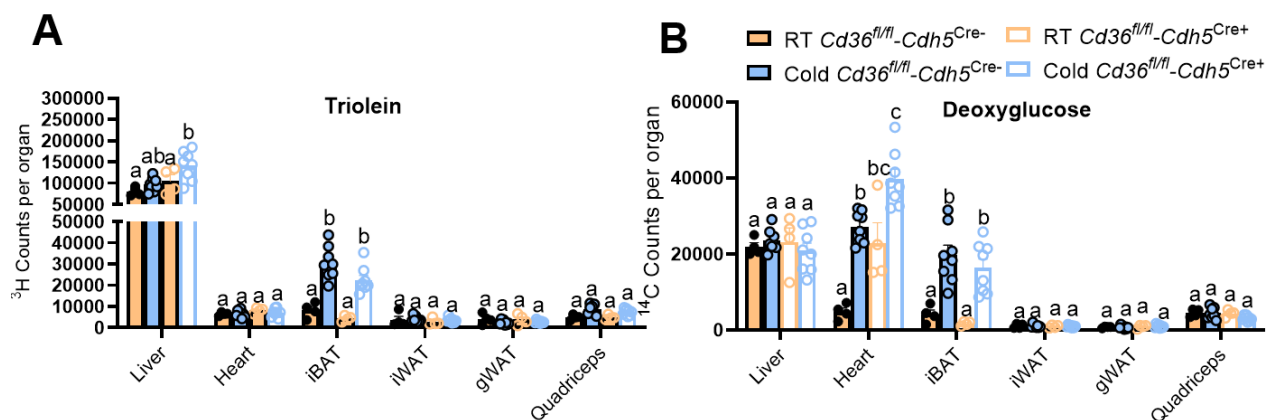


Figure 32. $\text{Cd}36^{\text{fl/fl}}\text{-Cd}h5^{\text{Cre}+}$ mice have increased DOG uptake in heart.

(A-B) 13-17 week old male $\text{Cd}36^{\text{fl/fl}}\text{-Cd}h5^{\text{Cre}+}$ and $\text{Cd}36^{\text{fl/fl}}\text{-Cd}h5^{\text{Cre}-}$ mice were kept at RT and exposed to cold (4°C) for 24h. Mice were fasted 4h in the morning and 2h before sacrifice they received an oral gavage with radio-labelled ^3H -Triolein and a tracer of ^{14}C -DOG.

(A) ^3H -Triolein counts per organ (B) ^{14}C -DOG counts per organ

We conclude that $\text{Cd}36^{\text{fl/fl}}\text{-Cd}h5^{\text{Cre}+}$ mice do not have altered lipid uptake compared to control littermates regardless of housing conditions. However, $\text{Cd}36^{\text{fl/fl}}\text{-Cd}h5^{\text{Cre}+}$ mice do have increased ^{14}C -DOG uptake in heart compared to control littermates regardless of housing conditions.

Do *Cd36^{fl/fl}-Cdh5^{Cre+}* mice have altered gene expression in BAT and WAT compared to control littermates at different housing temperatures?

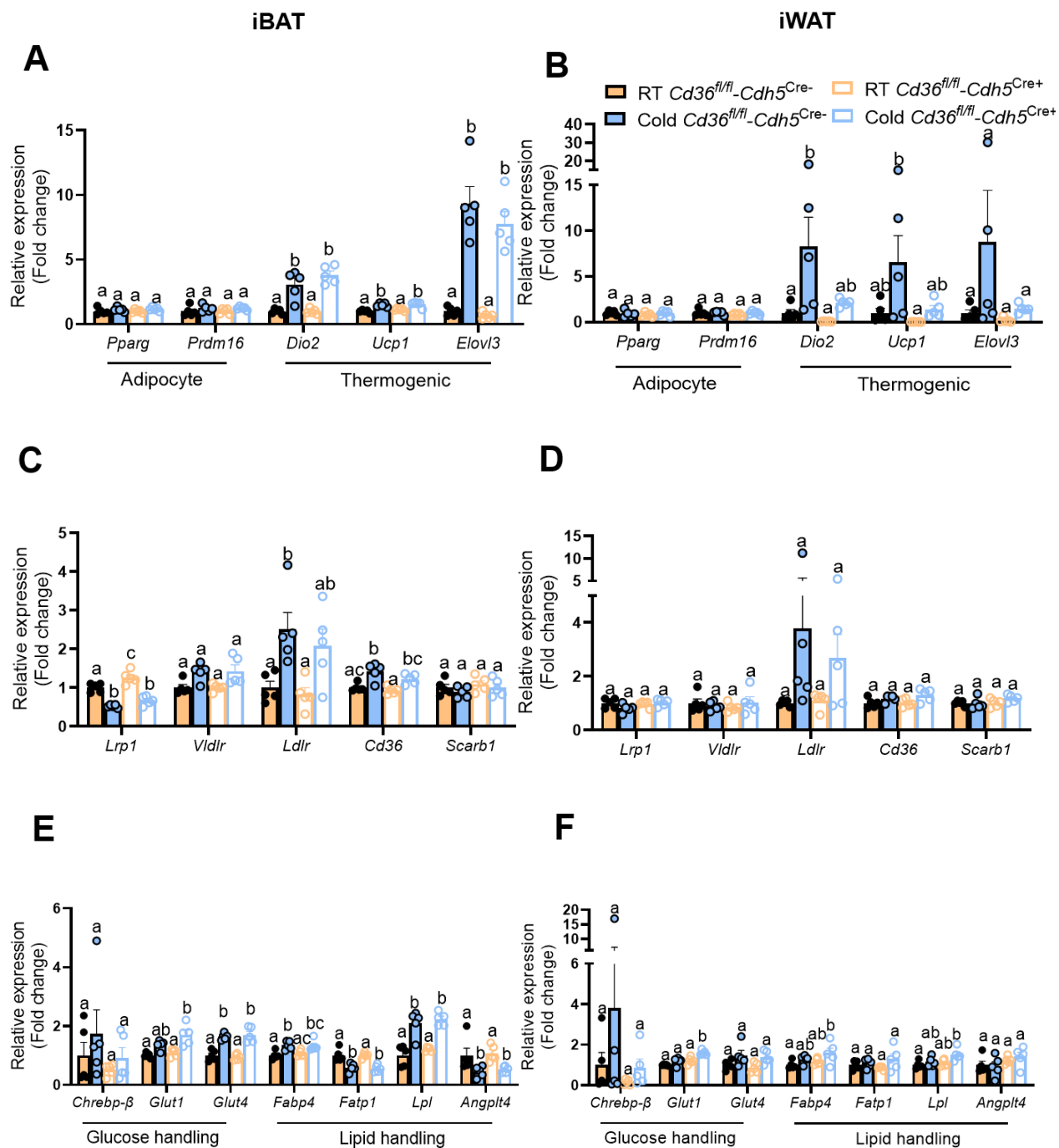
To check whether an endothelial-specific knockout of *Cd36* affects gene expression in BAT and WAT, we quantified expression of thermogenic markers, receptor as well as glucose and lipid handling genes in iBAT and iWAT of *Cd36^{fl/fl}-Cdh5^{Cre-}* and *Cd36^{fl/fl}-Cdh5^{Cre+}* mice kept at RT or at 4°C for 24h.

No differences were observed in *Pparγ* and *Prdm16* expression in BAT and WAT. Thermogenic markers *Dio2*, *Cdh5* and *Elovl3* were increased in BAT upon cold exposure and showed no differences between the genotypes (**Figure 33A**). In WAT, cold-exposure did increase *Ucp1* and *Dio2* expression but in cold-exposed *Cd36^{fl/fl}-Cdh5^{Cre+}* mice this increase was blunted compared to cold-exposed littermates (**Figure 33B**). No major differences in *Pparγ*, *Prdm16* and *Elovl3* expression were seen between the genotypes and housing temperatures in WAT (**Figure 33B**).

In BAT, *Cd36* expression was increased upon cold-exposure regardless of the genotype, but no knockout could be observed (**Figure 33C**). Expression of LDL receptor-related protein-1 (*Lrp1*), which interacts with VLDL particles and chylomicrons and is expressed by adipocytes (Hofmann *et al.*, 2007), was highest in *Cd36^{fl/fl}-Cdh5^{Cre+}* mice housed at RT. Cold-exposure decreased the expression of *Lrp1* to a similar level as cold-exposed *Cd36^{fl/fl}-Cdh5^{Cre-}* mice. Regarding expression of other receptors, aside from cold-induced effects no major differences were observed in BAT and WAT between the genotypes and housing temperatures (**Figure 33C-D**).

Regarding glucose handling genes, cold-exposed *Cd36^{fl/fl}-Cdh5^{Cre+}* mice had increased *Glut1* expression compared to cold-exposed control littermates in BAT and WAT. Aside from cold-induced increase in *Glut4* expression in BAT (**Figure 33E**), no major differences in gene expression of glucose handling were observed in BAT and WAT (**Figure 33E-F**).

Regarding lipid handling genes, mainly cold-induced increases or decreases were observed in BAT and WAT. Overall, cold-exposed *Cd36^{fl/fl}-Cdh5^{Cre+}* mice have decreased expression of thermogenic markers in WAT.



Endothelial-specific SR-B1ko mice

Validating endothelial-specific knockout of SR-B1 in *Scarb1^{fl/fl}-Cdh5^{Cre+}* mice

To validate the knockout model, we used MACS to separate the CD31⁺ endothelial cells (CD31), CD11b⁺ macrophages (CD11b) and mature adipocyte (mA) fraction isolated from iBAT of chow-fed *Scarb1^{fl/fl}-Cdh5^{Cre+}* and *Scarb1^{fl/fl}-Cdh5^{Cre-}* mice kept at RT.

The endothelial fraction of *Scarb1^{fl/fl}-Cdh5^{Cre+}* mice had decreased *Scarb1* expression compared to *Scarb1^{fl/fl}-Cdh5^{Cre-}* mice while the other fractions did not (**Figure 34A**). To confirm the specificity of the sorting, we measured genes specific for mature adipocytes (*Ucp1*, **Figure 34B**), endothelium (*Gpihbp1*, **Figure 34C**) and macrophages (adhesion G protein-coupled receptor E (*Adgre*), **Figure 34D**). *Adgre* and *Ucp1* expression were only expressed by the macrophage fraction and mA fraction, respectively, with no differences between *Scarb1^{fl/fl}-Cdh5^{Cre+}* and *Scarb1^{fl/fl}-Cdh5^{Cre-}* mice. *Gpihbp1* was expressed by the endothelial fraction as well as the mA fraction. This is probably explained by a contaminating association of endothelial cells in the brown adipocyte fraction. This could also explain the alleged decrease in *Scarb1* expression of *Scarb1^{fl/fl}-Cdh5^{Cre+}* mice (**Figure 34A**).

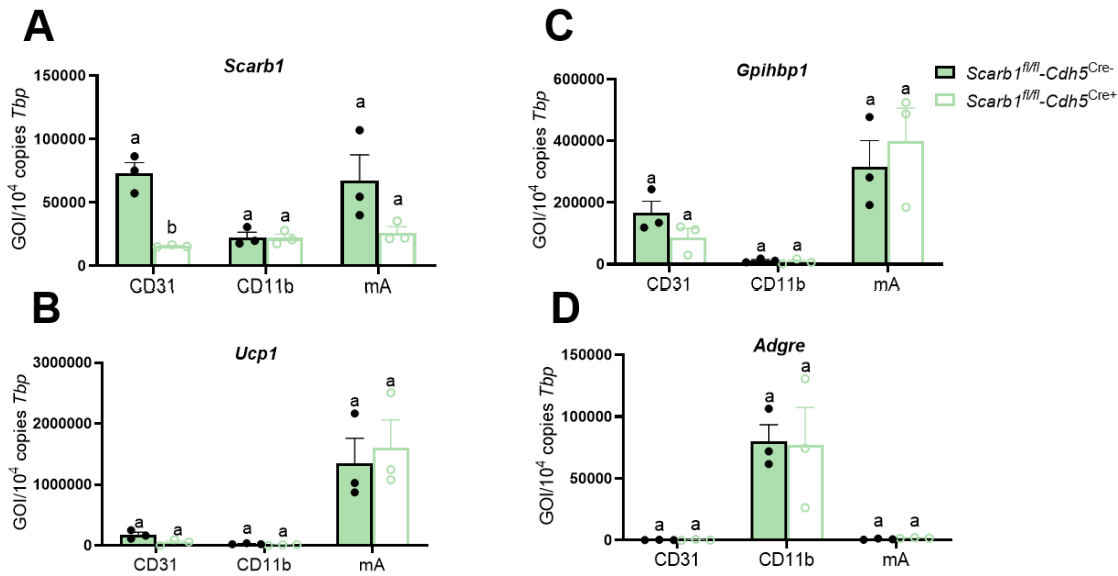


Figure 34. SR-B1 knockout is endothelial cell-specific.

(A-D) 15-18 week old female *Scarb1^{fl/fl}-Cdh5^{Cre+}* and *Scarb1^{fl/fl}-Cdh5^{Cre-}* mice were housed at 22°C and fed a chow diet (n=3; 4 BATs per pool). Gene expression in CD31⁺ endothelial cells, CD11b⁺ macrophages and mature adipocyte fraction isolated from BAT. Gene expression was normalized for *Tbp*.

(A) *Scarb1* expression (B) *Ucp1* expression (C) *Gpihbp1* expression (D) *Adgre* expression

Overall, the decrease in *Scarb1* expression was only observed in the endothelial fraction of *Scarb1^{fl/fl}-Cdh5^{Cre+}* mice, therefore we conclude that the knockout of SR-B1 is specific for endothelial cells.

Can an endothelial knockout of SR-B1 be detected on gene expression on whole organ level in *Scarb1^{fl/fl}-Cdh5^{Cre+}* mice?

To characterize the *Scarb1^{fl/fl}-Cdh5^{Cre+}* mice further, gene expression analysis was done in different organs of chow-fed *Scarb1^{fl/fl}-Cdh5^{Cre+}* and *Scarb1^{fl/fl}-Cdh5^{Cre-}* mice kept at RT.

Regarding body characteristics, no differences were observed between the genotypes except for *Scarb1^{fl/fl}-Cdh5^{Cre+}* had increased liver weight compared to control littermates (**Figure 35A-G**).

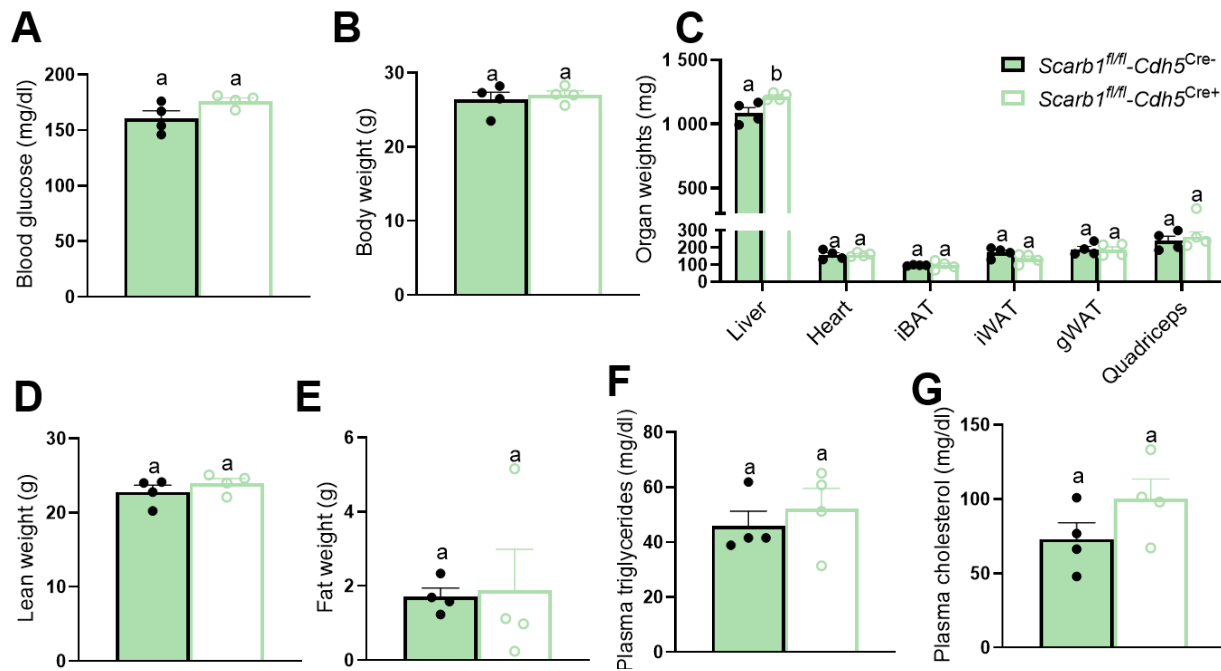


Figure 35. Body characteristics of *Scarb1^{fl/fl}-Cdh5^{Cre+}* and *Scarb1^{fl/fl}-Cdh5^{Cre-}* mice.

(A-G) 17-18 week old female and *Scarb1^{fl/fl}-Cdh5^{Cre+}* and *Scarb1^{fl/fl}-Cdh5^{Cre-}* mice were housed at 22°C and fed a chow diet. Only data from males are shown

(A) Blood glucose (B) Body weight (C) Organ weight (D) Lean weight (E) Fat weight (F) Plasma TGs (G) Plasma cholesterol

Interestingly, an endothelial-specific knockout of SR-B1 led to a decrease in *Scarb1* gene and SR-B1 protein expression on whole organ level for heart, iBAT, iWAT, gonadal WAT (gWAT) and quadriceps in *Scarb1^{fl/fl}-Cdh5^{Cre+}* mice compared to *Scarb1^{fl/fl}-Cdh5^{Cre-}* mice (**Figure 36A-C**). Underlining the contribution of the endothelial cells to whole organ expression. No differences in *Scarb1* and SR-B1 expression were observed in liver and adrenal glands of *Scarb1^{fl/fl}-Cdh5^{Cre+}* mice compared to *Scarb1^{fl/fl}-Cdh5^{Cre-}* mice (**Figure 36A-C**), as the main cells expressing SR-B1 in these organs are liver sinusoidal endothelial cells (Ganesan *et al.*, 2016) which are not affected by the *Cdh5* knockout as there is little *Cdh5* expression in these cells (Medina *et al.*, 2003, 2005) and the adrenal cells, respectively (Rigotti *et al.*, 1996).

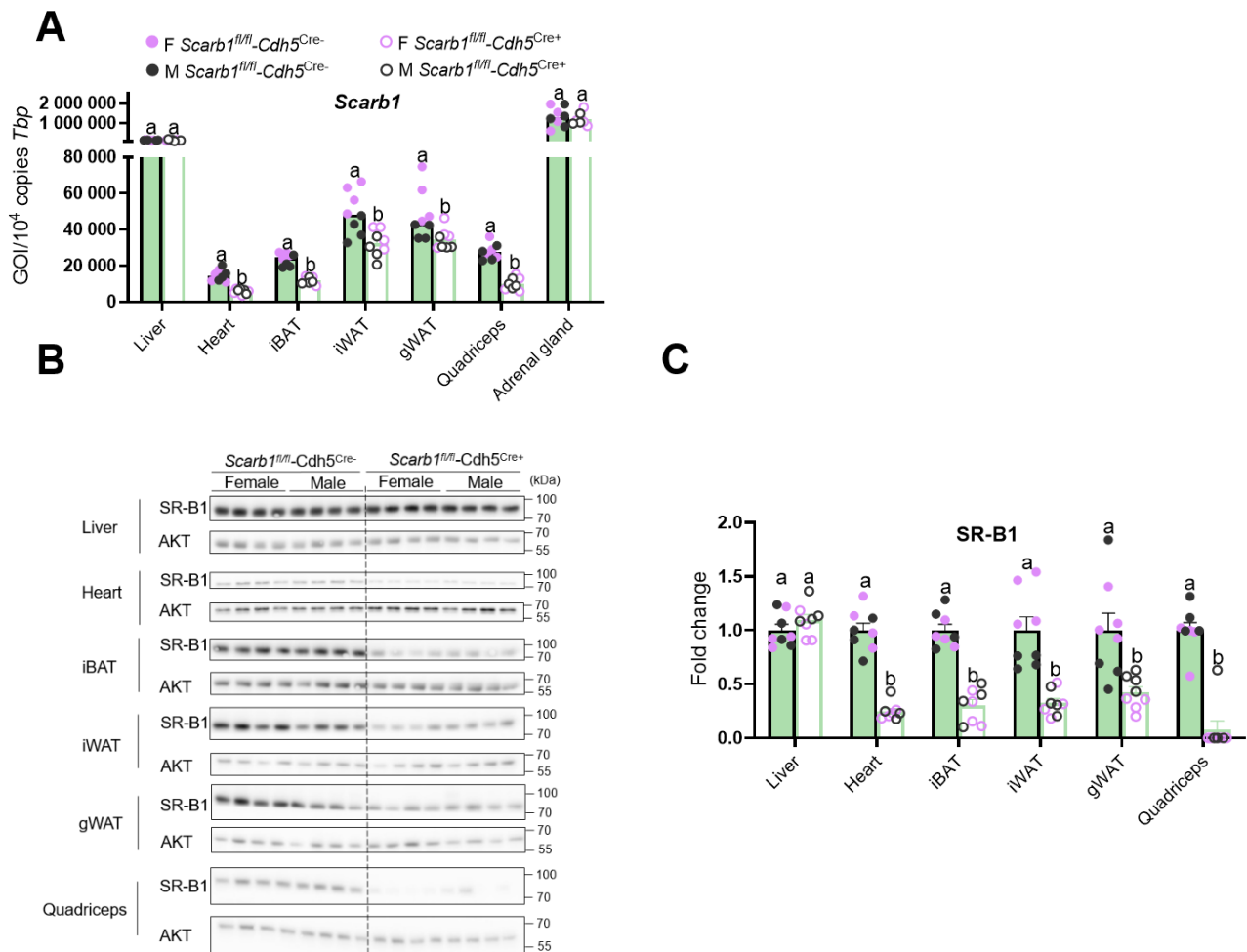


Figure 36. SR-B1 expressed by endothelial cells contributes majorly to whole organ SR-B1 expression.

(A-C) 17-18 week old female and *Scarb1^{fl/fl}-Cdh5^{Cre+}* and *Scarb1^{fl/fl}-Cdh5^{Cre-}* mice were housed at 22°C and fed a chow diet.

(A) Organ panel of *Scarb1* expression. *Scarb1* expression was normalized for *Tbp*.

(B-C) Organ panel of relative SR-B1 expression. Protein expression was normalized for AKT and the *Scarb1^{fl/fl}-Cdh5^{Cre-}* group was set to 1.

Next, we wanted to metabolically characterize the *Scarb1^{fl/fl}-Cdh5^{Cre+}* mice by housing them in metabolic cages at RT when fed a chow diet. No major differences between *Scarb1^{fl/fl}-Cdh5^{Cre+}* mice and *Scarb1^{fl/fl}-Cdh5^{Cre-}* mice were observed at RT regarding body temperature (**Figure 37A**), energy expenditure (**Figure 37B**), RER (**Figure 37C**), total distance (**Figure 37D**) and food intake (**Figure 37E**).

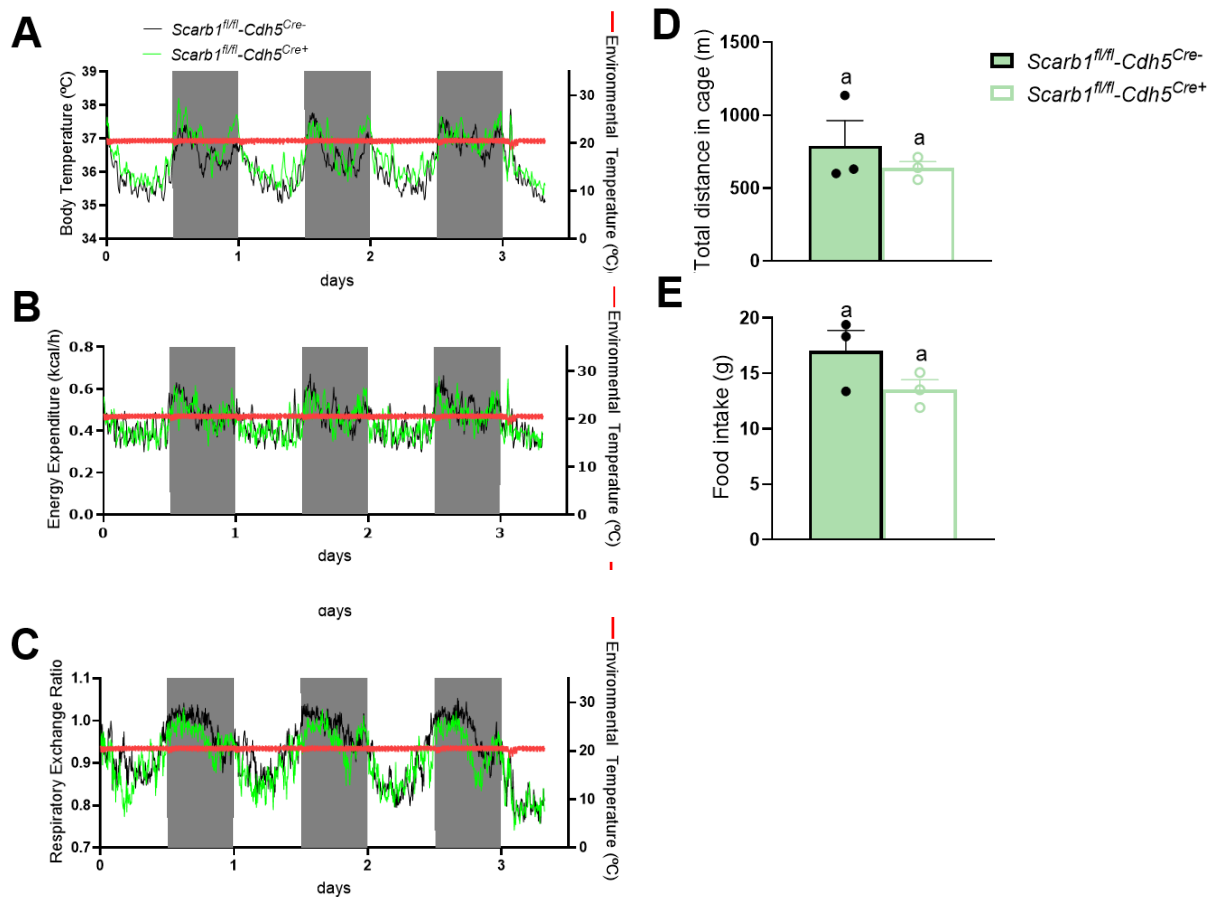


Figure 37. No differences in metabolic parameters at 22°C between *Scarb1^{fl/fl}-Cdh5^{Cre+}* and *Scarb1^{fl/fl}-Cdh5^{Cre-}* mice.

(A-E) 17-18 week old female and *Scarb1^{fl/fl}-Cdh5^{Cre+}* and *Scarb1^{fl/fl}-Cdh5^{Cre-}* mice were housed at 22°C in metabolic cages and fed a chow diet. Only data from males are shown.

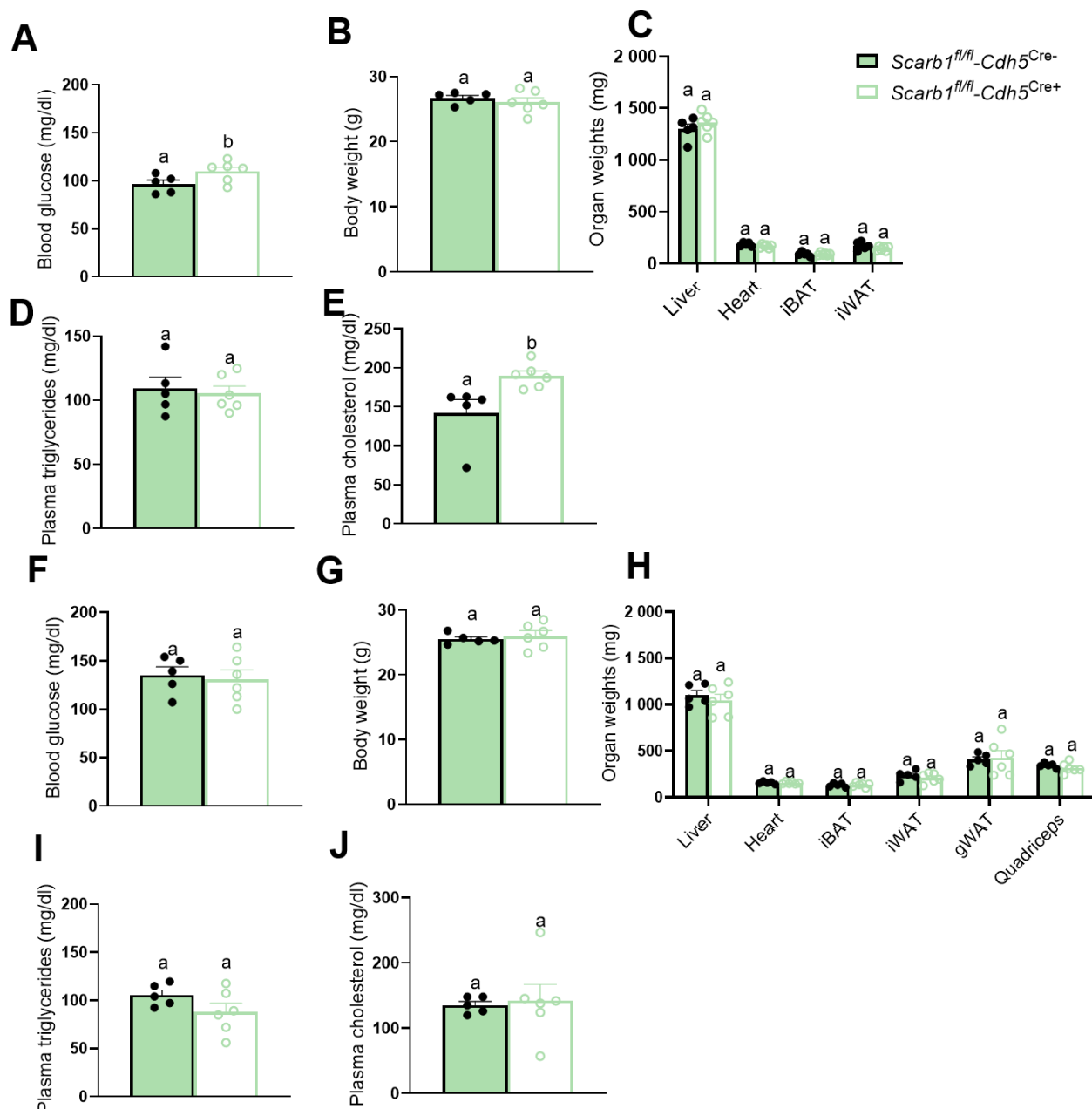
(A) Body temperature (B) Energy expenditure (C) RER (D) Total distance in cage (E) Food intake

So far, we conclude that SR-B1 expressed by endothelial cells contributes majorly to whole organ expression of heart, iBAT, iWAT, gWAT and quadriceps. *Scarb1^{fl/fl}-Cdh5^{Cre+}* mice not differ metabolically from *Scarb1^{fl/fl}-Cdh5^{Cre-}* mice at RT when fed a chow diet.

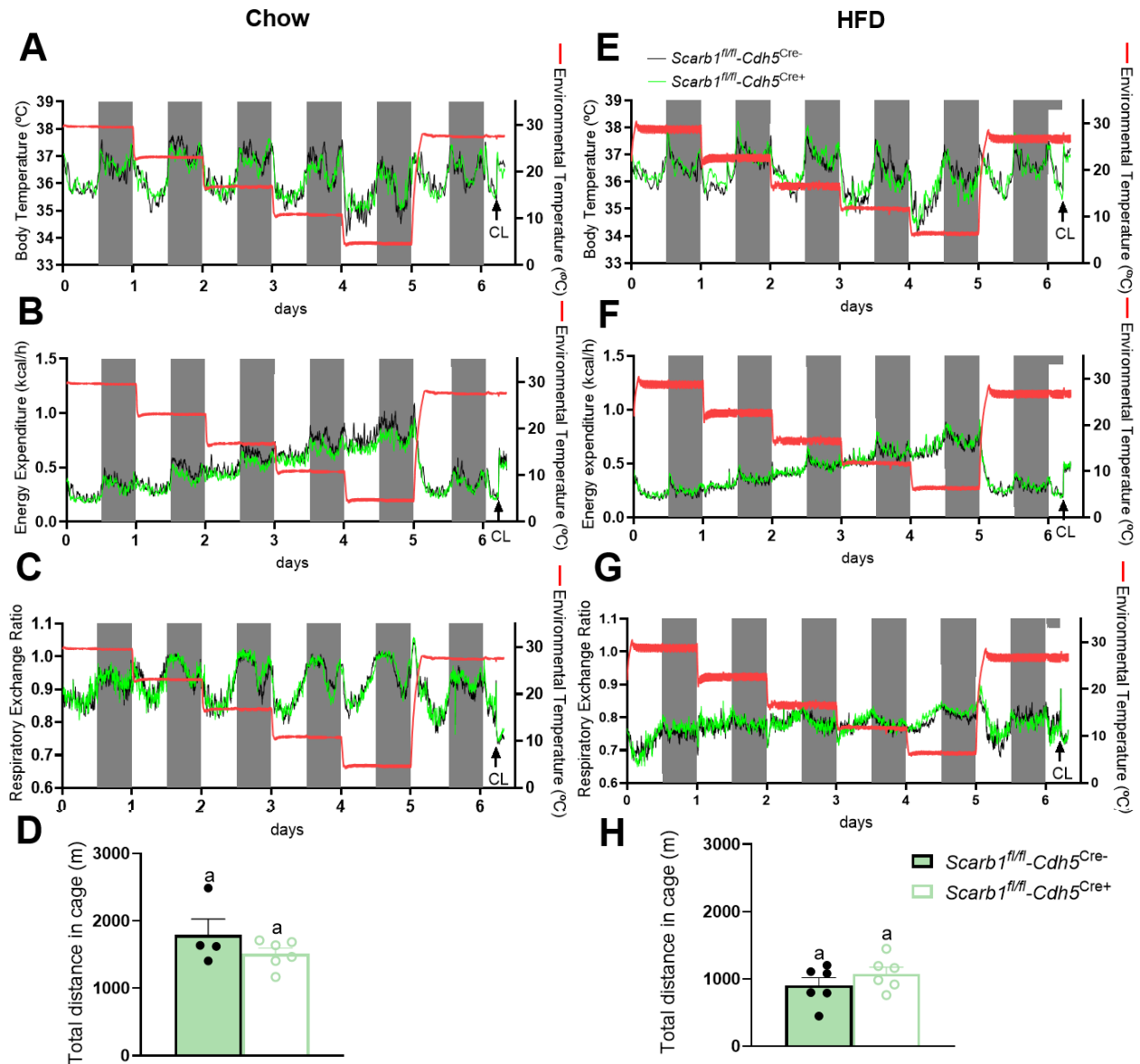
Are *Scarb1^{fl/fl}-Cdh5^{Cre+}* mice able to maintain their body temperature when the temperature is gradually decreased and is this influenced by diet?

To see whether endothelial-expressed SR-B1 affects cold adaptation, we housed *Scarb1^{fl/fl}-Cdh5^{Cre+}* mice and *Scarb1^{fl/fl}-Cdh5^{Cre-}* mice in metabolic cages and decreased the temperature from 30°C to 6°C, by decreasing the temperature each day with 6°C. The temperature was then increased to 28°C for 1.5 more day and 3h before sacrifice the mice received a CL injection, to measure the maximum oxygen consumption of the BAT. This experiment was done in chow-fed mice (**Figure 38A-E**) and mice fed a HFD for 4 weeks (**Figure 38F-J**).

Regarding body characteristics, chow-fed *Scarb1^{fl/fl}-Cdh5^{Cre+}* mice had increased blood glucose levels and plasma cholesterol levels compared to *Scarb1^{fl/fl}-Cdh5^{Cre-}* mice (**Figure 38A, E**). However, the increase in blood glucose levels and plasma cholesterol levels was not observed in *Scarb1^{fl/fl}-Cdh5^{Cre+}* mice after a HFD of 4 weeks (**Figure 38F, J**). No other differences in body characteristics were observed (**Figure 38B-D, F-J**).



Scarb1^{fl/fl}-Cdh5^{Cre+} mice were able to maintain their body temperature at all temperatures regardless of the diet (**Figure 39A, E**). The decreasing temperature resulted in an increase in energy expenditure in *Scarb1^{fl/fl}-Cdh5^{Cre+}* mice and *Scarb1^{fl/fl}-Cdh5^{Cre-}* mice (**Figure 39B, F**), as expected (Scholander *et al.*, 1950). RER differed between the diets as HFD contains little glucose and therefore the RER stayed around 0.7 and did not alternate between 0.7-1.0 as seen in the chow diet, as expected (Simonson and DeFronzo, 1990) (**Figure 39C, G**). No differences between *Scarb1^{fl/fl}-Cdh5^{Cre+}* mice and *Scarb1^{fl/fl}-Cdh5^{Cre-}* mice were observed regarding activity regardless of diet (**Figure 39D, H**).



In summary, *Scarb1^{fl/fl}-Cdh5^{Cre+}* mice were able to maintain their body temperature at all temperatures regardless of the diet. SR-B1 expressed by endothelial cells therefore is dispensable for adaptive thermogenesis.

Do *Scarb1^{fl/fl}-Cdh5^{Cre+}* mice have altered lipid uptake compared to control littermates at different housing temperatures and diet regiments?

To test whether endothelial expressed SR-B1 affects lipid and glucose uptake, we exposed *Scarb1^{fl/fl}-Cdh5^{Cre+}* mice and *Scarb1^{fl/fl}-Cdh5^{Cre-}* mice to 4°C for 24h or kept them at RT and 2h before sacrifice the mice received an OGFT with radioactive-labeled ³H-Triolein and ¹⁴C-DOG (2 g/kg). Then we measured the uptake of radioactive particles in the different organs. This experiment was done in chow-fed mice and mice fed a HFD for 4 weeks.

Regarding body characteristics, cold-exposed chow-fed *Scarb1^{fl/fl}-Cdh5^{Cre+}* mice had decreased liver weight compared to *Scarb1^{fl/fl}-Cdh5^{Cre-}* mice which was not observed in mice receiving a HFD for 4 weeks (**Figure 40C, H**). Aside from the cold-induced decrease in plasma TG levels (**Figure 40D, I**) no other differences in body characteristics were observed (**Figure 40A-B, E-H, J**).

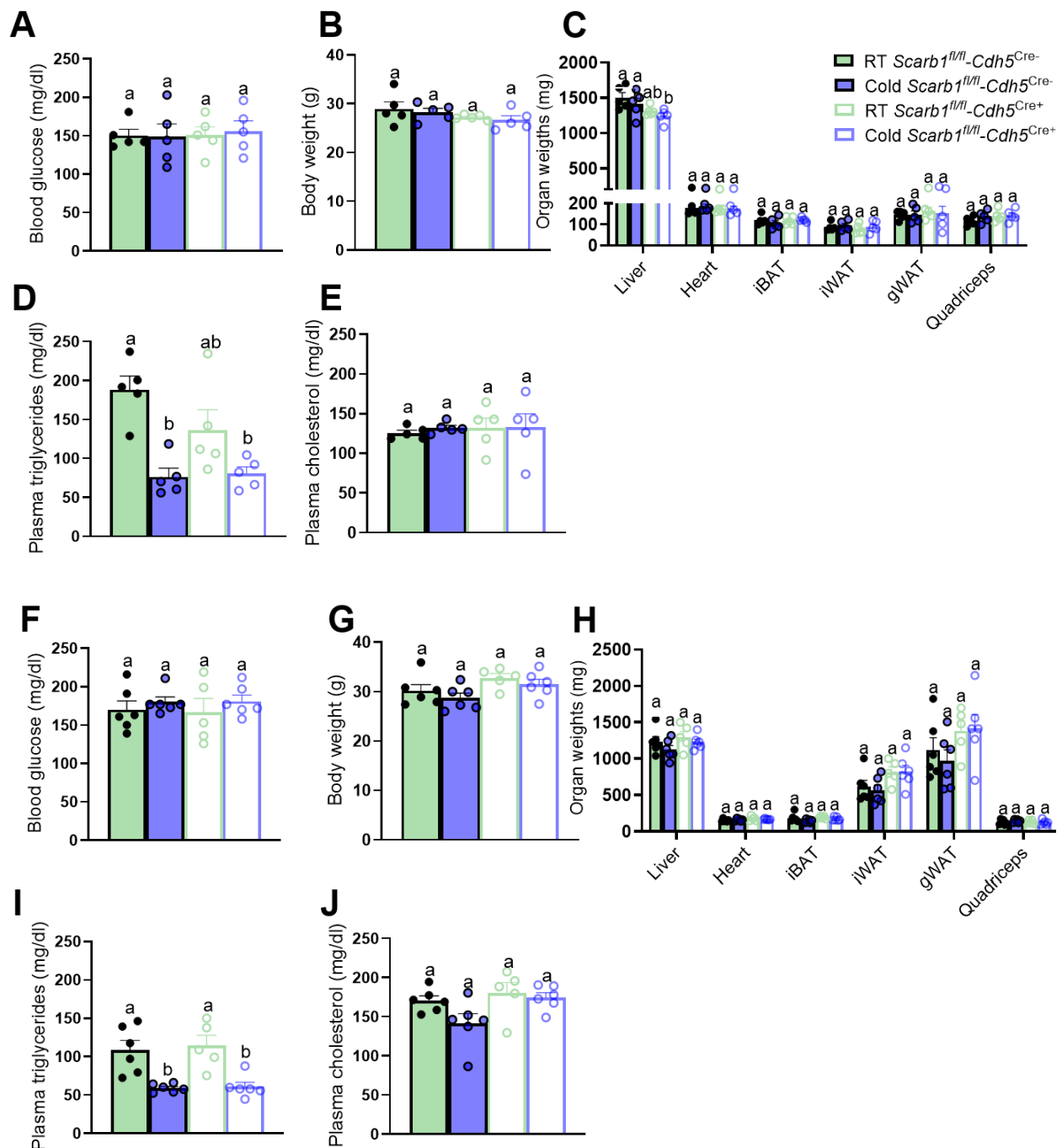


Figure 40. Body characteristics of *Scarb1*^{fl/fl}-*Cdh5*^{Cre+} and *Scarb1*^{fl/fl}-*Cdh5*^{Cre-} mice.

(A-E) 16-22 week old male *Scarb1*^{fl/fl}-*Cdh5*^{Cre+} and *Scarb1*^{fl/fl}-*Cdh5*^{Cre-} mice on a chow diet were housed at 22°C or 6°C for 24h. 2h before sacrifice the mice received an OGFT with radioactive-labeled ³H-Triolein and ¹⁴C-DOG (2g/kg).

(F-J) 11-15 week old male *Scarb1*^{fl/fl}-*Cdh5*^{Cre+} and *Scarb1*^{fl/fl}-*Cdh5*^{Cre-} mice were fed a HFD for 4 weeks and afterwards housed at 22°C or 6°C for 24h. 2h before sacrifice the mice received an OGFT with radioactive-labeled ³H-Triolein and ¹⁴C-DOG (2g/kg).

(A, F) Blood glucose (B, G) Body weight (C, H) Organ weight (D, I) Plasma TGs (E, J) Plasma cholesterol

Cold exposure increased uptake of ^3H -Triolein and ^{14}C -DOG in heart and iBAT regardless of the genotype and diet (**Figure 41A, C**). Cold exposure also increased ^3H -Triolein uptake in quadriceps of *Scarb1^{fl/fl}-Cdh5^{Cre-}* mice and slightly in cold-exposed *Scarb1^{fl/fl}-Cdh5^{Cre+}* mice fed a HFD for 4 weeks (**Figure 41C**), this was not observed in chow-fed mice (**Figure 41A**). HFD-fed cold-exposed *Scarb1^{fl/fl}-Cdh5^{Cre-}* mice showed a decrease in ^3H -Triolein uptake in gWAT, while this was not observed in HFD-fed cold-exposed *Scarb1^{fl/fl}-Cdh5^{Cre+}* mice (**Figure 41C**). Regarding ^{14}C -DOG uptake, the liver of chow-fed *Scarb1^{fl/fl}-Cdh5^{Cre-}* mice kept at RT had increased uptake of ^{14}C -DOG compared to cold-exposed mice and *Scarb1^{fl/fl}-Cdh5^{Cre+}* mice kept at RT (**Figure 41B**). Aside from cold-induced increases in ^{14}C -DOG uptake in heart and iBAT, no major differences were observed between *Scarb1^{fl/fl}-Cdh5^{Cre+}* mice and control littermates (**Figure 41B, D**).

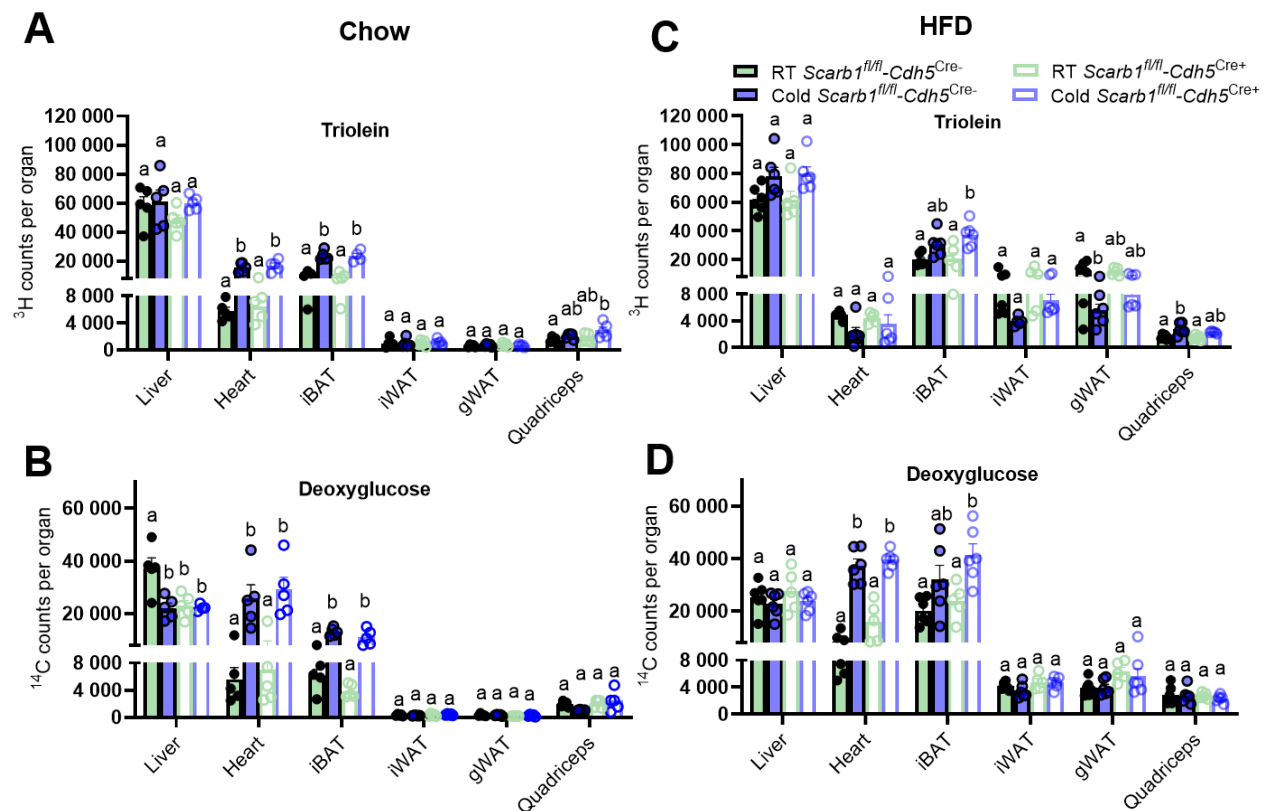


Figure 41. No differences in lipid and glucose uptake between *Scarb1^{fl/fl}-Cdh5^{Cre+}* and *Scarb1^{fl/fl}-Cdh5^{Cre-}* mice on chow and HFD at different housing conditions.

(A-B) 16-22 week old male *Scarb1^{fl/fl}-Cdh5^{Cre+}* and *Scarb1^{fl/fl}-Cdh5^{Cre-}* mice on a chow diet were housed at 22°C or 6°C for 24h. 2h before sacrifice the mice received an OGFT with radioactive-labeled ^3H -Triolein and ^{14}C -DOG (2g/kg).

(C-D) 11-15 week old male *Scarb1^{fl/fl}-Cdh5^{Cre+}* and *Scarb1^{fl/fl}-Cdh5^{Cre-}* mice were fed a HFD for 4 weeks and afterwards housed at 22°C or 6°C for 24h. 2h before sacrifice the mice received an OGFT with radioactive-labeled ^3H -Triolein and ^{14}C -DOG (2g/kg).

(A, C) ^3H -Triolein counts per organ (B, D) ^{14}C -DOG counts per organ

In summary, no major differences were observed in lipid and glucose uptake between *Scarb1^{fl/fl}-Cdh5^{Cre-}* and *Scarb1^{fl/fl}-Cdh5^{Cre+}* mice regardless of diet and housing conditions. Therefore, we conclude that SR-B1 expressed by endothelial cells is dispensable for lipid and glucose uptake.

Do *Scarb1^{fl/fl}-Cdh5^{Cre+}* mice have altered gene expression in BAT and WAT compared to control littermates at different housing temperatures and diet regiments?

To test whether the lack of differences in metabolic parameters is due to an alteration of thermogenic marker expression, we exposed chow-fed *Scarb1^{fl/fl}-Cdh5^{Cre+}* mice and *Scarb1^{fl/fl}-Cdh5^{Cre-}* mice to 4°C for 24h or kept them at RT and checked then the gene expression of iBAT and iWAT.

In iBAT, *Ucp1*, *Elovl3*, *Dio2*, *Ppargc1a* and *Lpl* expression increased upon cold exposure regardless of the genotype. *Scarb1^{fl/fl}-Cdh5^{Cre+}* mice have increased expression of *Dio2* and *Ppargc1a* upon cold compared to mice kept at RT or cold-exposed *Scarb1^{fl/fl}-Cdh5^{Cre-}* mice while no other differences were observed (**Figure 42A**). In iWAT, despite a high standard variation, we did observe an increase or trend to increase in *Ucp1*, fatty acid synthase (*Fasn*), *Elovl3*, *Ppargc1a* expression upon cold exposure regardless of the genotype (**Figure 42B**).

To test whether the lack of differences is due to a compensatory mechanism, we checked receptor gene expression in iBAT and iWAT. In iBAT, *Scarb1* expression was decreased in *Scarb1^{fl/fl}-Cdh5^{Cre+}* mice irrespective of housing conditions compared to *Scarb1^{fl/fl}-Cdh5^{Cre-}* mice (**Figure 42C**). Aside from the cold triggered increase in *Ldlr* and *Glut4* expression and decrease in *Lrp1* expression, no differences were observed between *Scarb1^{fl/fl}-Cdh5^{Cre+}* mice and *Scarb1^{fl/fl}-Cdh5^{Cre-}* mice regardless of the housing temperature (**Figure 42C**). In iWAT, *Scarb1* expression was decreased in *Scarb1^{fl/fl}-Cdh5^{Cre+}* mice kept at RT, but not in cold-exposed *Scarb1^{fl/fl}-Cdh5^{Cre+}* mice compared to *Scarb1^{fl/fl}-Cdh5^{Cre-}* mice regardless of housing temperature (**Figure 42D**). *Ldlr* expression showed a cold-induced increase in cold-exposed *Scarb1^{fl/fl}-Cdh5^{Cre-}* mice compared to *Scarb1^{fl/fl}-Cdh5^{Cre-}* mice kept at RT, the same trend was seen in *Scarb1^{fl/fl}-Cdh5^{Cre+}* mice. *Cd36* expression was increased in cold-exposed *Scarb1^{fl/fl}-Cdh5^{Cre+}* mice compared to cold-exposed *Scarb1^{fl/fl}-Cdh5^{Cre-}* mice. *Glut1* expression was increased in cold-exposed *Scarb1^{fl/fl}-Cdh5^{Cre+}* mice compared to *Scarb1^{fl/fl}-Cdh5^{Cre+}* mice kept at RT and *Scarb1^{fl/fl}-Cdh5^{Cre-}* mice. (**Figure 42D**).

To check whether HFD would affect thermogenic marker and receptor expression in iBAT and iWAT of *Scarb1^{fl/fl}-Cdh5^{Cre+}* mice and *Scarb1^{fl/fl}-Cdh5^{Cre-}* mice, we fed mice a HFD for 4 weeks before we repeated the experiment and 2h before sacrifice the mice received an OGFT with radioactive-labeled ³H-Triolein and ¹⁴C-DOG. Other than the cold triggered increase in several marker genes and a cold-induced decrease in the case of *Fasn*, no genotype differences between *Scarb1^{fl/fl}-Cdh5^{Cre+}* mice and *Scarb1^{fl/fl}-Cdh5^{Cre-}* mice in iBAT were observed (**Figure 42E**). In iWAT, due to the high variance in expression levels, we only observed a tendency that *Ucp1*, *Dio2*, *Elovl3*, and *Ppargc1a* increased upon cold exposure regardless of the genotype (**Figure 42F**), no other differences were observed.

Besides decreased *Scarb1* expression in iBAT and iWAT of *Scarb1^{fl/fl}-Cdh5^{Cre+}* mice compared to *Scarb1^{fl/fl}-Cdh5^{Cre-}* mice regardless of housing temperature (**Figure 42G-H**), *Ldlr* expression was also decreased in iBAT of cold-exposed *Scarb1^{fl/fl}-Cdh5^{Cre+}* mice and the same trend was observed in *Scarb1^{fl/fl}-Cdh5^{Cre+}* mice kept at RT compared to *Scarb1^{fl/fl}-Cdh5^{Cre-}* mice regardless of housing temperature (**Figure 42G**). In iWAT, cold-exposed *Scarb1^{fl/fl}-Cdh5^{Cre+}* mice had lower *Ldlr* expression compared to *Scarb1^{fl/fl}-Cdh5^{Cre-}* mice kept at RT, no other differences were observed **Figure 42H**). In iBAT, other than the tendency of cold-triggered increased expression of *Cd36*, *Vldlr*, *Scarb2* and *Glut4*, or decrease of *Lrp1* (**Figure 42G**), no increase in a receptor was observed that could act as a compensatory mechanism for the loss of endothelial expressed SR-B1.

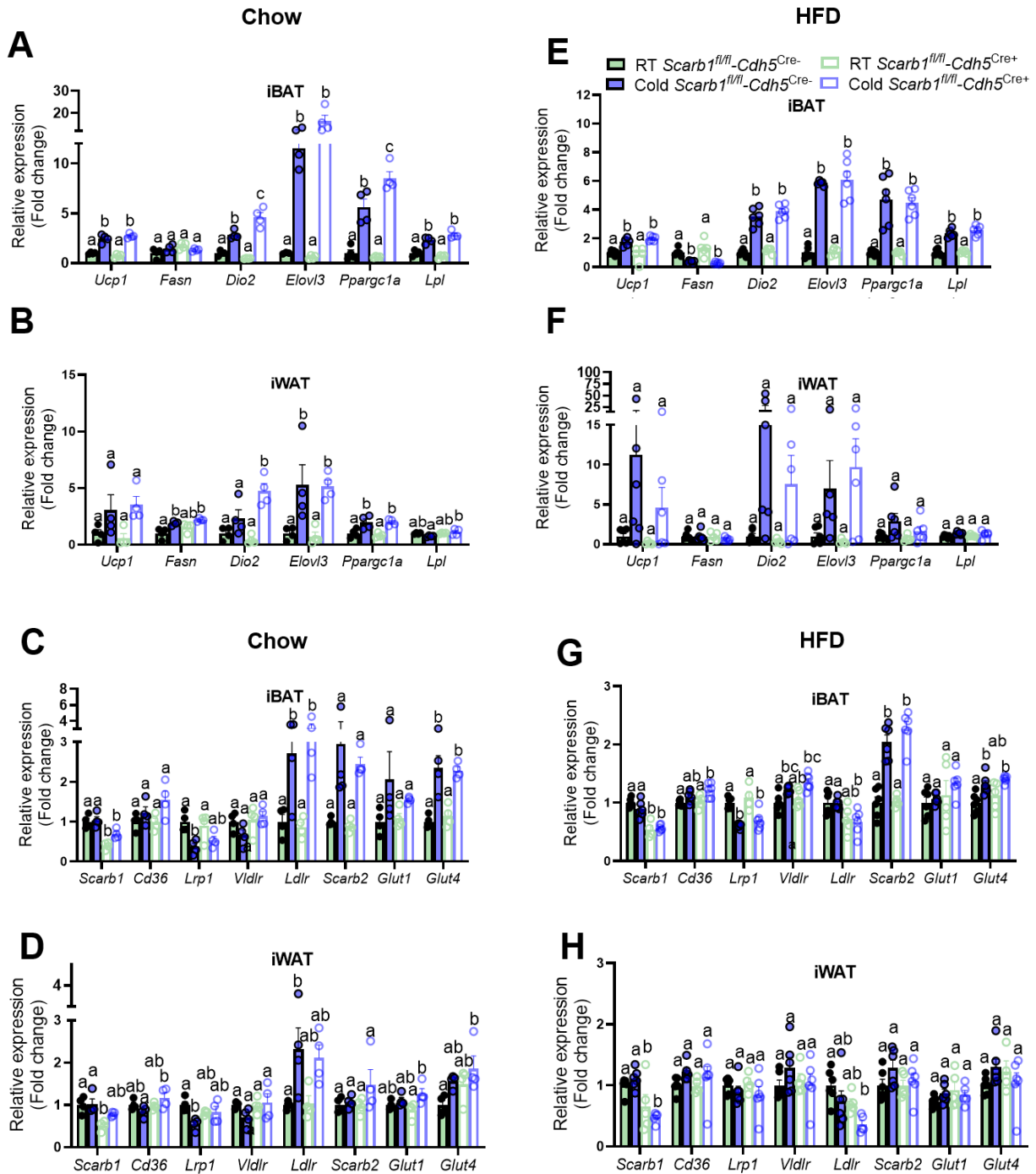


Figure 42. No differences in thermogenic marker and receptor expression in iBAT and iWAT between *Scarb1^{fl/fl}-Cdh5^{Cre+}* and *Scarb1^{fl/fl}-Cdh5^{Cre-}* mice on chow and HFD at different housing conditions.

(A-D) 10-13 week old female *Scarb1^{fl/fl}-Cdh5^{Cre+}* and *Scarb1^{fl/fl}-Cdh5^{Cre-}* mice were housed at 22°C or 4°C for 24h and fed a chow diet. (E-H) 11-15 week old male *Scarb1^{fl/fl}-Cdh5^{Cre+}* and *Scarb1^{fl/fl}-Cdh5^{Cre-}* mice were fed a HFD for 4 weeks and afterwards housed at 22°C or 4°C for 24h. 2h before sacrifice the mice received an OGFT with radioactive-labeled ³H-Triolein and ¹⁴C-DOG (2g/kg).

(A-B, E-F) Relative thermogenic marker expression in (A, E) iBAT (B, F) iWAT (C-D, G-H). Relative receptor expression in (C, G) iBAT (D, H) iWAT.

102

Gene expression was normalized for *Tbp* and RT *Scarb1^{fl/fl}-Cdh5^{Cre-}* group was set to 1.

Overall, although chow-fed cold-exposed *Scarb1^{fl/fl}-Cdh5^{Cre+}* mice have slightly increased thermogenic marker gene expression compared to cold-exposed littermates, no compensatory mechanisms could be detected that could explain the lack of differences regarding their capacity to do thermogenesis. Furthermore, knockout of SR-B1 in endothelial cells is not compensated by altered receptor gene expression.

Do *Scarb1^{fl/fl}-Cdh5^{Cre+}* mice have altered uptake of cholesteryl ethers and selective cholesterol uptake compared to *Scarb1^{fl/fl}-Cdh5^{Cre-}* mice?

As SR-B1 expressed by endothelial cells does not seem to play a role in adaptive thermogenesis or glucose and lipid uptake and since SR-B1 plays an important role in HDL metabolism, we were wondering if endothelial SR-B1 played a specific role in HDL metabolism. To test this, we performed a HDL turnover experiment where we injected radioactively-labeled HDL particles with radioactively-labeled ¹²⁵I HDL-apolipoprotein and ³H-cholesteryl ether in chow-fed *Scarb1^{fl/fl}-Cdh5^{Cre-}* and *Scarb1^{fl/fl}-Cdh5^{Cre+}* mice kept at RT.

No differences were observed in plasma FCR between *Scarb1^{fl/fl}-Cdh5^{Cre-}* and *Scarb1^{fl/fl}-Cdh5^{Cre+}* mice (**Figure 43A-C**). Liver and kidney are used as controls, as they take up high amounts of CEs and the apolipoprotein respectively (Pittman and Steinberg, 1984; Glass *et al.*, 1985), here we did not observe any differences between *Scarb1^{fl/fl}-Cdh5^{Cre-}* and *Scarb1^{fl/fl}-Cdh5^{Cre+}* mice (**Figure 43D-E**). Interestingly, in heart and iBAT, we observed a decrease in selective cholesteryl ether uptake in *Scarb1^{fl/fl}-Cdh5^{Cre+}* mice compared to *Scarb1^{fl/fl}-Cdh5^{Cre-}* mice (**Figure 43F-G**). No differences in uptake in other organs were observed (**Figure 43H-I**).

In summary, SR-B1 expressed by endothelial cells seems to be important for selective cholesterol uptake in iBAT and heart.

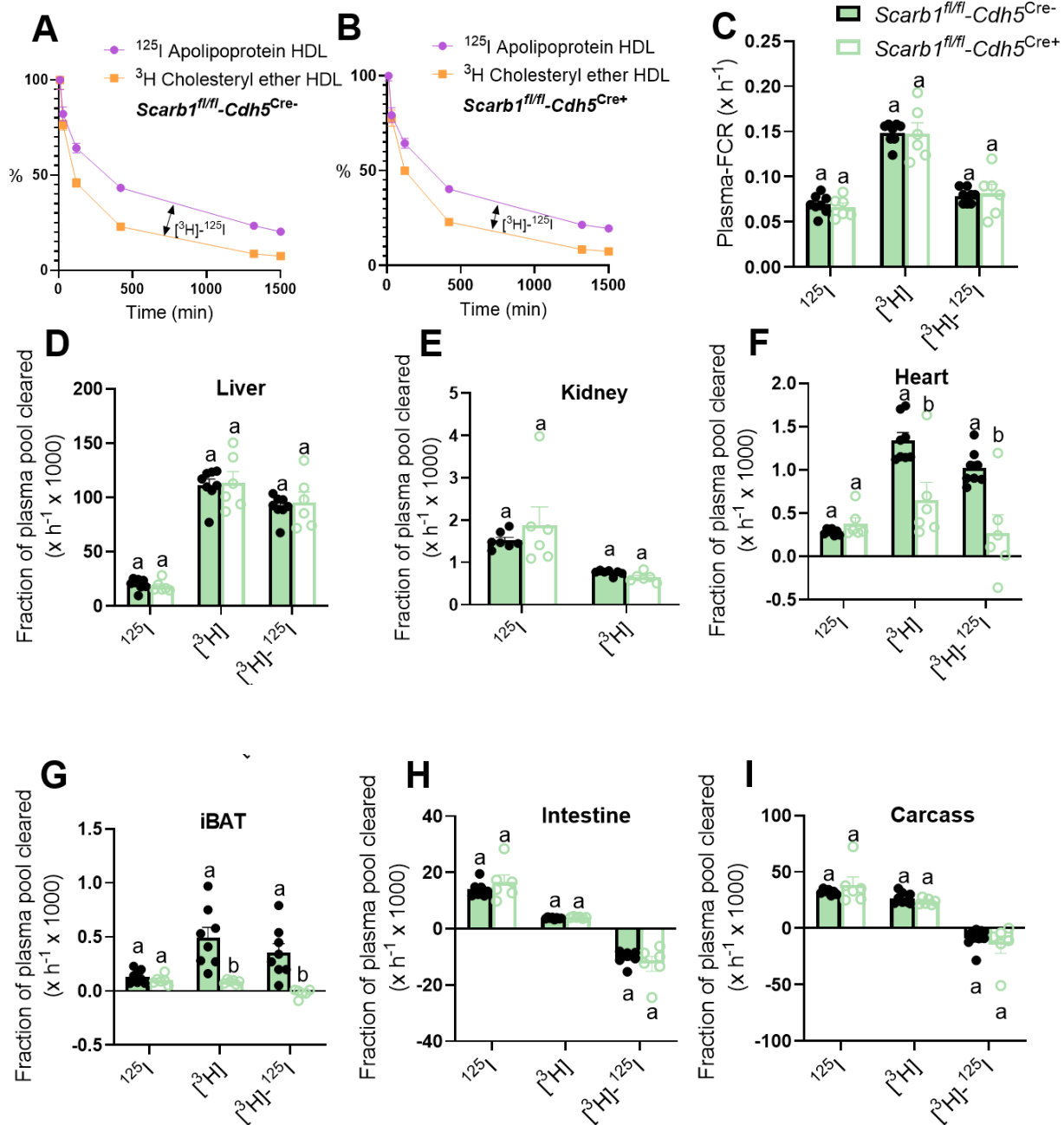


Figure 43. *Scarb1^{fl/fl}-Cdh5^{Cre+}* mice have strongly reduced uptake of ^3H -labelled cholesteryl ether in heart and iBAT.

(A-I) 24-30 week old male *Scarb1^{fl/fl}-Cdh5^{Cre+}* and *Scarb1^{fl/fl}-Cdh5^{Cre-}* mice on a chow diet were housed at 22°C and used for a HDL turnover experiment. Mice were given HDL with a ^{125}I radioactive-labelled core and ^3H labelled cholesteryl ether intravenously and sacrificed 24h later. (A) FCR rates of ^{125}I and ^3H in plasma of *Scarb1^{fl/fl}-Cdh5^{Cre-}* mice over a course of 24h. (B) FCR rates of ^{125}I and ^3H in plasma of *Scarb1^{fl/fl}-Cdh5^{Cre+}* mice over a course of 24h. (C) ^{125}I HDL core and ^3H cholesteryl ether in plasma

(D-I) The uptake of ^{125}I HDL core and ^3H cholesteryl ether in different organs

(D) Liver (E) Kidney (F) Heart (G) iBAT (H) Intestine (I) Carcass

Part G: Discussion

The interest to study BAT was regained in 2009, when BAT was rediscovered in human adults by several independent groups by the use of ^{18}F -fluoro-2-deoxy-D-glucose (^{18}F -FDG) positron emission tomography–computed tomography (PET-CT) (Cypess *et al.*, 2009; Saito *et al.*, 2009; van Marken Lichtenbelt *et al.*, 2009; Virtanen *et al.*, 2009). Before 2009, it was known that infants possessed functional BAT but thought that adults lost their functional BAT throughout their lifetime (Cannon and Nedergaard, 2004). The groups found that BAT mass is inversely correlated with age and BMI (Cypess *et al.*, 2009; Saito *et al.*, 2009; van Marken Lichtenbelt *et al.*, 2009). However, what sparked interest is that when BAT is activated, it takes up high amounts of lipids and glucose (Ouellet *et al.*, 2012; Chondronikola *et al.*, 2014; Alexander Iwen *et al.*, 2017). Therefore, activation of BAT in humans, might help counteract obesity by increasing the energy expenditure and in turn decrease the risk of cardiovascular disease. For example, in mice it was shown that activation of BAT could correct hyperlipidemia (Bartelt *et al.*, 2011), however the appearance of BAT in obese humans is low and BAT activity is impaired (Vijgen *et al.*, 2011; Carey *et al.*, 2013; Orava *et al.*, 2013).

Interestingly, a study by Becher and colleagues showed that individuals that have detectable BAT, have lower plasma glucose levels and TG levels regardless of BMI compared to individuals that have no detectable BAT. Moreover, the prevalence of type 2 diabetes, coronary heart disease and hypertension was lower in individuals with detectable BAT regardless of BMI compared to individuals that have no detectable BAT (Becher *et al.*, 2021).

All the above combined, makes BAT an interesting target to study also in relation to humans. For BAT to be functioning properly FFAs are needed to be imported into the mitochondria and heat is generated via UCP1 (Cannon and Nedergaard, 2004). The FFAs can be endogenously obtained via lipolysis of the intracellular lipid droplets or imported exogenously (Cannon and Nedergaard, 2004). In order for exogenous lipids to reach the brown adipocytes, they first need to cross the endothelial barrier and secondly need to be imported into the brown adipocytes. Therefore for efficient lipid uptake, receptors and transporters expressed on endothelial cells and brown adipocytes are indispensable (Abumrad *et al.*, 2021; Wade *et al.*, 2021).

CD36

CD36 is a LCFA transporter and is involved in numerous processes in the body (Silverstein and Febbraio, 2009). It is highly expressed in metabolic organs like heart (Koonen *et al.*, 2005), muscle (Bonen *et al.*, 2000) and BAT (Bartelt *et al.*, 2011). Moreover CD36 can be found in different cell-types, including immune cells (Cifarelli *et al.*, 2017), endothelial cells and adipocytes (Fischer *et al.*, 2021). In the scope of this thesis, we are specifically interested in expression of CD36 in endothelial cells and brown adipocytes.

The importance of CD36 for thermogenesis was shown years ago by our group, that CD36ko mice were just like UCP1 knockout (UCP1ko) mice unable to maintain their body temperature when exposed to cold (Enerback *et al.*, 1997; Bartelt *et al.*, 2011), in particular when the mice were fasted (Bartelt *et al.*, 2011; Putri *et al.*, 2015). Uptake studies showed that CD36ko mice had decreased uptake of lipids in heart, muscle and different BAT depots (Coburn *et al.*, 2000; Bartelt *et al.*, 2011). In order for brown adipocytes to fulfill their thermogenic function, lipids need to be combusted and a defect in lipid uptake could lead therefore to an impairment in thermogenic function as observed in the CD36ko mice (Bartelt *et al.*, 2011).

In order to be able to combust the exogenous lipids, lipids first need to cross the endothelial barrier and subsequently be internalized by the brown adipocytes (Cannon and Nedergaard, 2004). In BAT, CD36 is highly expressed in brown adipocytes and endothelial cells (Fischer *et al.*, 2021). Therefore, knocking CD36 out in one of these cell-types might greatly affect lipid uptake and therefore thermogenic capacity. Studies in EC-CD36ko mice showed that EC-CD36ko mice had decreased lipid uptake in heart, quadriceps and BAT, increased circulating NEFAs, decreased plasma blood glucose and enhanced glucose clearance (Son *et al.*, 2018; Daquinag *et al.*, 2021; Rekhi *et al.*, 2021; Dada *et al.*, 2024). To our knowledge, no mouse model has been generated with a CD36 knockout specific for brown adipocytes. Although Ad-CD36ko mice showed also decreased uptake of lipids in BAT and WAT and increased circulating NEFAs (Daquinag *et al.*, 2021).

How CD36 takes up lipids is not completely understood. CD36 is known to take up TRL particles (Bartelt *et al.*, 2011; Schlein *et al.*, 2016; Heine *et al.*, 2018). Fischer and colleagues showed that endothelial CD36 takes up TRL particles which then are subsequently processed by lysosomal acid lipase (LAL) (Fischer *et al.*, 2021). Besides TRL particle uptake, CD36 is mainly known for the uptake of LCFAs (Abumrad *et al.*, 1993). Work by Neculai and colleagues that elucidated the crystal structure of LIMP-2 suggests that CD36 also has a large cavity that spans the whole protein which allows for the uptake of lipids (Neculai *et al.*, 2013).

Currently, it is thought that FFAs are bound to FABPpm which helps it stabilize for CD36. CD36 then inserts the FAs into the plasma membrane, through flip-flop mechanism the FA is bound on the cytosolic side by FABPc and processed further (Glatz and Luiken, 2017). On the other hand, several studies show that in adipocytes, upon binding with LCFAs CD36 is internalized in an endocytic manner with caveolin-1 (CAV-1), is also found at lipid droplets and recycled back to the plasma membrane when FAs are taken out of the medium (Hao *et al.*, 2020; Daquinag *et al.*, 2021). Previously it was shown that endothelial cells could package protein and lipids in extracellular vesicles and deliver them to underlying adipocytes (Crewe *et al.*, 2018). Peche and colleagues showed that in endothelial cells, binding of FA to CD36 led to phosphorylation of CAV-1 and internal vesicles containing FAs, CD36, CAV-1 and ceramides were formed. These vesicles were then transported to the basolateral membrane and released the FFAs there (Peche *et al.*, 2023). This thesis aimed to elucidate the different roles of CD36 expressed by brown adipocytes and endothelial cells in adaptive thermogenesis and lipid uptake.

CD36 in brown adipocytes

To our knowledge, we are the first to generate brown adipocyte-specific CD36 knockout mice. Knockout of CD36 resulted in a 25% decrease of CD36 expression in *Cd36^{fl/fl}-Ucp1^{Cre+}* mice and was already visible on whole organ level, which underlines the contribution of brown adipocytes to total CD36 expression. Interestingly, cold exposure did increase CD36 expression in *Cd36^{fl/fl}-Ucp1^{Cre+}* mice but not to the same extent as in *Cd36^{fl/fl}-Ucp1^{Cre-}* mice. This is probably due to the other cell-types expressing CD36 (Fischer *et al.*, 2021). The contribution of CD36 expressed by brown adipocytes for adaptive thermogenesis was evident when the *Cd36^{fl/fl}-Ucp1^{Cre+}* mice were exposed to cold while fasted and could not maintain their body temperature. This is also in line with previous reports when CD36ko mice fasted in the cold and could not maintain their body temperature (Bartelt *et al.*, 2011; Putri *et al.*, 2015). Interestingly, the ability of *Cd36^{fl/fl}-Ucp1^{Cre+}* mice to maintain their body temperature in the cold when fasted varied between the mice. Other mechanisms to generate heat are increasing shivering thermogenesis or increasing browning of WAT and enhancing futile cycling in beige adipocytes (Pant, Bal and Periasamy, 2016; Ikeda and Yamada, 2020). We did not observe notable shivering of *Cd36^{fl/fl}-Ucp1^{Cre+}* mice by eye. Overall, *Cd36^{fl/fl}-Ucp1^{Cre+}* mice have blunted increase in thermogenic markers after cold exposure, suggesting impaired browning of WAT. However, the variance in gene expression was quite high which could also explain the variance in the ability to maintain their body temperature. More analyses will have to be performed to elucidate the variance of ability of *Cd36^{fl/fl}-Ucp1^{Cre+}* mice to maintain their body temperature.

In order for BAT to be able to generate heat, it needs to combust FFAs in mitochondria (Cannon and Nedergaard, 2004). Therefore, endogenous lipids and exogenous lipids are crucial for thermogenesis (Schreiber *et al.*, 2017; Shin *et al.*, 2017). Our group showed that cold-exposed CD36ko mice have decreased uptake in heart, muscle and different depots of BAT (Bartelt *et al.*, 2011). We showed that at RT *Cd36^{fl/fl}-Ucp1^{Cre+}* mice also have lower ³H-Triolein uptake in BAT and upon cold exposure uptake increases but not to the same extent as in *Cd36^{fl/fl}-Ucp1^{Cre-}* mice. This also corresponds with gene expression data where lipid handling genes show a blunted cold-induced increase in BAT of *Cd36^{fl/fl}-Ucp1^{Cre+}* compared to *Cd36^{fl/fl}-Ucp1^{Cre-}* mice. Moreover, gene expression data also showed no increase in other lipid receptors to compensate for the loss of CD36. Therefore, knockout of CD36 in brown adipocytes impairs lipid handling in BAT. To compensate, lipids can also be generated by converting glucose to lipids via DNL (Sanchez-Gurmaches *et al.*, 2018). It is known that CD36ko mice have enhanced glucose clearance after an OGTT and that heart and muscle take up more glucose (Hajri *et al.*, 2002, 2007; Goudriaan *et al.*, 2003; McFarlan *et al.*, 2012). However, the BAT of cold-exposed *Cd36^{fl/fl}-Ucp1^{Cre+}* mice did not increase the uptake of DOG. Moreover, glucose handling genes were also not affected in cold-exposed *Cd36^{fl/fl}-Ucp1^{Cre+}* mice. Therefore, knockout of CD36 in brown adipocytes does not impact glucose handling in BAT.

Overall, we show that CD36 expressed by brown adipocytes is indispensable for thermogenesis and lipid uptake in BAT. Other cell-types expressing CD36 and other receptors in general are not able to compensate for the loss of CD36 in brown adipocytes.

CD36 in endothelial cells

Interestingly, in our endothelial-specific CD36 knockout mouse model, the depletion of CD36 on whole organ expression could only be detected on protein level in BAT of *Cd36^{fl/fl}-Cdh5^{Cre+}* mice. This is in contrast to another report showing a 50% decrease in BAT of EC-CD36ko mice on gene and protein expression (Son *et al.*, 2018). It has to be noted that they created an EC-CD36ko mouse model using the Tie2 promoter, while in our experiments endothelial-specific CD36 mice Cre is expressed under the Cdh5 promoter. These differences might be explained by the expression of CD36 by other cell-types, as Cre expression driven by the Tie2 promoter results also in recombination in hematopoietic cells. Although, the cold-induced *Cd36* expression does seem to be slightly impaired in *Cd36^{fl/fl}-Cdh5^{Cre+}* mice similar to *Cd36^{fl/fl}-Ucp1^{Cre+}* mice. Notably, immunofluorescence data indicate that endothelial cells do not express CD36 in *Cd36^{fl/fl}-Cdh5^{Cre+}* mice, therefore we conclude that *Cd36^{fl/fl}-Cdh5^{Cre+}* mice do not express CD36 in endothelial cells.

CD36 is highly expressed in endothelial cells of BAT (Fischer *et al.*, 2021) and lipids have to be transported over the endothelial cells to get to the brown adipocytes (Cannon and Nedergaard, 2004; Peche *et al.*, 2023). Surprisingly, knockout of CD36 in endothelial cells did not affect adaptive thermogenesis in $Cd36^{fl/fl}-Cdh5^{Cre+}$ mice. Even when $Cd36^{fl/fl}-Cdh5^{Cre+}$ mice were fasted under cold exposure conditions, they were able to maintain their body temperature, which is different compared to either CD36ko mice (Bartelt *et al.*, 2011; Putri *et al.*, 2015) or, as described in the current study, $Cd36^{fl/fl}-Ucp1^{Cre+}$ mice. In line with this, thermogenic marker expression in BAT was not altered in $Cd36^{fl/fl}-Cdh5^{Cre+}$ mice. Although, in WAT cold-exposed $Cd36^{fl/fl}-Cdh5^{Cre+}$ mice had decreased thermogenic marker expression just like $Cd36^{fl/fl}-Ucp1^{Cre+}$ mice, suggesting impaired browning of WAT.

It was reported that EC-CD36ko mice have decreased uptake of lipids in heart, muscle and BAT (Son *et al.*, 2018). However, in our experiments we did not observe a decrease in lipid uptake in any organ of $Cd36^{fl/fl}-Cdh5^{Cre+}$ mice. This also corresponds with the gene expression data where lipid handling genes in BAT and WAT were not affected in $Cd36^{fl/fl}-Cdh5^{Cre+}$ mice. Interestingly, gene expression data also showed no increase in other lipid receptors to compensate for the loss of CD36. Moreover, $Cd36^{fl/fl}-Cdh5^{Cre+}$ mice have increased uptake of ^{14}C -DOG in heart, but not in other organs. This is in line with the gene expression data of BAT and WAT as glucose handling genes were not affected in $Cd36^{fl/fl}-Cdh5^{Cre+}$ mice. On the other hand, for EC-CD36ko mice it was reported that besides heart, WAT and muscle also had increased uptake of glucose (Son *et al.*, 2018).

It is puzzling that an endothelial knockout of CD36 did not affect lipid handling. Especially, considering that lipids need to be transported over endothelial cells before reaching the parenchymal cells (Peche *et al.*, 2023) and EC-CD36ko have decreased lipid uptake (Son *et al.*, 2018). Moreover, it is interesting that an endothelial knockout of CD36 does not affect adaptive thermogenesis considering that CD36 is highly expressed in endothelial cells of BAT (Fischer *et al.*, 2021). Based on our data, as none of the usual receptors are compensating for the loss of CD36 in $Cd36^{fl/fl}-Cdh5^{Cre+}$ mice, alternative uptake mechanisms need to take place in $Cd36^{fl/fl}-Cdh5^{Cre+}$ mice. In a recent study it was reported that EC-CD36ko mice have increased gut permeability, increased inflammation and decreased levels of tight junction proteins (Cifarelli *et al.*, 2017). In case the endothelial barrier integrity is also impaired in BAT of $Cd36^{fl/fl}-Cdh5^{Cre+}$ mice, this could explain the lack of differences in lipid and glucose uptake and that thermogenic capacity of BAT is not impaired. In that case, instead of transendothelial lipid transport which requires receptors/transporters, paracellular lipid transport could be enhanced and compensate endothelial lipid uptake (Von Eckardstein and Rohrer, 2009).

Altogether, as summarized in **Figure 44** we conclude that CD36 expressed by brown adipocytes is essential for thermogenesis and lipid uptake in BAT while CD36 by endothelial cells is not. However, endothelial cells differ per organ as they take on characteristics of the tissue and display therefore a huge variety (Festa, AlZaim and Kalucka, 2023). Thus, it could be that deletion of CD36 affects the different endothelial cell populations in a different manner (Festa, AlZaim and Kalucka, 2023). Moreover, it is unknown how CD36 interacts with components of endothelial cells, how this affects endothelial cell behavior and could affect signal transduction. Therefore, it would be interesting to look deeper into BAT endothelial cells and compare the different CD36 knockout models, for example by quantitative electron microscopic studies. Moreover, it would be interesting to investigate the permeability of the vascular endothelium and to study TRL processing with fluorescently labeled TRLs. Lastly, to confirm the IF data, cell-type sorted approach like MACS to validate the knockout in endothelial cells.

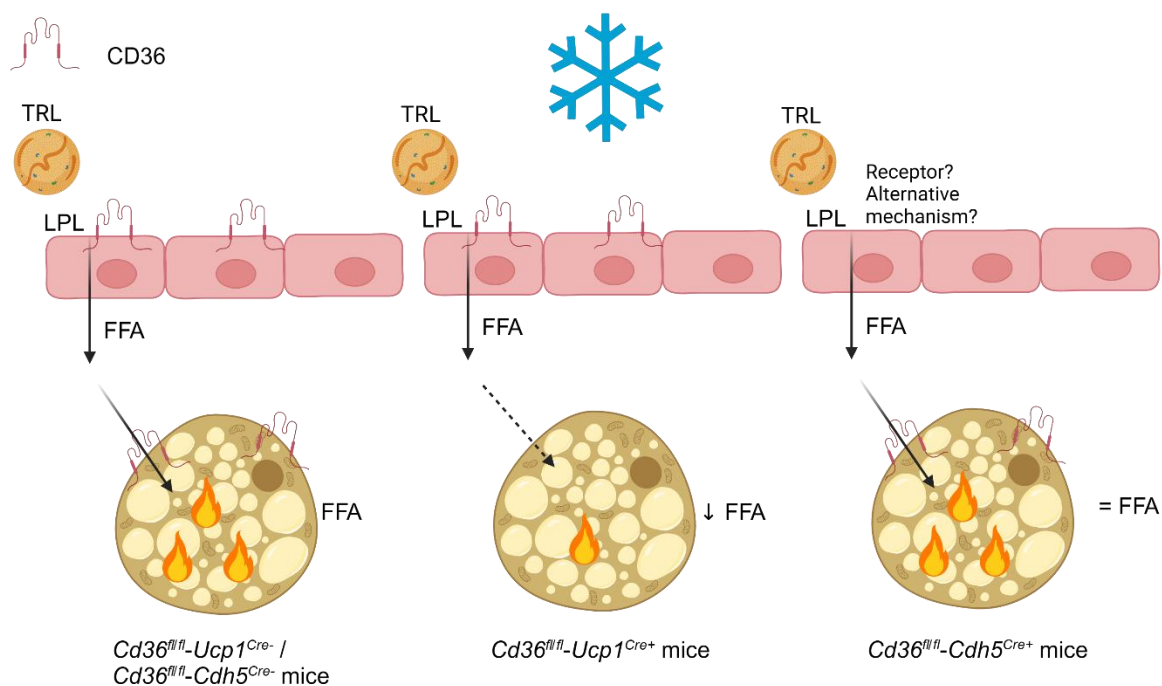


Figure 44. Graphical summary of brown adipocyte-specific and endothelial-specific CD36 knockout on lipid handling and thermogenesis.

SR-B1

SR-B1 is a multifunctional receptor that is known to bind a variety of lipoproteins (Calvo *et al.*, 1997), but mainly known as the HDL receptor (Acton *et al.*, 1996). The role of SR-B1 in RCT and cholesterol metabolism was evident when SR-B1ko mice were generated. SR-B1ko mice had enlarged HDL particles, had reduced cholesterol stores and total plasma cholesterol levels were dramatically increased (Rigotti, B. Trigatti, *et al.*, 1997). The function of SR-B1 depends in which cell it is expressed. For example, in hepatocytes and adrenal cells, SR-B1 extracts CEs from HDL particles without internalization of the particle (Acton *et al.*, 1996; Rigotti, B. L. Trigatti, *et al.*, 1997), while in the periphery SR-B1 is involved in cholesterol efflux from macrophages (De La Llera-Moya *et al.*, 1999). The bidirectional flux of cholesterol is thought to be possible due to the large cavity that spans the whole protein of SR-B1 like a LIMP-2 (Neculai *et al.*, 2013).

RCT is important as cells in the periphery do not have the ability to get rid of excess cholesterol and an excess of cholesterol can be toxic. Therefore, cholesterol efflux to lipid-poor HDL particles via ABCA1 and mature HDL particles via ABCG1 and SR-B1 is essential (De La Llera-Moya *et al.*, 1999; Thuahnai *et al.*, 2004; Phillips, 2014). HDL particles are then transported back to the liver where SR-B1 extracts the CEs and HDL can be recycled back into the bloodstream (Shen, Azhar and Kraemer, 2018).

In order for HDL particles to reach the parenchymal cells, they need to cross the endothelial barrier. It was shown that SR-B1 and ABCG1 in endothelial cells are involved in the transcytosis of HDL particles, therefore allowing cholesterol efflux of the parenchymal cells (Rohrer *et al.*, 2009). Besides the role of HDL in RCT, it is also atheroprotective via signaling via nitric oxide (NO). It was shown that endothelial NO synthase (eNOS) activation was induced by HDL binding SR-B1 (Yuhanna *et al.*, 2001). Moreover, HDL promotes endothelial cell migration and reendothelization via SR-B1 in endothelial cells (Seetharam *et al.*, 2006). For the protective effects of cell migration and reendothelization the adapter protein PDZK1 is needed in endothelial cells (Zhu *et al.*, 2008). Besides its role in HDL transcytosis, endothelial SR-B1 is also involved in transcytosis of LDL (Armstrong *et al.*, 2015; Huang *et al.*, 2019). Due to the affinity for HDL and LDL, SR-B1 expressed by arterial endothelial cells has been suggested to be atheroprotective (Vaisman *et al.*, 2015) and atherogenic (Huang *et al.*, 2019).

Overall, SR-B1 is a key player in cholesterol metabolism and its function is depending on the cell-type it is expressed in.

The role of SR-B1 expressed by endothelial cells in BAT and WAT has to our knowledge, not been studied. SR-B1 is an interesting target as our group found that SR-B1 is highly expressed in endothelial cells of BAT and WAT in mice and different WAT depots in humans. In combination with the fact that SR-B1 is from the same receptor family as CD36 and it can bind different TRL particles (Calvo *et al.*, 1997; Out *et al.*, 2004; Van Eck *et al.*, 2008; Wiersma *et al.*, 2010), we wanted to investigate the role of SR-B1 expressed by endothelial cells in relation to adaptive thermogenesis and lipid uptake. As our group had already showed that during CL administration, that pharmacologically mimics cold exposure, mice had enhanced HDL particle clearance via SR-B1 in the liver and enhanced RCT (Bartelt *et al.*, 2017).

SR-B1 in endothelial cells

In this study, we showed that SR-B1 expressed by endothelial cells, contributes majorly to whole organ SR-B1 expression of BAT, WAT and other organs, but SR-B1 expressed by endothelial cells is dispensable for adaptive thermogenesis and lipid and glucose uptake regardless of diet. Aside from cold-exposed *Scarb1^{fl/fl}-Cdh5^{Cre+}* mice having increased expression in some thermogenic genes in iBAT, we did not observe any differences in BAT and WAT regarding thermogenic markers. We also did not observe increased expression of other receptors which could compensate for the loss of endothelial SR-B1. The lack in differences between *Scarb1^{fl/fl}-Cdh5^{Cre+}* mice and control littermates is probably due to the fact that CD36 is still present and contributes majorly to the amount of lipid being able to be taken up by (endothelial cells of) BAT (Bartelt *et al.*, 2011).

Notably, we did observe a decrease in the selective uptake of cholesteryl ether in BAT, heart and lungs of *Scarb1^{fl/fl}-Cdh5^{Cre+}* mice compared to *Scarb1^{fl/fl}-Cdh5^{Cre-}* mice which to our best knowledge was not reported before. Most of the studies regarding SR-B1 in the periphery are focused on the efflux of cholesterol from macrophages to HDL particles (De La Llera-Moya *et al.*, 1999; Thuahnai *et al.*, 2004; Phillips, 2014). SR-B1 is known to mediate selective cholesterol uptake not just in liver but also in steroidogenic organs (Rigotti, Miettinen and Krieger, 2003; Hu *et al.*, 2010). Currently it is thought that the main role of SR-B1 expressed by endothelial cells is involved in the transcytosis of HDL and LDL particles (Rohrer *et al.*, 2009; Armstrong *et al.*, 2015; Fung *et al.*, 2017; Huang *et al.*, 2019). Although, almost 50 years ago, it was already shown that endothelial cells take up cholesterol from HDL particles (Collet *et al.*, 1988). More recently, a study investigating the role of SR-B1 in arterial and venous endothelial cells of the placenta showed an increased selective uptake of cholesterol in arterial endothelial cells of the placenta compared to the venous endothelial cells (Strahlhofer-Augsten *et al.*, 2022).

Therefore, it seems that besides transcytosis of HDL by SR-B1, SR-B1 expressed by endothelial cells also extract CE from HDL in a bidirectional manner (Stangl, Hyatt and Hobbs, 1999). Interestingly, it was shown that HDL transcytosis was SR-B1-dependent but cholesterol transfer to endothelial cells was independent of SR-B1 (Muñoz-Vega *et al.*, 2018). Why we observe a difference in BAT, heart and lungs probably has to do with high expression of SR-B1 in these organs. It is very likely that the same results would be observed when studying iWAT, gWAT and quadriceps. Moreover, the type of endothelium in these organs also plays a role. These organs have a continuous endothelium, which means that the endothelium is tightly linked together via tight junctions and transport of cargos need to be transported via receptors. While in organs with a fenestrated endothelium or discontinuous endothelium, there are openings in the endothelium allowing for passages of cargos (Urbanczyk, Zbinden and Schenke-Layland, 2022). In addition, most experiments studying selective uptake of CE are done *in vitro*, not accounting for organ cross talk and organ dynamics. Therefore, results between our data might also differ from the *in vitro* data.

Overall, SR-B1 expressed by endothelial cells is dispensable for thermogenesis and lipid and glucose uptake in BAT. Notably, as presented in **Figure 45**, SR-B1 expressed by endothelial cells is involved in cholesterol influx in iBAT and the heart. The importance of selective uptake of cholesterol from HDL particles for cellular cholesterol metabolism and the biology of endothelial cells, however, remains to be elucidated.

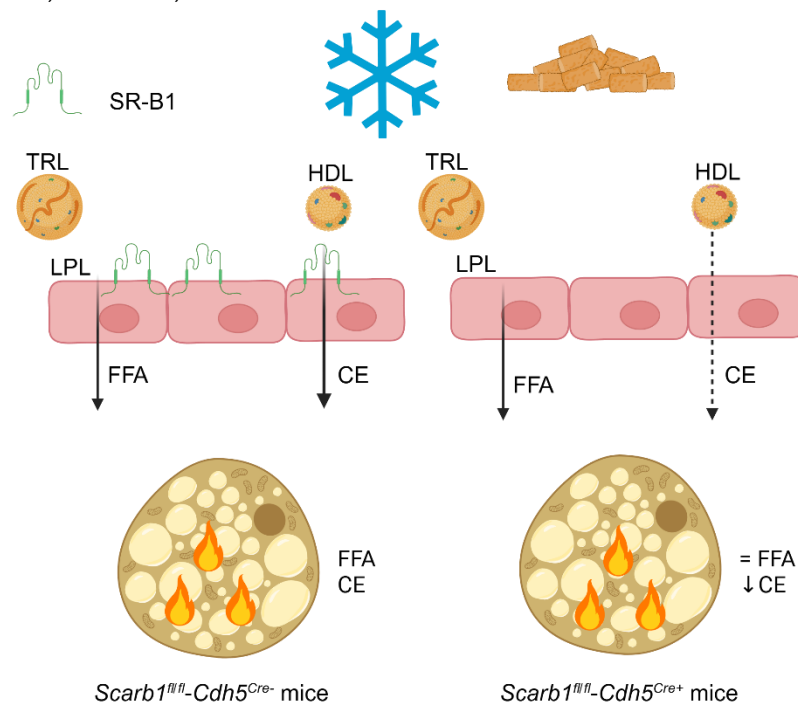


Figure 45. Graphical summary of endothelial-specific SR-B1 knockout on lipid handling and thermogenesis.

Part H: References

Abumrad, N. A. *et al.* (1993) 'Cloning of a rat adipocyte membrane protein implicated in binding or transport of long-chain fatty acids that is induced during preadipocyte differentiation. Homology with human CD36', *Journal of Biological Chemistry*, 268(24), pp. 17665–17668. doi: 10.1016/s0021-9258(17)46753-6.

Abumrad, N. A. *et al.* (2021) 'Endothelial Cell Receptors in Tissue Lipid Uptake and Metabolism', *Circulation Research*, 128(3), pp. 433–450. doi: 10.1161/CIRCRESAHA.120.318003.

Acton, S. *et al.* (1996) 'Identification of scavenger receptor SR-BI as a high density lipoprotein receptor', *Science*, 271(5248), pp. 518–520. doi: 10.1126/science.271.5248.518.

Acton, S. *et al.* (1999) 'Association of polymorphisms at the SR-BI gene locus with plasma lipid levels and body mass index in a white population', *Arteriosclerosis, Thrombosis, and Vascular Biology*, 19(7), pp. 1734–1743. doi: 10.1161/01.ATV.19.7.1734.

Acton, S. L. *et al.* (1994) 'Expression cloning of SR-BI, a CD36-related class B scavenger receptor', *Journal of Biological Chemistry*, 269(33), pp. 21003–21009. doi: 10.1016/s0021-9258(17)31921-x.

Alexander Iwen, K. *et al.* (2017) 'Cold-induced brown adipose tissue activity alters plasma fatty acids and improves glucose metabolism in men', *Journal of Clinical Endocrinology and Metabolism*, 102(11), pp. 4226–4234. doi: 10.1210/jc.2017-01250.

An, S. M., Cho, S. H. and Yoon, J. C. (2023) 'Adipose Tissue and Metabolic Health', *Diabetes and Metabolism Journal*, 47(5), pp. 595–611. doi: 10.4093/dmj.2023.0011.

Anderson, C. M. *et al.* (2015) 'Dependence of brown adipose tissue function on CD36-mediated coenzyme Q uptake', *Cell Reports*, 10(4), pp. 505–515. doi: 10.1016/j.celrep.2014.12.048.

Armstrong, S. M. *et al.* (2015) 'A novel assay uncovers an unexpected role for SR-BI in LDL transcytosis', *Cardiovascular Research*, 108(2), pp. 268–277. doi: 10.1093/cvr/cvv218.

Asch, A. S. *et al.* (1987) 'Isolation of the thrombospondin membrane receptor', *Journal of Clinical Investigation*, 79(4), pp. 1054–1061. doi: 10.1172/JCI112918.

Babitt, J. *et al.* (1997) 'Murine SR-BI, a high density lipoprotein receptor that mediates selective lipid uptake, is N-glycosylated and fatty acylated and colocalizes with plasma membrane caveolae', *Journal of Biological Chemistry*, 272(20), pp. 13242–13249. doi: 10.1074/jbc.272.20.13242.

Baillie, A. G. S., Coburn, C. T. and Abumrad, N. A. (1996) 'Reversible binding of long-chain fatty acids to purified FAT, the adipose CD36 homolog', *Journal of Membrane Biology*, 153(1), pp. 75–81. doi: 10.1007/s002329900111.

Barbatelli, G. *et al.* (2010) 'The emergence of cold-induced brown adipocytes in mouse white fat depots is determined predominantly by white to brown adipocyte transdifferentiation', *American Journal of Physiology - Endocrinology and Metabolism*, 298(6), pp. 1244–1253. doi: 10.1152/ajpendo.00600.2009.

Bartelt, A. *et al.* (2011) 'Brown adipose tissue activity controls triglyceride clearance', *Nature Medicine*, 17(2), pp. 200–206. doi: 10.1038/nm.2297.

Bartelt, A. *et al.* (2017) 'Thermogenic adipocytes promote HDL turnover and reverse cholesterol transport', *Nature Communications*, 8. doi: 10.1038/ncomms15010.

Bartelt, A. and Heeren, J. (2014) 'Adipose tissue browning and metabolic health', *Nature Reviews Endocrinology*, 10(1), pp. 24–36. doi: 10.1038/nrendo.2013.204.

Baruch, D. I. *et al.* (1999) 'CD36 peptides that block cytoadherence define the CD36 binding region for Plasmodium falciparum-infected erythrocytes', *Blood*, 94(6), pp. 2121–2127. doi: 10.1182/blood.v94.6.2121.

Becher, T. *et al.* (2021) 'Brown adipose tissue is associated with cardiometabolic health', *Nature Medicine*, 27(1), pp. 58–65. doi: 10.1038/s41591-020-1126-7.

Berbee, J. F. P. *et al.* (2015) 'Brown fat activation reduces hypercholesterolaemia and protects from atherosclerosis development', *Nature Communications*, 6. doi: 10.1038/ncomms7356.

Blondin, D. P. *et al.* (2020) 'Human Brown Adipocyte Thermogenesis Is Driven by β 2-AR Stimulation', *Cell Metabolism*, 32(2), pp. 287–300.e7. doi: 10.1016/j.cmet.2020.07.005.

Bonen, A. *et al.* (2000) 'Acute regulation of fatty acid uptake involves the cellular redistribution of fatty acid translocase', *Journal of Biological Chemistry*, 275(19), pp. 14501–14508. doi: 10.1074/jbc.275.19.14501.

Borel, P. *et al.* (2013) 'CD36 and SR-BI Are Involved in Cellular Uptake of Provitamin A Carotenoids by Caco-2 and HEK Cells, and Some of Their Genetic Variants Are Associated with Plasma Concentrations of These Micronutrients in Humans', *Journal of Nutrition*, 143(4), pp. 448–456. doi: 10.3945/jn.112.172734.

Braun, A. *et al.* (2002) 'Loss of SR-BI expression leads to the early onset of occlusive atherosclerotic coronary artery disease, spontaneous myocardial infarctions, severe cardiac dysfunction, and premature death in apolipoprotein E-deficient mice', *Circulation Research*, 90(3), pp. 270–276. doi: 10.1161/hh0302.104462.

Braun, K. *et al.* (2018) 'Non-adrenergic control of lipolysis and thermogenesis in adipose tissues', *Journal of Experimental Biology*, 121, pp. 1–14. doi: 10.1242/jeb.165381.

Brown, M. S. and Goldstein, J. L. (1986) 'A Receptor-Mediated Pathway for Cholesterol Homeostasis', *Science*, 232(5), pp. 34–47.

Calvo, D. *et al.* (1997) 'CLA-1 Is an 85-kD Plasma Membrane Glycoprotein That Acts as a High-Affinity Receptor for Both Native (HDL, LDL, and VLDL) and Modified (OxLDL and AcLDL) Lipoproteins', *Arteriosclerosis, Thrombosis, and Vascular Biology*, 17(11), pp. 2341–2349.

Calvo, D. *et al.* (1998) 'Human CD36 is a high affinity receptor for the native lipoproteins HDL, LDL, and VLDL', *Journal of Lipid Research*, 39(4), pp. 777–788. doi: 10.1016/s0022-2275(20)32566-9.

Calvo, D. and Vega, M. A. (1993) 'Identification, primary structure, and distribution of CLA-1, a novel member of the CD36/LIMPII gene family', *Journal of Biological Chemistry*, 268(25), pp. 18929–18935. doi: 10.1016/s0021-9258(17)46716-0.

Cannon, B. and Nedergaard, J. (2004) 'Brown Adipose Tissue: Function and Physiological Significance', *Physiological Reviews*, 84(1), pp. 277–359. doi: 10.1152/physrev.00015.2003.

Carey, A. L. *et al.* (2013) 'Ephedrine activates brown adipose tissue in lean but not obese humans', *Diabetologia*, 56(1), pp. 147–155. doi: 10.1007/s00125-012-2748-1.

Chadwick, A. C. *et al.* (2017) 'NMR structure of the C-terminal transmembrane domain of the HDL receptor, SR-BI, and a functionally-relevant leucine zipper motif', 25(3), pp. 446–457. doi: 10.1016/j.str.2017.01.001.NMR.

Chondronikola, M. *et al.* (2014) 'Brown adipose tissue improves whole-body glucose homeostasis and insulin sensitivity in humans', *Diabetes*, 63(12), pp. 4089–4099. doi: 10.2337/db14-0746.

Cifarelli, V. *et al.* (2017) 'CD36 Deficiency Impairs the Small Intestinal Barrier and Induces Subclinical Inflammation in Mice', *Cmgh*, 3(1), pp. 82–98. doi: 10.1016/j.jcmgh.2016.09.001.

Coburn, C. T. *et al.* (2000) 'Defective uptake and utilization of long chain fatty acids in muscle and adipose tissues of CD36 knockout mice', *Journal of Biological Chemistry*, 275(42), pp. 32523–32529. doi: 10.1074/jbc.M003826200.

Collet, X. *et al.* (1988) 'Uptake of HDL unesterified and esterified cholesterol by human endothelial cells. Modulation by HDL phospholipolysis and cell cholesterol content', *Biochimica et Biophysica Acta (BBA)/Lipids and Lipid Metabolism*, 958(1), pp. 81–92. doi: 10.1016/0005-2760(88)90248-2.

Coort, S. L. M. *et al.* (2002) 'Sulfo-N-succinimidyl esters of long chain fatty acids specifically inhibit fatty acid translocase (FAT/CD36)-mediated cellular fatty acid uptake', *Molecular and Cellular Biochemistry*, 239(1–2), pp. 213–219. doi: 10.1023/A:1020539932353.

Crewe, C. *et al.* (2018) 'An Endothelial-to-Adipocyte Extracellular Vesicle Axis Governed by Metabolic State', *Cell*, 175(3), pp. 695-708.e13. doi: 10.1016/j.cell.2018.09.005.

Cypess, A. M. *et al.* (2009) 'Identification and Importance of Brown Adipose Tissue in Adult Humans', *New England Journal of Medicine*, 360(15), pp. 1509–1517. doi: 10.1056/NEJMoa0810780.

Dada, A. *et al.* (2024) 'Enhanced ECCD36 Signaling Promotes Skeletal Muscle Insulin Resistance in Female Mice', *American Journal of Physiology-Endocrinology and Metabolism*, (July), pp. 533–543. doi: 10.1152/ajpendo.00246.2024.

Dallner, O. S. *et al.* (2006) 'B3-Adrenergic Receptors Stimulate Glucose Uptake in Brown Adipocytes By Two Mechanisms Independently of Glucose Transporter 4 Translocation', *Endocrinology*, 147(12), pp. 5730–5739. doi: 10.1210/en.2006-0242.

Daquinag, A. C. *et al.* (2021) 'Fatty acid mobilization from adipose tissue is mediated by CD36 posttranslational modifications and intracellular trafficking', *JCI Insight*, 6(17), pp. 1–16. doi: 10.1172/jci.insight.147057.

Dijk, W. *et al.* (2015) 'ANGPTL4 mediates shuttling of lipid fuel to brown adipose tissue during sustained cold exposure', *eLife*, 4(OCTOBER2015), pp. 1–23. doi: 10.7554/eLife.08428.

Dole, V. P. (1956) 'A relation between non-esterified fatty acids in plasma and the metabolism of glucose.', *The Journal of clinical investigation*, 35(2), pp. 150–154. doi: 10.1172/JCI103259.

Van Eck, M. *et al.* (2003) 'Differential effects of scavenger receptor BI deficiency on lipid metabolism in cells of the arterial wall and in the liver', *Journal of Biological Chemistry*, 278(26), pp. 23699–23705. doi: 10.1074/jbc.M211233200.

Van Eck, M. *et al.* (2008) 'Scavenger receptor BI facilitates the metabolism of VLDL lipoproteins in vivo', *Journal of Lipid Research*, 49(1), pp. 136–146. doi: 10.1194/jlr.M700355-JLR200.

Von Eckardstein, A. and Rohrer, L. (2009) 'Transendothelial lipoprotein transport and regulation of endothelial permeability and integrity by lipoproteins', *Current Opinion in Lipidology*, 20(3), pp. 197–205. doi: 10.1097/MOL.0b013e32832afd63.

Elias, I. *et al.* (2012) 'Adipose tissue overexpression of vascular endothelial growth factor protects against diet-induced obesity and insulin resistance', *Diabetes*, 61(7), pp. 1801–1813. doi: 10.2337/db11-0832.

Endemann, G. *et al.* (1993) 'CD36 is a receptor for oxidized low density lipoprotein', *Journal of Biological Chemistry*, 268(16), pp. 11811–11816. doi: 10.1016/s0021-9258(19)50272-1.

Enerback, S. *et al.* (1997) 'Mice lacking mitochondrial uncoupling protein are cold-sensitive but not obese', *Nature*, 387(5537), pp. 90–94.

Febbraio, M. *et al.* (1999) 'A null mutation in murine CD36 reveals an important role in fatty acid and lipoprotein metabolism', *Journal of Biological Chemistry*, 274(27), pp. 19055–19062. doi: 10.1074/jbc.274.27.19055.

Fedorenko, A., Lishko, P. V. and Kirichok, Y. (2012) 'Mechanism of fatty-acid-dependent UCP1 uncoupling in brown fat mitochondria', *Cell*, 151(2), pp. 400–413. doi: 10.1016/j.cell.2012.09.010.

Feingold, K. R. (2022) 'Lipid and Lipoprotein Metabolism', *Endocrinology and Metabolism Clinics of North America*, 51(3), pp. 437–458. doi: 10.1016/j.ecl.2022.02.008.

Festa, J., AlZaim, I. and Kalucka, J. (2023) 'Adipose tissue endothelial cells: insights into their heterogeneity and functional diversity', *Current Opinion in Genetics and Development*, 81, p. 102055. doi: 10.1016/j.gde.2023.102055.

Fischer, A. W. *et al.* (2021) 'Lysosomal lipoprotein processing in endothelial cells stimulates adipose tissue thermogenic adaptation', *Cell Metabolism*, 33(3), pp. 547-564.e7. doi: 10.1016/j.cmet.2020.12.001.

Fong, L. G. *et al.* (2016) 'GPIHBP1 and Plasma Triglyceride Metabolism', *Trends in Endocrinology and Metabolism*, 27(7), pp. 455–469. doi: 10.1016/j.tem.2016.04.013.

Fung, K. Y. *et al.* (2017) 'SR-BI mediated transcytosis of HDL in brain microvascular endothelial cells is independent of caveolin, clathrin, and PDZK1', *Frontiers in Physiology*, 8(OCT), pp. 1–16. doi: 10.3389/fphys.2017.00841.

Gaidukov, L. *et al.* (2011) 'Glycine dimerization motif in the N-terminal transmembrane domain of the high density lipoprotein receptor SR-BI required for normal receptor oligomerization and lipid transport', *Journal of Biological Chemistry*, 286(21), pp. 18452–18464. doi: 10.1074/jbc.M111.229872.

Ganesan, L. P. *et al.* (2016) 'Scavenger receptor B1, the HDL receptor, is expressed abundantly in liver sinusoidal endothelial cells', *Scientific Reports*, 6(January), pp. 1–13. doi: 10.1038/srep20646.

Glass, C. *et al.* (1985) 'Uptake of high-density lipoprotein-associated apoprotein A-I and cholesterol esters by 16 tissues of the rat in vivo and by adrenal cells and hepatocytes in vitro', *Journal of Biological Chemistry*, 260(2), pp. 744–750. doi: 10.1016/s0021-9258(20)71160-9.

Glatz, J. F. C. and Luiken, J. (2017) 'From fat to FAT (CD36/SR-B2): Understanding the regulation of cellular fatty acid uptake', *Biochimie*, 136, pp. 21–26. doi: 10.1016/j.biochi.2016.12.007.

Glatz, J. F. C., Luiken, J. J. F. P. and Bonen, A. (2010) 'Membrane fatty acid transporters as regulators of lipid metabolism: Implications for metabolic disease', *Physiological Reviews*, 90(1), pp. 367–417. doi: 10.1152/physrev.00003.2009.

Goldberg, I. J., Eckel, R. H. and Abumrad, N. A. (2009) 'Regulation of fatty acid uptake into tissues: Lipoprotein lipase- And CD36-mediated pathways', *Journal of Lipid Research*, 50(SUPPL.), pp. S86–S90. doi: 10.1194/jlr.R800085-JLR200.

Goudriaan, J. R. *et al.* (2003) 'CD36 deficiency increases insulin sensitivity in muscle, but induces insulin resistance in the liver in mice', *Journal of Lipid Research*, 44(12), pp. 2270–2277. doi: 10.1194/jlr.M300143-JLR200.

Hajri, T. *et al.* (2002) 'Defective fatty acid uptake modulates insulin responsiveness and metabolic responses to diet in CD36-null mice', *Journal of Clinical Investigation*, 109(10), pp. 1381–1389. doi: 10.1172/jci200214596.

Hajri, T. *et al.* (2007) 'CD36-facilitated fatty acid uptake inhibits leptin production and signaling in adipose tissue', *Diabetes*, 56(7), pp. 1872–1880. doi: 10.2337/db06-1699.

Hao, J. W. *et al.* (2020) 'CD36 facilitates fatty acid uptake by dynamic palmitoylation-regulated endocytosis', *Nature Communications*, 11(1), pp. 1–16. doi: 10.1038/s41467-020-18565-8.

Harmon, C. M. *et al.* (1991) 'Labeling of adipocyte membranes by sulfo-N-succinimidyl derivatives of long-chain fatty acids: Inhibition of fatty acid transport', *The Journal of Membrane Biology*, 121(3), pp. 261–268. doi: 10.1007/BF01951559.

Harmon, C. M. and Abumrad, N. A. (1993) 'Binding of sulfosuccinimidyl fatty acids to adipocyte membrane proteins: Isolation and amino-terminal sequence of an 88-kD protein implicated in transport of long-chain fatty acids', *The Journal of Membrane Biology*, 133(1), pp. 43–49. doi: 10.1007/BF00231876.

Havel, R. J., Eder, H. A. and Bragdon, J. H. (1955) 'The distribution and chemical composition of ultracentrifugally separated lipoproteins in human serum.', *The Journal of clinical investigation*, 34(9), pp. 1345–1353. doi: 10.1172/JCI103182.

Heeren, J. and Scheja, L. (2018) 'Brown adipose tissue and lipid metabolism', *Current Opinion in Lipidology*, 29(3), pp. 180–185. doi: 10.1097/MOL.0000000000000504.

Heine, M. *et al.* (2018) 'Lipolysis Triggers a Systemic Insulin Response Essential for Efficient Energy Replenishment of Activated Brown Adipose Tissue in Mice', *Cell Metabolism*, 28(4), pp. 644-655.e4. doi: 10.1016/j.cmet.2018.06.020.

Himms-Hagen, J. *et al.* (2000) 'Multilocular fat cells in WAT of CL-316243-treated rats derive directly from white adipocytes', *American Journal of Physiology - Cell Physiology*, 279(3 48-3), pp. 670–681. doi: 10.1152/ajpcell.2000.279.3.c670.

Hoeke, G. *et al.* (2016) 'Role of Brown Fat in Lipoprotein Metabolism and Atherosclerosis', *Circulation Research*, 118(1), pp. 173–182. doi: 10.1161/CIRCRESAHA.115.306647.

Hofmann, S. M. *et al.* (2007) 'Adipocyte LDL receptor-related protein-1 expression modulates postprandial lipid transport and glucose homeostasis in mice', *Journal of Clinical Investigation*, 117(11), pp. 3271–3282. doi: 10.1172/JCI31929.

Hoosdally, S. J. *et al.* (2009) 'The human scavenger receptor CD36. Glycosylation status and its role in trafficking and function', *Journal of Biological Chemistry*, 284(24), pp. 16277–16288. doi: 10.1074/jbc.M109.007849.

Hosomi, K. *et al.* (2023) 'NanoSPECT imaging reveals the uptake of ¹²³I-labelled oxidized low-density lipoprotein in the brown adipose tissue of mice via CD36', *Cardiovascular Research*, 119(4), pp. 1008–1020. doi: 10.1093/cvr/cvac167.

Hu, J. *et al.* (2010) 'Cellular cholesterol delivery, intracellular processing and utilization for biosynthesis of steroid hormones', *Nutrition and Metabolism*, 7(Table 1), pp. 7–9. doi: 10.1186/1743-7075-7-47.

Hu, Z. *et al.* (2013) 'Regulation of expression and function of scavenger receptor class B, type I (SR-BI) by Na⁺/H⁺ exchanger regulatory factors (NHERFs)', *Journal of Biological Chemistry*, 288(16), pp. 11416–11435. doi: 10.1074/jbc.M112.437368.

Huang, L. *et al.* (2019) 'SR-B1 drives endothelial cell LDL transcytosis via DOCK4 to promote atherosclerosis', *Nature*, 569(7757), pp. 565–569. doi: 10.1038/s41586-019-1140-4.

Huby, T. *et al.* (2006) 'Knockdown expression and hepatic deficiency reveal an atheroprotective role for SR-BI in liver and peripheral tissues', *Journal of Clinical Investigation*, 116(10), pp. 2767–2776. doi: 10.1172/JCI26893.

Ikeda, K. and Yamada, T. (2020) 'UCP1 Dependent and Independent Thermogenesis in Brown and Beige Adipocytes', *Frontiers in Endocrinology*, 11(July), pp. 1–6. doi: 10.3389/fendo.2020.00498.

Kajimura, S. and Saito, M. (2014) 'A New Era in Brown Adipose Tissue Biology: Molecular Control of Brown Fat Development and Energy Homeostasis', *Annual Review of Physiology*, 76, pp. 225–249. doi: 10.1146/annurev-physiol-021113-170252.

Kalucka, J. *et al.* (2020) 'Single-Cell Transcriptome Atlas of Murine Endothelial Cells', *Cell*, 180(4), pp. 764–779.e20. doi: 10.1016/j.cell.2020.01.015.

Kocher, O. *et al.* (2003) 'Targeted Disruption of the PDZK1 Gene in Mice Causes Tissue-specific Depletion of the High Density Lipoprotein Receptor Scavenger Receptor Class B Type I and Altered Lipoprotein Metabolism', *Journal of Biological Chemistry*, 278(52), pp. 52820–52825. doi: 10.1074/jbc.M310482200.

Koonen, D. P. Y. *et al.* (2005) 'Long-chain fatty acid uptake and FAT/CD36 translocation in heart and skeletal muscle', *Biochimica et Biophysica Acta - Molecular and Cell Biology of Lipids*, 1736(3), pp. 163–180. doi: 10.1016/j.bbalip.2005.08.018.

Kozarsky, K. F. *et al.* (1997) 'Overexpression of the HDL receptor SR-BI alters plasma HDL and bile cholesterol levels', *Nature*, 387(6631), pp. 414–417. doi: 10.1038/387414a0.

Kuda, O. *et al.* (2013) 'Sulfo-N-succinimidyl oleate (SSO) inhibits fatty acid uptake and signaling for intracellular calcium via binding CD36 lysine 164: SSO also inhibits oxidized low density lipoprotein uptake by macrophages', *Journal of Biological Chemistry*, 288(22), pp. 15547–15555. doi: 10.1074/jbc.M113.473298.

Kuniyasu, A., Hayashi, S. and Nakayama, H. (2002) 'Adipocytes recognize and degrade oxidized low density lipoprotein through CD36', *Biochemical and Biophysical Research Communications*, 295(2), pp. 319–323. doi: 10.1016/S0006-291X(02)00666-6.

De La Llera-Moya, M. *et al.* (1999) 'Scavenger receptor BI (SR-BI) mediates free cholesterol flux independently of HDL tethering to the cell surface', *Journal of Lipid Research*, 40(3), pp. 575–580. doi: 10.1016/s0022-2275(20)32462-7.

Labbé, S. M. *et al.* (2015) 'In vivo measurement of energy substrate contribution to cold-induced brown adipose tissue thermogenesis', *FASEB Journal*, 29(5), pp. 2046–2058. doi: 10.1096/fj.14-266247.

Lafferty, M. J. *et al.* (2013) 'Angiopoietin-like protein 4 inhibition of lipoprotein lipase: Evidence for reversible complex formation', *Journal of Biological Chemistry*, 288(40), pp. 28524–28534. doi: 10.1074/jbc.M113.497602.

Laugerette, F. *et al.* (2005) 'CD36 involvement in orosensory detection of dietary lipids, spontaneous fat preference, and digestive secretions', *Journal of Clinical Investigation*, 115(11), pp. 3177–3184. doi: 10.1172/JCI25299.

Lee, M. W., Lee, M. and Oh, K. J. (2019) 'Adipose tissue-derived signatures for obesity and type 2 diabetes: Adipokines, batokines and microRNAs', *Journal of Clinical Medicine*, 8(6), p. 854. doi: 10.3390/jcm8060854.

Luo, L. and Liu, M. (2016) 'Adipose tissue in control of metabolism', *Journal of Endocrinology*, 231(3), pp. R77–R99. doi: 10.1530/JOE-16-0211.

Lynes, M. D. *et al.* (2017) 'The cold-induced lipokine 12,13-diHOME promotes fatty acid transport into brown adipose tissue', *Nature Publishing Group*, 23(5), pp. 631–637. doi: 10.1038/nm.4297.The.

Ma, X. *et al.* (2004) 'A common haplotype at the CD36 locus is associated with high free fatty acid levels and increased cardiovascular risk in Caucasians', *Human Molecular Genetics*, 13(19), pp. 2197–2205. doi: 10.1093/hmg/ddh233.

Manichaikul, A. *et al.* (2015) 'Association of the lipoprotein receptor SCARB1 common missense variant rs4238001 with incident coronary heart disease', *PLoS ONE*, 10(5), pp. 1–16. doi: 10.1371/journal.pone.0125497.

van Marken Lichtenbelt, W. D. *et al.* (2009) 'Cold-Activated Brown Adipose Tissue in Healthy Men', *New England Journal of Medicine*, 360(15), pp. 1500–1508. doi: 10.1056/nejmoa0808718.

Marques, P. E. *et al.* (2019) 'Multimerization and Retention of the Scavenger Receptor SR-B1 in the Plasma Membrane', *Developmental Cell*, 50(3), pp. 283-295.e5. doi: 10.1016/j.devcel.2019.05.026.

Martin, C. *et al.* (2011) 'CD36 as a lipid sensor', *Physiology and Behavior*, 105(1), pp. 36–42. doi: 10.1016/j.physbeh.2011.02.029.

Masuda, D. *et al.* (2009) 'Chylomicron remnants are increased in the postprandial state in CD36 deficiency', *Journal of Lipid Research*, 50(5), pp. 999–1111. doi: 10.1194/jlr.P700032-JLR200.

McFarlan, J. T. *et al.* (2012) 'In vivo, fatty acid translocase (CD36) critically regulates skeletal muscle fuel selection, exercise performance, and training-induced adaptation of fatty acid oxidation', *Journal of Biological Chemistry*, 287(28), pp. 23502–23516. doi: 10.1074/jbc.M111.315358.

Medina, J. *et al.* (2003) 'Hepatocyte growth factor activates endothelial proangiogenic mechanisms relevant in chronic hepatitis C-associated neoangiogenesis', *Journal of Hepatology*, 38, pp. 660–667. doi: 10.1016/S0168-8278(03)00053-9.

Medina, J. *et al.* (2005) 'Evidence of angiogenesis in primary biliary cirrhosis: An immunohistochemical descriptive study', *Journal of Hepatology*, 42(1), pp. 124–131. doi: 10.1016/j.jhep.2004.09.024.

Min, S. Y. *et al.* (2016) 'Human "brite/beige" adipocytes develop from capillary networks, and their implantation improves metabolic homeostasis in mice', *Nature Medicine*, 22(3), pp. 312–318. doi: 10.1038/nm.4031.

Motojima, K. *et al.* (1998) 'Expression of putative fatty acid transporter genes are regulated by peroxisome proliferator-activated receptor α and γ activators in a tissue- and inducer-specific manner', *Journal of Biological Chemistry*, 273(27), pp. 16710–16714. doi: 10.1074/jbc.273.27.16710.

Moussa, M. *et al.* (2011) 'CD36 is involved in lycopene and lutein uptake by adipocytes and adipose tissue cultures', *Molecular Nutrition and Food Research*, 55(4), pp. 578–584. doi: 10.1002/mnfr.201000399.

Muñoz-Vega, M. *et al.* (2018) 'Hdl-mediated lipid influx to endothelial cells contributes to regulating intercellular adhesion molecule (Icam)-1 expression and enos phosphorylation', *International Journal of Molecular Sciences*, 19(11). doi: 10.3390/ijms19113394.

Nassir, F. *et al.* (2007) 'CD36 is important for fatty acid and cholesterol uptake by the proximal but not distal intestine', *Journal of Biological Chemistry*, 282(27), pp. 19493–19501. doi: 10.1074/jbc.M703330200.

Neculai, D. *et al.* (2013) 'Structure of LIMP-2 provides functional insights with implications for SR-BI and CD36', *Nature*, 504(7478), pp. 172–176. doi: 10.1038/nature12684.

Oquendo, P. *et al.* (1989) 'CD36 directly mediates cytoadherence of *Plasmodium falciparum* parasitized erythrocytes', *Cell*, 58(1), pp. 95–101. doi: 10.1016/0092-8674(89)90406-6.

Orava, J. *et al.* (2013) 'Blunted metabolic responses to cold and insulin stimulation in brown adipose tissue of obese humans', *Obesity*, 21(11), pp. 2279–2287. doi: 10.1002/oby.20456.

Ouellet, V. *et al.* (2012) 'Brown adipose tissue oxidative metabolism contributes to energy expenditure during acute cold exposure in humans', 122(2), pp. 545–552. doi: 10.1172/JCI60433DS1.

Out, R. *et al.* (2004) 'Scavenger Receptor BI Plays a Role in Facilitating Chylomicron Metabolism', *Journal of Biological Chemistry*, 279(18), pp. 18401–18406. doi: 10.1074/jbc.M401170200.

Pagnon, J. *et al.* (2012) 'Identification and functional characterization of protein kinase A phosphorylation sites in the major lipolytic protein, adipose triglyceride lipase', *Endocrinology*, 153(9), pp. 4278–4289. doi: 10.1210/en.2012-1127.

Pant, M., Bal, N. C. and Periasamy, M. (2016) 'Sarcoplin: A Key Thermogenic and Metabolic Regulator in Skeletal Muscle', *Trends in Endocrinology and Metabolism*, 27(12), pp. 881–892. doi: 10.1016/j.tem.2016.08.006.

Papale, G. A. *et al.* (2010) 'Extracellular hydrophobic regions in scavenger receptor BI play a key role in mediating HDL-cholesterol transport', *Archives of Biochemistry and Biophysics*, 496(2), pp. 132–139. doi: 10.1016/j.abb.2010.02.011.

Park, K. *et al.* (2022) 'Endothelial Cells Induced Progenitors Into Brown Fat to Reduce Atherosclerosis', *Circulation Research*, 131(2), pp. 168–183. doi: 10.1161/CIRCRESAHA.121.319582.

Peche, V. S. *et al.* (2023) 'Endothelial cell CD36 regulates membrane ceramide formation, exosome fatty acid transfer and circulating fatty acid levels', *Nature Communications*, 14(1), pp. 1–19. doi: 10.1038/s41467-023-39752-3.

Petrovic, N. *et al.* (2010) 'Chronic peroxisome proliferator-activated receptor γ (PPAR γ) activation of epididymally derived white adipocyte cultures reveals a population of thermogenically competent, UCP1-containing adipocytes molecularly distinct from classic brown adipocytes', *Journal of Biological Chemistry*, 285(10), pp. 7153–7164. doi: 10.1074/jbc.M109.053942.

Phillips, M. C. (2014) 'Molecular mechanisms of cellular cholesterol efflux', *Journal of Biological Chemistry*, 289(35), pp. 24020–24029. doi: 10.1074/jbc.R114.583658.

Pittman, R. C. *et al.* (1987) 'A nonendocytotic mechanism for the selective uptake of high density lipoprotein-associated cholesterol esters.', *Journal of Biological Chemistry*, 262(6), pp. 2443–2450. doi: 10.1016/s0021-9258(18)61524-8.

Pittman, R. C. and Steinberg, D. (1984) 'Sites and mechanisms of uptake and degradation of high density and low density lipoproteins', *Journal of Lipid Research*, 25(13), pp. 1577–1585. doi: 10.1016/s0022-2275(20)34435-7.

Polkinghorne, M. D., West, H. W. and Antoniadou, C. (2024) 'Adipose Tissue in Cardiovascular Disease: From Basic Science to Clinical Translation', *Annual Review of Physiology*, 86, pp. 175–198. doi: 10.1146/annurev-physiol-042222-021346.

Powers, H. R. and Sahoo, D. (2022) 'SR-B1's Next Top Model: Structural Perspectives on the Functions of the HDL Receptor', *Current Atherosclerosis Reports*, 24(4), pp. 277–288. doi: 10.1007/s11883-022-01001-1.

Putri, M. *et al.* (2015) 'CD36 is indispensable for thermogenesis under conditions of fasting and cold stress', *Biochemical and Biophysical Research Communications*, 457(4), pp. 520–525. doi: 10.1016/j.bbrc.2014.12.124.

Raheel, H. *et al.* (2019) 'CD36 mediates albumin transcytosis by dermal but not lung microvascular endothelial cells: Role in fatty acid delivery', *American Journal of Physiology - Lung Cellular and Molecular Physiology*, 316(5), pp. L740–L750. doi: 10.1152/ajplung.00127.2018.

Reaven, E. *et al.* (2004) 'Dimerization of the scavenger receptor class B type I: Formation, function, and localization in diverse cells and tissues', *Journal of Lipid Research*, 45(3), pp. 513–528. doi: 10.1194/jlr.M300370-JLR200.

Rekhi, U. R. *et al.* (2021) 'Endothelial Cell CD36 Reduces Atherosclerosis and Controls Systemic Metabolism', *Frontiers in Cardiovascular Medicine*, 8(November), pp. 1–14. doi: 10.3389/fcvm.2021.768481.

Ren, B. Y. *et al.* (1995) 'CD36 Gene Transfer Confers Capacity for Phagocytosis of Cells Undergoing Apoptosis', *The Journal of experimental medicine*, 181(May), pp. 1857–1862.

Rigotti, A. *et al.* (1996) 'Regulation by adrenocorticotrophic hormone of the in vivo expression of scavenger receptor class B type I (SR-BI), a high density lipoprotein receptor, in steroidogenic cells of the murine adrenal gland', *Journal of Biological Chemistry*, 271(52), pp. 33545–33549. doi: 10.1074/jbc.271.52.33545.

Rigotti, A., Trigatti, B. L., *et al.* (1997) 'A targeted mutation in the murine gene encoding the high density lipoprotein (HDL) receptor scavenger receptor class B type I reveals its key role in HDL metabolism', *Proceedings of the National Academy of Sciences of the United States of America*, 94(23), pp. 12610–12615. doi: 10.1073/pnas.94.23.12610.

Rigotti, A., Trigatti, B., *et al.* (1997) 'Scavenger receptor BI - A cell surface receptor for high density lipoprotein', *Current Opinion in Lipidology*, pp. 181–188. doi: 10.1097/00041433-199706000-00009.

Rigotti, A., Acton, S. L. and Krieger, M. (1995) 'The class B scavenger receptors SR-BI and CD36 are receptors for anionic phospholipids', *Journal of Biological Chemistry*, 270(27), pp. 16221–16224. doi: 10.1074/jbc.270.27.16221.

Rigotti, A., Miettinen, H. E. and Krieger, M. (2003) 'The role of the high-density lipoprotein receptor SR-BI in the lipid metabolism of endocrine and other tissues', *Endocrine Reviews*, 24(3), pp. 357–387. doi: 10.1210/er.2001-0037.

Roberts, C. G. P. *et al.* (2007) 'Variants in scavenger receptor class B type I gene are associated with HDL cholesterol levels in younger women', *Human Heredity*, 64(2), pp. 107–113. doi: 10.1159/000101962.

Rohrer, L. *et al.* (2009) 'High-density lipoprotein transport through aortic endothelial cells involves scavenger receptor BI and ATP-binding cassette transporter G1', *Circulation Research*, 104(10), pp. 1142–1150. doi: 10.1161/CIRCRESAHA.108.190587.

Rosen, E. D. *et al.* (1999) 'PPAR γ is required for the differentiation of adipose tissue in vivo and in vitro', *Molecular Cell*, 4(4), pp. 611–617. doi: 10.1016/S1097-2765(00)80211-7.

Rosenwald, M. *et al.* (2013) 'Bi-directional interconversion of brite and white adipocytes', *Nature Cell Biology*, 15(6), pp. 659–667. doi: 10.1038/ncb2740.

Sahoo, D. *et al.* (2007) 'Scavenger receptor class B Type I (SR-BI) assembles into detergent-sensitive dimers and tetramers', *Biochimica et Biophysica Acta - Molecular and Cell Biology of Lipids*, 1771(7), pp. 807–817. doi: 10.1016/j.bbalip.2006.03.003.

Saito, M. *et al.* (2009) 'High incidence of metabolically active brown adipose tissue in healthy adult humans: Effects of cold exposure and adiposity', *Diabetes*, 58(7), pp. 1526–1531. doi: 10.2337/db09-0530.

Sanchez-Gurmaches, J. *et al.* (2018) 'Brown Fat AKT2 Is a Cold-Induced Kinase that Stimulates ChREBP-Mediated De Novo Lipogenesis to Optimize Fuel Storage and Thermogenesis', *Cell Metabolism*, 27(1), pp. 195-209.e6. doi: 10.1016/j.cmet.2017.10.008.

Schlein, C. *et al.* (2016) 'FGF21 lowers plasma triglycerides by accelerating lipoprotein catabolism in white and brown adipose tissues', *Cell Metabolism*, 23(3), pp. 441–453. doi: 10.1016/j.cmet.2016.01.006.

Scholander, P. F. *et al.* (1950) 'Heat regulation in some arctic and tropical mammals and birds.', *The Biological bulletin*, 99(2), pp. 237–258. doi: 10.2307/1538741.

Schreiber, R. *et al.* (2017) 'Cold-Induced Thermogenesis Depends on ATGL-Mediated Lipolysis in Cardiac Muscle, but Not Brown Adipose Tissue', *Cell Metabolism*, 26(5), pp. 753-763.e7. doi: 10.1016/j.cmet.2017.09.004.

Schwenk, R. W. *et al.* (2010) 'Fatty acid transport across the cell membrane: Regulation by fatty acid transporters', *Prostaglandins Leukotrienes and Essential Fatty Acids*, 82(4–6), pp. 149–154. doi: 10.1016/j.plefa.2010.02.029.

Seale, P. *et al.* (2008) 'PRDM16 controls a brown fat/skeletal muscle switch', *Nature*, 454(7207), pp. 961–967. doi: 10.1038/nature07182.

Seetharam, D. *et al.* (2006) 'High-density lipoprotein promotes endothelial cell migration and reendothelialization via scavenger receptor-B type I', *Circulation Research*, 98(1), pp. 63–72. doi: 10.1161/01.RES.0000199272.59432.5b.

Seki, T. *et al.* (2016) 'Endothelial PDGF-CC regulates angiogenesis-dependent thermogenesis in beige fat', *Nature Communications*, 7, pp. 1–16. doi: 10.1038/ncomms12152.

Seki, T. *et al.* (2018) 'Ablation of endothelial VEG FR1 improves metabolic dysfunction by inducing adipose tissue browning', *Journal of Experimental Medicine*, 215(2), pp. 611–626. doi: 10.1084/jem.20171012.

Sfeir, Z. *et al.* (1997) 'Regulation of FAT/CD36 gene expression: Further evidence in support of a role of the protein in fatty acid binding/transport', *Prostaglandins Leukotrienes and Essential Fatty Acids*, 57(1), pp. 17–21. doi: 10.1016/S0952-3278(97)90487-7.

Shen, W. J., Azhar, S. and Kraemer, F. B. (2018) 'SR-B1: A Unique Multifunctional Receptor for Cholesterol Influx and Efflux', *Annual Review of Physiology*, 80(3), pp. 95–116. doi: 10.1146/annurev-physiol-021317-121550.

Shibao, C. A. *et al.* (2016) 'A common CD36 variant influences endothelial function and response to treatment with phosphodiesterase 5 inhibition', *Journal of Clinical Endocrinology and Metabolism*, 101(7), pp. 2751–2758. doi: 10.1210/jc.2016-1294.

Shin, H. *et al.* (2017) 'Lipolysis in Brown Adipocytes Is Not Essential for Cold-Induced Thermogenesis in Mice', *Cell Metabolism*, 26(5), pp. 764-777.e5. doi: 10.1016/j.cmet.2017.09.002.

Shin, K. C. *et al.* (2022) 'VLDL-VLDLR axis facilitates brown fat thermogenesis through replenishment of lipid fuels and PPAR β/δ activation', *Cell Reports*, 41(11), p. 111806. doi: 10.1016/j.celrep.2022.111806.

Silva, J. E. (2003) 'The Thermogenic Effect of Thyroid Hormone and Its Clinical Implications', *Annals of Internal Medicine*, 139(3), pp. 205–213. doi: 10.7326/0003-4819-139-3-200308050-00010.

Silverstein, R. L. and Febbraio, M. (2009) 'CD36, a Scavenger Receptor Involved in Immunity, Metabolism, Angiogenesis, and Behavior', *Science Signaling*, 2(72). doi: 10.1126/scisignal.272re3.

Simcox, J. *et al.* (2017) 'Global Analysis of Plasma Lipids Identifies Liver-Derived Acylcarnitines as a Fuel Source for Brown Fat Thermogenesis', *Cell Metabolism*, 26(3), pp. 509–522.e6. doi: 10.1016/j.cmet.2017.08.006.

Simonson, D. C. and DeFronzo, R. A. (1990) 'Indirect calorimetry: Methodological and interpretative problems', *American Journal of Physiology - Endocrinology and Metabolism*, 258(3 21-3). doi: 10.1152/ajpendo.1990.258.3.e399.

Son, N. H. *et al.* (2018) 'Endothelial cell CD36 optimizes tissue fatty acid uptake', *Journal of Clinical Investigation*, 128(10), pp. 4329–4342. doi: 10.1172/JCI99315.

Stangl, H., Hyatt, M. and Hobbs, H. H. (1999) 'Transport of lipids from high and low density lipoproteins via scavenger receptor-BI', *Journal of Biological Chemistry*, 274(46), pp. 32692–32698. doi: 10.1074/jbc.274.46.32692.

Strahlhofer-Augsten, M. *et al.* (2022) 'The Distinct Role of the HDL Receptor SR-BI in Cholesterol Homeostasis of Human Placental Arterial and Venous Endothelial Cells', *International Journal of Molecular Sciences*, 23(10). doi: 10.3390/ijms23105364.

Tao, N., Wagner, S. J. and Lublin, D. M. (1996) 'CD36 is palmitoylated on both N- and C-terminal cytoplasmic tails', *Journal of Biological Chemistry*, 271(37), pp. 22315–22320. doi: 10.1074/jbc.271.37.22315.

Teboul, L. *et al.* (2001) 'Structural and functional characterization of the mouse fatty acid translocase promoter: Activation during adipose differentiation', *Biochemical Journal*, 360(2), pp. 305–312. doi: 10.1042/0264-6021:3600305.

Thorne, R. F. *et al.* (2010) 'Palmitoylation of CD36/FAT regulates the rate of its post-transcriptional processing in the endoplasmic reticulum', *Biochimica et Biophysica Acta - Molecular Cell Research*, 1803(11), pp. 1298–1307. doi: 10.1016/j.bbamcr.2010.07.002.

Thuahnai, S. T. *et al.* (2004) 'Scavenger receptor class B type I-mediated cholesteryl ester-selective uptake and efflux of unesterified cholesterol: Influence of high density lipoprotein size and structure', *Journal of Biological Chemistry*, 279(13), pp. 12448–12455. doi: 10.1074/jbc.M311718200.

Tian, T. *et al.* (2020) 'The P2X7 ion channel is dispensable for energy and metabolic homeostasis of white and brown adipose tissues', *Purinergic Signalling*, 16(4), pp. 529–542. doi: 10.1007/s11302-020-09738-7.

Torres Irizarry, V. C. *et al.* (2022) 'Hypothalamic Estrogen Signaling and Adipose Tissue Metabolism in Energy Homeostasis', *Frontiers in Endocrinology*, 13(June), pp. 1–19. doi: 10.3389/fendo.2022.898139.

Trigatti, B. *et al.* (1999) 'Influence of the high density lipoprotein receptor SR-BI on reproductive and cardiovascular pathophysiology', *Proceedings of the National Academy of Sciences of the United States of America*, 96(16), pp. 9322–9327. doi: 10.1073/pnas.96.16.9322.

Tvrdek, P. *et al.* (1997) 'Cig30, a mouse member of a novel membrane protein gene family, is involved in the recruitment of brown adipose tissue', *Journal of Biological Chemistry*, 272(50), pp. 31738–31746. doi: 10.1074/jbc.272.50.31738.

Tvrdek, P. *et al.* (2000) 'Role of a new mammalian gene family in the biosynthesis of very long chain fatty acids and sphingolipids', *Journal of Cell Biology*, 149(3), pp. 707–717. doi: 10.1083/jcb.149.3.707.

Urbanczyk, M., Zbinden, A. and Schenke-Layland, K. (2022) 'Organ-specific endothelial cell heterogeneity and its impact on regenerative medicine and biomedical engineering applications', *Advanced Drug Delivery Reviews*, 186, p. 114323. doi: 10.1016/j.addr.2022.114323.

Vaisman, B. L. *et al.* (2015) 'Endothelial Expression of Scavenger Receptor Class B, Type I Protects against Development of Atherosclerosis in Mice', *BioMed Research International*, 2015. doi: 10.1155/2015/607120.

Varban, M. L. *et al.* (1998) 'Targeted mutation reveals a central role for SR-BI in hepatic selective uptake of high density lipoprotein cholesterol', *Proceedings of the National Academy of Sciences of the United States of America*, 95(8), pp. 4619–4624. doi: 10.1073/pnas.95.8.4619.

Vijay, J. *et al.* (2020) 'Single-cell analysis of human adipose tissue identifies depot- and disease-specific cell types', *Nature Metabolism*, 2(1), pp. 97–109. doi: 10.1038/s42255-019-0152-6.

Vijgen, G. H. E. J. *et al.* (2011) 'Brown adipose tissue in morbidly obese subjects', *PLoS ONE*, 6(2), pp. 2–7. doi: 10.1371/journal.pone.0017247.

Viñals, M. *et al.* (2003) 'Identification of the N-linked glycosylation sites on the high density lipoprotein (HLD) receptor SR-BI and assessment of their effects on HDL binding and selective lipid uptake', *Journal of Biological Chemistry*, 278(7), pp. 5325–5332. doi: 10.1074/jbc.M211073200.

Virtanen, K. A. *et al.* (2009) 'Functional Brown Adipose Tissue in Healthy Adults', *The New England Journal of Medicine*, 360(15), pp. 1518–1525.

Wade, G. *et al.* (2021) 'Lipid Transport in Brown Adipocyte Thermogenesis', *Frontiers in Physiology*, 12(December), pp. 1–16. doi: 10.3389/fphys.2021.787535.

Wang, N. *et al.* (1998) 'Liver-specific overexpression of scavenger receptor BI decreases levels of very low density lipoprotein ApoB, low density lipoprotein ApoB, and high density lipoprotein in transgenic mice', *Journal of Biological Chemistry*, 273(49), pp. 32920–32926. doi: 10.1074/jbc.273.49.32920.

Webb, N. R. *et al.* (1998) 'SR-BII, an isoform of the scavenger receptor BI containing an alternate cytoplasmic tail, mediates lipid transfer between high density lipoprotein and cells', *Journal of Biological Chemistry*, 273(24), pp. 15241–15248. doi: 10.1074/jbc.273.24.15241.

Westerberg, R. *et al.* (2006) 'ELOVL3 is an important component for early onset of lipid recruitment in brown adipose tissue', *Journal of Biological Chemistry*, 281(8), pp. 4958–4968. doi: 10.1074/jbc.M511588200.

Westerterp, M. *et al.* (2006) 'Cholesteryl ester transfer protein decreases high-density lipoprotein and severely aggravates atherosclerosis in APOE*3-Leiden mice', *Arteriosclerosis, Thrombosis, and Vascular Biology*, 26(11), pp. 2552–2559. doi: 10.1161/01.ATV.0000243925.65265.3c.

- Whytock, K. L. *et al.* (2022) 'Single cell full-length transcriptome of human subcutaneous adipose tissue reveals unique and heterogeneous cell populations', *iScience*, 25(8), p. 104772. doi: 10.1016/j.isci.2022.104772.
- Wiersma, H. *et al.* (2010) 'Scavenger receptor BI facilitates hepatic very low density lipoprotein production in mice', *Journal of Lipid Research*, 51(3), pp. 544–553. doi: 10.1194/jlr.M000844.
- Worthmann, A. *et al.* (2017) 'Cold-induced conversion of cholesterol to bile acids in mice shapes the gut microbiome and promotes adaptive thermogenesis', *Nature Medicine*, 23(7), pp. 839–849. doi: 10.1038/nm.4357.
- Wu, J. *et al.* (2012) 'Beige adipocytes are a distinct type of thermogenic fat cell in mouse and human', *Cell*, 150(2), pp. 366–376. doi: 10.1016/j.cell.2012.05.016.
- Xu, S. *et al.* (1997) 'Apolipoproteins of HDL can directly mediate binding to the scavenger receptor SR-BI, an HDL receptor that mediates selective lipid uptake', *Journal of Lipid Research*, 38(7), pp. 1289–1298. doi: 10.1016/s0022-2275(20)37413-7.
- Yamashita, S. *et al.* (2007) 'Physiological and pathological roles of a multi-ligand receptor CD36 in atherogenesis; insights from CD36-deficient patients', *Molecular and Cellular Biochemistry*, 299(1–2), pp. 19–22. doi: 10.1007/s11010-005-9031-4.
- Yau, W. W. *et al.* (2019) 'Thyroid hormone (T3) stimulates brown adipose tissue activation via mitochondrial biogenesis and MTOR-mediated mitophagy', *Autophagy*, 15(1), pp. 131–150. doi: 10.1080/15548627.2018.1511263.
- Yu, J. *et al.* (2015) 'Lipid droplet remodeling and interaction with mitochondria in mouse brown adipose tissue during cold treatment', *Biochimica et Biophysica Acta - Molecular Cell Research*, 1853(5), pp. 918–928. doi: 10.1016/j.bbamcr.2015.01.020.
- Yu, M. *et al.* (2011) 'Exoplasmic cysteine Cys384 of the HDL receptor SR-BI is critical for its sensitivity to a small-molecule inhibitor and normal lipid transport activity', *Proceedings of the National Academy of Sciences of the United States of America*, 108(30), pp. 12243–12248. doi: 10.1073/pnas.1109078108.
- Yuhanna, I. S. *et al.* (2001) 'High-density lipoprotein binding to scavenger receptor-BI activates endothelial nitric oxide synthase', *Nature Medicine*, 7(7), pp. 853–857. doi: 10.1038/89986.

Zechner, R., Madeo, F. and Kratky, D. (2017) 'Cytosolic lipolysis and lipophagy: Two sides of the same coin', *Nature Reviews Molecular Cell Biology*, 18(11), pp. 671–684. doi: 10.1038/nrm.2017.76.

Zeng, T. T. *et al.* (2017) 'Influence of SCARB1 gene SNPs on serum lipid levels and susceptibility to coronary heart disease and cerebral infarction in a Chinese population', *Gene*, 626(May), pp. 319–325. doi: 10.1016/j.gene.2017.05.020.

Zeng, Y. *et al.* (2003) 'Endocytosis of Oxidized Low Density Lipoprotein through Scavenger Receptor CD36 Utilizes a Lipid Raft Pathway That Does Not Require Caveolin-1', *Journal of Biological Chemistry*, 278(46), pp. 45931–45936. doi: 10.1074/jbc.M307722200.

Zhang, X. and Fernández-Hernando, C. (2019) 'The Janus-faced role of SR-BI in atherosclerosis', *Nature Metabolism*, 1(6), pp. 586–587. doi: 10.1038/s42255-019-0072-5.

Zhao, L. *et al.* (2018) 'CD36 palmitoylation disrupts free fatty acid metabolism and promotes tissue inflammation in non-alcoholic steatohepatitis', *Journal of Hepatology*, 69(3), pp. 705–717. doi: 10.1016/j.jhep.2018.04.006.

Zhu, W. *et al.* (2008) 'The scavenger receptor class B type I adaptor protein PDZK1 maintains endothelial monolayer integrity', *Circulation Research*, 102(4), pp. 480–487. doi: 10.1161/CIRCRESAHA.107.159079.

Part I: Attachments

Table 11. Buffers and solutions

Buffer/Solution	Composition
1.5M Tris-HCl	<ul style="list-style-type: none"> 181.7 g Tris-Base Adjust pH 8.8 with HCl 25% in final volume of 1 L of H₂O dest.
1M Tris-HCl	<ul style="list-style-type: none"> 121.1 g Tris-Base Adjust pH 6.8 with HCl 25% in final volume of 1 L of H₂O dest.
3% BSA in PBS	<ul style="list-style-type: none"> 1.5 g BSA in final volume of 50 mL of TBST
Anesthesia	ketamine (100 mg/ml)/xylazin (2 %)/NaCl (0.9 %); 2.3/1.0/6.7, v/v/v; 15 µL/g bodyweight
Blocking buffer BSA 5%	<ul style="list-style-type: none"> 2.5 g BSA in final volume of 50 mL of TBST
Blocking buffer milk 5%	<ul style="list-style-type: none"> 2.5 g Milk Skim Powder in final volume of 50 mL of TBST
Blotting buffer	<ul style="list-style-type: none"> 56.2 g Glycine 12.1 g Tris-base 1 L Methanol in final volume of 5 L of H₂O dest.
Citric acid buffer pH 6.0	<ul style="list-style-type: none"> 1.92 g Citric acid Adjust pH with 2M NaOH 0.5 mL Tween20 in final volume of 1 L of H₂O dest.
Formaldehyde solution 3.7%	<ul style="list-style-type: none"> 100 mL Formaldehyde solution 37% in final volume of 1 L of PBS
NaCl 5M	<ul style="list-style-type: none"> 14.61 g NaCl in final volume of 50 mL of H₂O dest.
MACS buffer 2mM EDTA 0.5% BSA	<ul style="list-style-type: none"> 744 mg EDTA 5 g BSA in final volume of 1 L of PBS

MACS digestion solution (prepare fresh)	<ul style="list-style-type: none"> • 1.5 U/mL Collagenase D • 2.4 U/mL Dispase • 1 mM CaCl₂ in final volume of 10 mL PBS
Primary antibody solution 5% BSA with NaAzid 0.02%	<ul style="list-style-type: none"> • 2.5 g BSA • 50 µL Sodium azide 20% in final volume of 50 mL of TBST (filtered)
RIPA buffer stock solution	<ul style="list-style-type: none"> • 20 mL Tris-HCL pH 7.4 1M • 1.862 g EDTA • 2.92 g NaCl • 2.22 g Sodium pyrophosphate • 2.1 g Sodiumfluoride • 10 mL NP-40% in final volume of 1 L of H ₂ O dest. (filtered)
RIPA	<ul style="list-style-type: none"> • 50 µL Na₃VO₄ • 100 µL Phosphatase inhibitors A (Sigma) • 100 µL Phosphatase inhibitors B (Sigma) • 100 µL 10% SDS • 1 cOmplete Mini Protease Inhibitor Cocktail Tablets (Roche) in final volume of 10 mL of RIPA stock solution
Running buffer (10X)	<ul style="list-style-type: none"> • 54 g Tris-Base • 144 g Glycine • 10 g SDS in final volume of 1 L of H ₂ O dest.
SDS 10 %	<ul style="list-style-type: none"> • 10 g SDS in final volume of 100 mL of H ₂ O dest.
Sodium azide 20% (w/v)	<ul style="list-style-type: none"> • 10 g Sodium Azide in final volume of 50 mL of H ₂ O dest.

STE buffer	<ul style="list-style-type: none"> • 2.92 g NaCl • 1.21 g Tris-Base • 5 g SDS • 3.72 g EDTA • Adjust pH 7.4 in of 1 L of H ₂ O dest.
TBE-Buffer (5X)	<ul style="list-style-type: none"> • 54 g Tris-Base • 27.5 g Boric acid • 3.7 g EDTA in final volume of 1 L of H ₂ O dest.
TBS - Tween 0.1%	<ul style="list-style-type: none"> • 100 mL TBS 10X • 1 mL TWEEN® 20 in final volume of 1 L of H ₂ O dest.
TBS buffer (10X)	<ul style="list-style-type: none"> • 0.2M Tris-Base • 1.37M NaCl in final volume of 1 L of H ₂ O dest., pH 7.4

Part J: Register of figures

Table 12. Register of figures

Figure title	Page #
Figure 1. Location of different BAT and WAT depots in humans and mice.	23
Figure 2. Cell origin and differentiation of skeletal muscle, brown, beige and white adipocytes.	24
Figure 3. Overview of characteristics of white, brown and beige adipocytes.	25
Figure 4. Browning and whitening of WAT.	26
Figure 5. White adipocytes during feeding and fasting.	28
Figure 6. Signaling cascade upon adrenergic stimulation of BAT.	30
Figure 7. Lipoprotein metabolism during NST.	31
Figure 8. Schematic overview of structure of CD36.	33
Figure 9. Schematic overview of FA uptake via CD36.	35
Figure 10. Schematic overview of structure of SR-B1.	38
Figure 11. Role of SR-B1 in endothelial cells and RCT.	40
Figure 12. Exemplary PCR results of the CD36flox PCR.	50
Figure 13. Exemplary PCR results of the SR-B1flox PCR.	53
Figure 14. Exemplary PCR results of the CreCs PCR.	56
Figure 15. Workflow of MACS.	57
Figure 16. Body characteristics of $Cd36^{fl/fl}-Ucp1^{Cre+}$ and $Cd36^{fl/fl}-Ucp1^{Cre-}$ mice.	62
Figure 17. $Cd36^{fl/fl}-Ucp1^{Cre+}$ mice have decreased $Cd36$ gene and CD36 protein expression compared to control littermates.	63
Figure 18. Localization of CD36 in iBAT of $Cd36^{fl/fl}-Ucp1^{Cre-}$ and $Cd36^{fl/fl}-Ucp1^{Cre+}$ mice.	64

Figure 19. Body characteristics of $Cd36^{fl/fl}-Ucp1^{Cre+}$ and $Cd36^{fl/fl}-Ucp1^{Cre-}$ mice.	66
Figure 20. $Cd36^{fl/fl}-Ucp1^{Cre+}$ mice are able to maintain their body temperature when exposed to cold in a fed state.	67
Figure 21. Body characteristics of $Cd36^{fl/fl}-Ucp1^{Cre+}$ and $Cd36^{fl/fl}-Ucp1^{Cre-}$ mice.	69
Figure 22. $Cd36^{fl/fl}-Ucp1^{Cre+}$ mice are unable to maintain their body temperature when exposed to cold in a fasted state.	71
Figure 23. Body characteristics of $Cd36^{fl/fl}-Ucp1^{Cre+}$ and $Cd36^{fl/fl}-Ucp1^{Cre-}$ mice.	72
Figure 24. Cold-exposed $Cd36^{fl/fl}-Ucp1^{Cre+}$ mice have blunted uptake in iBAT compared to cold-exposed control littermates.	73
Figure 25. Cold-exposed $Cd36^{fl/fl}-Ucp1^{Cre+}$ mice have decreased expression of lipid handling genes in BAT and decreased expression of thermogenic markers in WAT.	76
Figure 26. Body characteristics of $Cd36^{fl/fl}-Cdh5^{Cre+}$ and $Cd36^{fl/fl}-Cdh5^{Cre-}$ mice.	77
Figure 27. $Cd36^{fl/fl}-Cdh5^{Cre+}$ mice have decreased CD36 protein expression compared to control littermates housed at RT.	78
Figure 28. Localization of CD36 in iBAT of $Cd36^{fl/fl}-Cdh5^{Cre-}$ and $Cd36^{fl/fl}-Cdh5^{Cre+}$ mice.	79
Figure 29. Body characteristics of $Cd36^{fl/fl}-Cdh5^{Cre+}$ and $Cd36^{fl/fl}-Cdh5^{Cre-}$ mice.	80
Figure 30. $Cd36^{fl/fl}-Cdh5^{Cre+}$ mice are able to maintain their body temperature when exposed to cold in a fed and fasted state.	81
Figure 31. Body characteristics of $Cd36^{fl/fl}-Cdh5^{Cre+}$ and $Cd36^{fl/fl}-Cdh5^{Cre-}$ mice.	82
Figure 32. $Cd36^{fl/fl}-Cdh5^{Cre+}$ mice have increased DOG uptake in heart.	83
Figure 33. Cold-exposed $Cd36^{fl/fl}-Cdh5^{Cre+}$ mice have decreased expression of thermogenic markers in WAT.	85

Figure 34. SR-B1 knockout is endothelial cell-specific.	86
Figure 35. Body characteristics of <i>Scarb1^{fl/fl}-Cdh5^{Cre+}</i> and <i>Scarb1^{fl/fl}-Cdh5^{Cre-}</i> mice.	88
Figure 36. SR-B1 expressed by endothelial cells contributes majorly to whole organ SR-B1 expression.	89
Figure 37. No differences in metabolic parameters at 22°C between <i>Scarb1^{fl/fl}-Cdh5^{Cre+}</i> and <i>Scarb1^{fl/fl}-Cdh5^{Cre-}</i> mice.	90
Figure 38. Body characteristics of <i>Scarb1^{fl/fl}-Cdh5^{Cre+}</i> and <i>Scarb1^{fl/fl}-Cdh5^{Cre-}</i> mice.	92
Figure 39. No differences in metabolic parameters at between <i>Scarb1^{fl/fl}-Cdh5^{Cre+}</i> and <i>Scarb1^{fl/fl}-Cdh5^{Cre-}</i> mice on chow and HFD during cold adaptation.	94
Figure 40. Body characteristics of <i>Scarb1^{fl/fl}-Cdh5^{Cre+}</i> and <i>Scarb1^{fl/fl}-Cdh5^{Cre-}</i> mice.	97
Figure 41. No differences in lipid and glucose uptake between <i>Scarb1^{fl/fl}-Cdh5^{Cre+}</i> and <i>Scarb1^{fl/fl}-Cdh5^{Cre-}</i> mice on chow and HFD at different housing conditions.	98
Figure 42. No differences in thermogenic marker and receptor expression in iBAT and iWAT between <i>Scarb1^{fl/fl}-Cdh5^{Cre+}</i> and <i>Scarb1^{fl/fl}-Cdh5^{Cre-}</i> mice on chow and HFD at different housing conditions.	102
Figure 43. <i>Scarb1^{fl/fl}-Cdh5^{Cre+}</i> mice have strongly reduced uptake of ³ H-labelled cholesteryl ether in heart and iBAT.	105
Figure 44. Graphical summary of brown adipocyte-specific and endothelial-specific CD36 knockout on lipid handling and thermogenesis.	111
Figure 45. Graphical summary of endothelial-specific SR-B1 knockout on lipid handling and thermogenesis.	114

Part K: Register of tables

Table 13. Register of tables

Table title	Page #
Table 1. PCR reaction mix for CD36flox	48
Table 2. PCR primer sequences of CD36flox from 5' to 3'	49
Table 3. PCR program CD36flox	49
Table 4. PCR reaction mix for SR-B1flox	51
Table 5. PCR primer sequences of SR-B1flox from 5' to 3'	51
Table 6. PCR program SR-B1flox	52
Table 7. PCR reaction mix for CreCs	54
Table 8. PCR primer sequences of CreCs from 5' to 3'	54
Table 9. PCR program CreCs	55
Table 10. Gene names and TaqMan® Assays-on-Demand™	58-59
Table 11. Buffers and solutions	135-137
Table 12. Register of figures	138-140
Table 13. Register of tables	141

Acknowledgements

Over the past 3.5 years, many people crossed my path and helped me to be able to write this thesis & to become doctor Kim. Words cannot express all the gratitude and experiences lived, but I'll try.

Om te beginnen **Maaïke** en **Martijn**. Ik wist niet goed wat ik na mijn master wilde doen. Ik ben nieuwsgierig en hou van kennis vergaren, maar een PhD doen voelde niet als een optie. Jullie lieten me inzien dat ik het wel in me had, dat dit wel een optie voor me zou kunnen zijn en nu bijna 4 jaar later, I did it! Dankjewel voor jullie vertrouwen en dat jullie de weg hebben geopend voor dit fantastische avontuur.

Dit was ook niet mogelijk geweest zonder **Bart**, die naar me toe kwam op de laatste dag van mijn stage. "Zou je ervoor openstaan om een PhD in het buitenland te doen? In het internationale consortium waar ik onderdeel van ben, zoeken ze nog een PhD student in Hamburg." Natuurlijk greep ik deze gelegenheid met beide handen aan.

This led me to Jörg. After spending a day at the lab in Hamburg, talking to the PhD students, Pablo and Markus. I decided to join the lab and become part of EndoConnect. **Jörg**, I'm so grateful that you took a chance on me and allowed me to become part of the Heeren lab. Thank you for all the guidance, the many discussions and all the pizzas during the kicker tournaments. I will never forget you during the first kicker tournament, in your St Pauli t-shirt, ready to take anyone down and gloat even though you knew we were (back then) way worse than you. Thanks for everything.

Wenn wir über Kicker reden, dann kann ich natürlich **Walter** nicht vergessen. Als neu angestellte Doktorandin, hatte ich so viele Geschichte über Kickerturniere gehört, dass ich das selbst ausprobieren wollte. Mit Walter habe ich mein erstes Kickerspiel gespielt, natürlich verloren, aber es war der Anfang neuer Kickerturniere und vieler weiterer Spiele. **Walter**, **Birgit** und **Sandra**, ihr habt eine große Rolle darin gespielt dass ich mich im Labor wohlfühle. Durch gute Ratschläge, die Ermutigung, Deutsch zu sprechen („Kim in Hamburg heißt es Moin nicht MoinMoin, dann klingst du wie eine Touristin“) und zusammen zu tanzen habe ich viele schöne Erinnerungen an mein erstes Jahr als Doktorandin.

I didn't just become part of the Heeren lab, I also became part of EndoConnect. It was amazing how quickly we connected and bonded in Groningen, still in the aftermath of Corona, singing 'Despacito' in a half empty bar and nice that we made it full circle in Cambridge. I sometimes felt like an outsider, talking about brown adipose tissue or mice, while the rest of you were busy

unraveling the recycling pathways, getting excited about 'Retriever', 'Corvet' and other pathways and proteins that I had never heard of before joining. Let's just say I learned a lot. It was a pleasure to be EndoConnected to you: **Shrestha, Rebeka, Camilla, Matteo (Sponge), Joël (superJoel), Klevis (K-Levi), Carmen, Lipsa, Orsolya, Ankia, Alejandra, David (Frank), Annabel, Lorinda, Haoran & Markus**. Forever EndoConnected <3 I won't name all the PIs individually, although you must know that your feedback and presence was very much appreciated. I want to give a shout out to Albert, Alain and Pablo. **Albert**, thank you so much for allowing me to spend 2 months in beautiful Barcelona, I learned a lot about lipid droplets and microscopy (couldn't have done it without **Marta & Alba**), some Catalan and enjoyed great paella. **Alain**, Utrecht was weer zoals thuiskomen. Aan de ene kant vertrouwd, want in een keer weer Nederlands praten, maar ook niet, want wel weer een heel ander onderwerp. Dank voor je enthousiasme, je doortastende vragen die me nog een keer na lieten denken, maar vooral dank voor de steun en ruimte die je geboden hebt, die ik op dat moment nodig had. En ook **Thomas** bedankt voor je begeleiding. **Pablo**, we met each other when I was coming to Hamburg. I think that most of our conversations didn't revolve around actual science, but the way science is organized, what could be improved, how the UKE could be improved, the challenges internationals face and I can only say that I really enjoyed these conversations. It changed the way I view certain things and made the fire to change things even bigger and I would like to thank you for that. **Heleen, Eleni & Karen** you had some work cut out for you to make sure everything within the EndoConnect framework ran smoothly. Thanks for all the organization, answering all the e-mails and if Teams didn't work again still sent us all the documents via e-mail without complaining. **Karen**, jou wil ik graag nog even apart benoemen. Er werd aangeraden om een mentor te nemen binnen het consortium en na Groningen klikte het zo, dat ik jou graag als mentor wilde hebben. Dat was een hele goede keuze. Het was een welkome adempauze in de maand, waar weer even Nederlands gepraat mocht worden, geklaagd, om advies gevraagd en soms ook gewoon lekker een uurtje ouwehoeren. Je daagde me uit om verder (na mijn PhD) te kijken en was ook een grote steun toen ik het nodig had. Heel erg bedankt daarvoor.

Then, back to the Heeren lab. It took a lot of time, effort, discussions and help to be where I am today. From genotyping, to countless OEs and experiments, advice, MACS, administrative things but also fun stuff like the unofficial Christmas parties, kicker tournaments and playing pool & darts. Thank you for helping me in these past 3.5 years: **Anna, Ludger, Markus, Laura, Manka, Friederike, Michelle, Anastasia, Paul, Nadia, Janina, Peter, Meike, Laura, Jenny, Vivi, Luka, Lisa, Ronja, Victoria, Alina, Anastasiia, Finja, Sophia, Judy and Aurora**.

Also a special thanks to **Franz Rinniger** for your help with the HDL turnover experiment. Someone I have to put into the spotlight is Markus. Dear **Markus**, what a ride it has been these past years. Quickly, I realized that with your knowledge and my memory and organizational skills, we made quite the team. During my first Mitarbeitersjahresgespräch with you, you said: "It has been such a joy working with you, thank you for the past year." I would like to return the favor: Thank you, it has been a joy working with you these past years. It was always great to walk into the office of you and Ludger. If not for you, I would've never known who Udo Jürgens is, you made sure that I was well educated in science as well as in German culture. We could do serious, but more often we also had time to joke around and I really appreciate that. I hope that you'll never forget the 5th of November & that someone else will sing songs that will stuck in your head.

Then a special mention to the people who made Hamburg feel like home. Science is great and I learned a lot, but you are the ones that made this time here special and is what I will remember most. Dear **Giannis, Johanna, Jenny, David, Karthik, Simon, Sebastian, Martina, Tami, Magda, Marie, Johan, Macarena, Javi, Lola, Anna & Martin**. Thank you for the discussions about science or what life is about, the support during long ass experiments and after when the experiment didn't go as planned, to relax would it be playing kicker, singing in the karaoke bar, dancing on the Kiez, go to a festival, wine nights or eating Fricke fries after a long week. Friendships have been solidified over broken freezers, kicker tournaments, Fischbrötchen, memes, long nights in the Fricke and the Kiez, language lessons, long deep conversations and work out session in the gym. I'm so glad I've been stuck with all of you. Many memories were made, some were lost, but you always will have a special place in my heart.

Before I move on out of Hamburg, I want to thank **Hartmut Schlüter & Caroline Jung** for being part of my exam committee and for the feedback during the annual meetings.

Als laatst, lieve **papa, mama, Joep, Annemiek, Anouk** & al mijn lieve vrienden en vriendinnen uit Utrecht, Amsterdam en Groningen. Voor sommige was dit de eerste keer afscheid nemen omdat ik ergens anders heen verhuisde, voor anderen die al langer meeliepen was het de zoveelste keer. Ik ben zo ontzettend dankbaar voor jullie in mijn leven. Dat jullie er (nog) steeds zijn, de wandelingen of elkaar in het echt zien vervangen voor belletjes (die dan 3 uur duren), er oké mee zijn dat de tussenpozen dat we elkaar zien steeds langer worden. Dat als ik jullie nodig heb, jullie er zijn. Mijn thuis op afstand. Bedankt voor de lieve woorden, aanmoedigingen, luisterend oor zijn, de check-ins & de afleiding of de was (thanks mam!). I did it! Op naar het volgende avontuur.

Curriculum vitae

Lebenslauf entfällt aus datenschutzrechtlichen Gründen

Eidesstattliche Versicherung

Ich versichere ausdrücklich, dass ich die Arbeit selbständig und ohne fremde Hilfe verfasst, andere als die von mir angegebenen Quellen und Hilfsmittel nicht benutzt und die aus den benutzten Werken wörtlich oder inhaltlich entnommenen Stellen einzeln nach Ausgabe (Auflage und Jahr des Erscheinens), Band und Seite des benutzten Werkes kenntlich gemacht habe.

Ferner versichere ich, dass ich die Dissertation bisher nicht einem Fachvertreter an einer anderen Hochschule zur Überprüfung vorgelegt oder mich anderweitig um Zulassung zur Promotion beworben habe.

Ich erkläre mich einverstanden, dass meine Dissertation vom Dekanat der Medizinischen Fakultät mit einer gängigen Software zur Erkennung von Plagiaten überprüft werden kann.

Unterschrift:



10.03.2025, Hamburg